ANALYSIS OF DIELECTRIC SLAB WAVEGUIDE DISCONTINUITIES

A Thesis

Presented to

The Faculty of Graduate Studies

The University of Manitoba

In Partial Fulfillment

of the Requirements for the Degree of

Doctor of Philosophy

in

Electrical Engineering

by

APISAK ITTIPIBOON

January 1980

ANALYSIS OF DIELECTRIC SLAB WAVEGUIDE DISCONTINUITIES

BY

APISAK ITTIPIBOON

A thesis submitted to the Faculty of Graduate Studies of
the University of Manitoba in partial fulfillment of the requirements
of the degree of

To My Parents

ABSTRACT

The need for the study of the effects of discontinuity on a surface waveguide is given. A brief discussion of previous investigations including their disadvantages and limitations when applied to the problem of a slab waveguide discontinuity is outlined, after which two new techniques for solutions are presented. The first proposed technique is based on the Wiener-Hopf technique, where the Wiener-Hopf equations of the dielectric slab waveguide are derived for both TE and TM incidence by applying the Fourier transform to the wave equations, together with the proper boundary conditions. Because of the complicated functions involved, the factorizations and decompositions are obtained numerically by applying Lee-Mittra and Noble techniques. The transform equation can then be separated into two parts, regular in the upper and lower halves of the transform plane,which are set equal to zero after assuming an algebraic asymptotic behaviour of the transformed field. A second technique which is based on the residue-calculus and is somewhat more general than the Wiener-Hopf is also given. The unknown fields on both sides of the junction at the discontinuity are expanded in terms of surface wave and radiation modes after which, following the mode matching technique, two simultaneous equations for the unknown mode amplitudes are obtained. With a properly constructed function together with the assumption of algebraic behaviour of the field, these equations are solved by an application of residue-calculus. Simple expressions for the reflection coefficient, the transmitted power and radiation loss are then obtained. Numerical results are given for special cases leading to a discussion of the methods and their applications. The accuracy of the results is

confirmed by good agreement with the available data from Marcuse, for simple cases, and with those obtained by the reciprocity theorem and the application of Kay's technique, for more general cases.

ACKNOWLEDGEMENTS

The author would like to express his gratitude to Professor M. Hamid for his guidance throughout and his financial assistance in the last year of this research. The author would also like to thank Professor L. Shafai for his suggestions and discussions about the dielectric edge condition, Dr. T.C.K. Rao for his suggestions in the early stage of the research, and Dr. A. Mohsen for his suggestions in the preparation of this thesis. The discussions and assistances given to the author by his colleagues, Dr. A. Shoamanesh and Dr. K. Iskander and typing skill of Ms. M. Tyler are also appreciated.

The author would also like to acknowledge the financial assistance of the Department of Electrical Engineering, University of Manitoba in the form of a teaching assistantship and the Thai Government for the time granted to the author to complete the research.

TABLE OF CONTENTS

LIST OF FIGURES

LIST OF TABLES

CHAPTER 1

INTRODUCTION

A definition of a surface wave is given by Barlow and Brown as the wave that propagates along an interface between two different media without radiation; such radiation being construed to mean energy converted from surface wave field to some other forms [1]. If the two media concerned have finite losses, the energy flowing along the interface must supply those losses as well as the transmitted power. This does not invalidate the description of the surface wave, since the radiation is construed to mean energy absorbed from the wave independent of the supporting media. The important characteristic of a surface wave field is that its tangential components to the supporting surface will always decay with distance away from the surface. Three distinctive forms of a surface wave [1] which are usually the subject of study are:

(i) the inhomogeneous plane wave supported by a flat surface, sometimes called the Zenneck wave,

(ii) the inhomogeneous radial cylindrical wave, also supported by a flat surface and sometimes described as the radial form of a Zenneck wave,

(iii) the axial cylindrical wave associated with a surface of circular profile in the transverse plane and referred to as the Sommerfeld-Goubau wave.

In order to establish these pure surface waves, the supporting surface must be straight in the propagating direction of surface waves. Any curvature or taper in the direction of propagation of wave will always

introduce radiation and cause a departure from the pure-surface wave field [2,3]. These effects are also introduced by any sudden discontinuity or wall distortion [4,5] along the length of the supporting surface in the propagating direction.

For engineering applications, surface wave structures can be used as transmission lines [6] to provide means for transmitting information from point to point like trunk lines of hollow waveguides. They have advantages and potential applications in the millimeter and submillimeter wavelength regions and in optical communication systems [7-12], using fiber optics, in which the construction of a conventional hollow waveguide is difficult or impossible. Furthermore, they offer cost-effective solutions to many communication problems owing to their inherent features, which include wide bandwidth and low loss transmission. Because of the open-boundary characteristic of the surface wave structure, it has been applied as a means to provide a continuous access for vehicular communications [7], which permits continuous coupling to every vehicle and every station including the control center. For such applications, discontinuities in the supporting surface in the direction of propagation are undesirable because of the transmission loss they introduce due to radiation and reflection.

Another application of surface wave structures is surface wave aerials which make use of the radiation property at discontinuities. With the proper choice of type and location of the discontinuities, the radiation can also be controlled [13,14].

From these applications, it is clear that a better performance of the systems can be achieved if the behaviour of the surface wave at the discontinuities is fully understood. There are three main groups of

discontinuities which are the most common topics of interest, namely:

1. bends
2. variation of surface impedance of the guiding structure, which also includes a variation of material properties or surface deformations
3. the presence of obstacles.

Each of these discontinuities has been the topic of recent study by many investigators [2-5,16]. The main purpose of the present research is to find new techniques to solve for a solution of the second type discontinuity, and specifically the step discontinuity, in a slab waveguide for which it appears that all the previous studies do not lead to a satisfactory result.

Several techniques have been applied by various investigators to solve this type of problem. The surface wave structure under consideration can, in general, be represented by a surface impedance, dielectric slab or a dielectric rod. The rigorous solution, by comparison, is easier to obtain for the surface impedance than the dielectric slab while both are still easier than that of the dielectric rod which always involves a more complicated field, *i.e.*, hybrid modes. Before presenting new methods, the previous techniques will be summarized in order to justify the need for the proposed techniques.

Marcuvitz's modal synthesis [15] together with Schwinger's variational principle, were applied by Angulo [17] to solve for the diffraction of a surface wave by a semi-infinite dielectric slab, *i.e.*, slab of thickness $2d$ in the region of $-\infty \leq z \leq 0$ which terminates in free space at $z = 0$. In this technique, the field is expressed as the sum of discrete modes, satisfying the boundary condition, together with continuous modes, which are combined in pairs in such a way as to obtain

modes satisfying the boundary condition and the condition of orthogonality with respect to modes from a discrete spectrum. It was indicated by Shevchenko [18] at this point, that if the modes of the continuous spectrum satisfy the radiation condition in the radial direction from the waveguide before their transformation, then after the transformation they no longer satisfy this condition. Neither Marcuvitz nor Angulo seem to have paid attention to this point. Moreover, Angulo's problem cannot be reduced to the problem of an infinite dielectric slab with a discontinuity at $z = 0$ which is being considered in this thesis.

The Wiener-Hopf technique had been applied by Jones [19] for the problem of the diffraction of a surface wave by a semi-infinite grounded dielectric slab, which was transformed to an approximately equivalent problem suitable for this technique by using the approximate boundary conditions to replace the original exact boundary conditions, together with the Fourier transform technique. Again this problem cannot be reduced to the problem of an infinite dielectric slab as mentioned above. Kay [20] applied the Wiener-Hopf technique to obtain the exact solution for the problem of scattering at the junction of two surface reactances and Johansen [21] applied it to the problem of a surface wave scattering at the junction of two semi-infinite planes joined together by a step. As pointed out by Waldron [22], the concept of surface impedances is valid only under very restricted circumstances and it is very difficult or sometimes impossible to construct structures which have the prescribed value of impedance. Thus the solution by Kay is expected to give good results for a dielectric slab problem under certain specific conditions which are given later. However, Kay's technique will be applied to obtain the results which are compared with those obtained by the proposed techniques.

By representing the arbitrary deformations as a succession of infinitely many infinitesmal steps, Marcuse [23] was able to obtain the solution for the radiation loss of a slab waveguide due to an abrupt step or wall distortion. But as pointed out by Collin and Zucker [24], the results thus obtained cannot be very accurate, since the steps, if chosen small to represent the deformation, are so numerous that they lie in the near field of each other.

Applying the mode matching technique of the closed waveguide to the open waveguide, Clarricoats and Sharpe [25] were able to solve for the scattering at the junction of two planar waveguides under restricted conditions that make the radiation field at the junction negligible. The closed waveguide approach was also applied by Hu and Bergstein [26] to solve the problem of discontinuity in a slab waveguide. Using a similar technique to study the scattering of surface waves at a discontinuity in a planar waveguide, Mahmoud and Beal [27] converted the resulting integral equation into an infinite set of linear algebraic equations, which is then solved numerically by truncation. The acceptable solution for this finite truncated set of equations must satisfy an energy-balanced argument. This procedure for obtaining a solution is time-consuming and, as pointed out by Rulf [28], it is not necessary that the solution which satisfies the condition is indeed a good approximation of the solution.

The integral equation technique was applied by Hockham and Sharpe [29] to solve the same problem as that of Clarricoats and Sharpe. The accuracy of the result depends on a knowledge of the field (which is generally unknown) at the plane of discontinuity by approximating it as the sum of incident and reflected fields. Rulf [28] also formulated the problem in a form of an integral equation of a special type (*i.e.*, the

singular integral equation). But since it is difficult to obtain the general solution from this integral equation, Rulf only gave the solution for a simple case. Furthermore, the variational approach was applied by Rozzi [30], to solve for the step discontinuity in a planar dielectric waveguide.

As already mentioned, there are three main groups of discontinuities which are of particular interest, however this thesis is mainly confined to the problem of the second type discontinuity as they are the biggest class of the three groups. This type of discontinuity includes the termination of a waveguide into another waveguide which is different in both the material property, (*i.e.*, different dielectric constant) and geometry (*i.e.*, different thickness). It also includes the problem of arbitrary deformation of the guiding structure. It is therefore, the main purpose of this thesis to present two new techniques, the Wiener-Hopf and the residue-calculus, to solve for the problem of discontinuity, which involves the change in both the material property and thickness, on dielectric slab waveguide for single mode operation for both TE and TM incidence.

The general theoretical analysis of a dielectric slab waveguide is given in Chapter 2 which also includes the application of the reciprocity theorem, for the determination of the transmission coefficient at a discontinuity, and the derivation of the conditions under which Kay's analysis can be applied to the problem of a dielectric slab waveguide discontinuity.

The detailed theoretical analysis of the Wiener-Hopf technique which includes the derivation of the Wiener-Hopf equation for the dielectric slab waveguide is given in Chapter 3, together with the numerical

results. In Chapter 4, the detailed analysis of the residue-calculus is presented. Various numerical examples of the results are also included.

The general discussion of the techniques and the results are given in Chapter 5, followed by the conclusion and suggestions for future research.

CHAPTER 2

DIELECTRIC SLAB WAVEGUIDE

2.1 INTRODUCTION

A surface wave is defined as the wave that propagates along an interface between two different media without radiation [1]. The surface wave field is intimately bound to the surface of the supporting structure and decays exponentially away from the surface with the usual propagation function $e^{-j\beta z}$ (for $e^{j\omega t}$ time dependence) along the z-axis of the structure. It is found from this definition that there exists a class of open structures, such as a dielectric slab, dielectric-coated plane, corrugated plane, etc., shown schematically in figure 2.1 which are capable of supporting the surface wave.

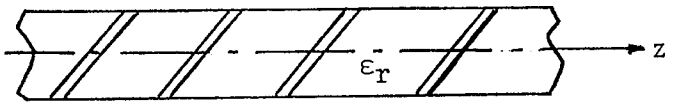

a) Dielectric slab

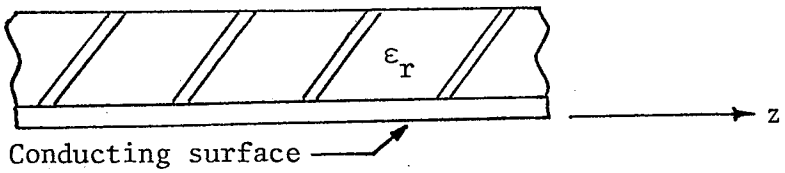

b) Dielectric-coated plane

c) Corrugated plane

Figure 2.1 Surface wave structures

The theoretical analysis for the surface wave supported by this class of structures can be found in texts which deal with waveguides or electromagnetic fields such as Collin [31], Barlow and Brown [32], Harrington [33], Marcuse [34,35], Kapany and Burke [36], Hessel [56], Tamir [57], Zucker [24], Arnaud [8] and Walter [37]. However, in this chapter, only the theoretical analysis of the surface wave supported by the dielectric slab waveguide is given. This is because the discontinuity problem which will be considered in later chapters is confined to this type of structure which in turn can give insight into the effects of discontinuities in more complicated structures. Also included in this chapter is the application of Kay's analysis [20] of the scattering of a surface wave by a discontinuity in a supporting reactance surface to the present problem of dielectric slab, and the application of the reciprocity theorem [16] for the determination of the transmission coefficient at the discontinuity. The results obtained from these two techniques are then used to check for the accuracy of the proposed novel techniques in later chapters.

2.2 GUIDED MODES OF SLAB WAVEGUIDES

The configuration of the slab waveguide is given in figure 2.2 The z-axis is the direction along which the wave is propagating, the transverse dimension y is assumed of infinite length such that there is no field variation along y (*i.e.*, $\frac{\partial}{\partial y} = 0$). Thus, the field of a slab waveguide can be decomposed into TE and TM modes.

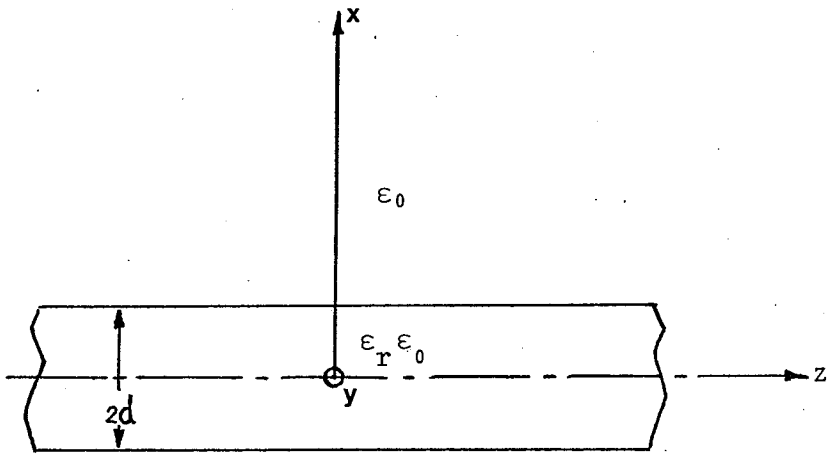

Figure 2.2 A planar dielectric slab waveguide

2.2.1 TE Modes

By the definition of a TE mode, $E_z = 0$. From Maxwell's equations under the above restriction (*i.e.*, $\frac{\partial}{\partial y} = 0$), the only nonvanishing field components are H_z, H_x and E_y. Furthermore, using Maxwell's equations the field components H_z and H_x can be expressed in terms of E_y as

$$H_x = \frac{-j}{\omega\mu} \frac{\partial E_y}{\partial z} \tag{2.2.1}$$

$$H_z = \frac{j}{\omega\mu} \frac{\partial E_y}{\partial x} \tag{2.2.2}$$

The E_y component is obtained from the solution of the reduced wave equation

$$\frac{\partial^2 E_y}{\partial x^2} + \frac{\partial^2 E_y}{\partial z^2} + \varepsilon_r k_0^2 E_y = 0 \qquad (2.2.3)$$

where ε_r is the dielectric constant of the medium through which the wave propagates and

$$k_0 = \omega \sqrt{\varepsilon_0 \mu_0} = \frac{2\pi}{\lambda_0} \qquad (2.2.4)$$

With the time dependence $e^{j\omega t}$ and z dependence $e^{-j\beta z}$, equation (2.2.3) is reduced to

$$\frac{\partial^2 E_y}{\partial x^2} + (\varepsilon_r k_0^2 - \beta^2) E_y = 0 \qquad (2.2.5)$$

The solution of this equation will be found separately for the region inside the slab and the surrounding medium. By applying the boundary condition which requires the continuity of the tangential field components at the interface of the two media, an eigenvalue equation for the propagation constant of the surface wave mode is obtained. In order to simplify the treatment, even and odd modes will be considered separately.

Even guided TE modes

The mode solution for even modes (E_y is an even function of x) inside the slabs, $|x| < d$ (omitting $e^{j(\omega t - \beta z)}$ term), is

$$E_y = A \cos Kx \qquad (2.2.6)$$

$$H_z = \frac{-jK}{\omega\mu_0} A \sin Kx \qquad (2.2.7)$$

$$H_x = \frac{-\beta}{\omega\mu_0} A \cos Kx \qquad (2.2.8)$$

where $$K^2 = \varepsilon_r k_0^2 - \beta^2 \qquad (2.2.9)$$

The field outside the slab, $|x| > d$ is

$$E_y = A \cos Kd \, e^{-\gamma(|x| - d)} \tag{2.2.10}$$

$$H_z = \frac{-x}{|x|} \frac{j\gamma}{\omega\mu_0} A \cos Kd \, e^{-\gamma(|x| - d)} \tag{2.2.11}$$

$$H_x = \frac{-\beta}{\omega\mu_0} A \cos Kd \, e^{-\gamma(|x| - d)} \tag{2.2.12}$$

where $$\gamma^2 = \beta^2 - k_0^2 \tag{2.2.13}$$

Both K^2 and γ^2 can be positive quantities since $\varepsilon_r > 1$. For positive value of γ^2, the field on the outside of the slab decays with increasing values of $|x|$. Thus, the condition for a guided surface wave mode is

$$\gamma^2 > 0 \tag{2.2.14}$$

Applying the boundary condition at $x = \pm d$ for E_y and H_z, the eigenvalue equation is thus obtained

$$\tan Kd = \frac{\gamma}{K} \tag{2.2.15}$$

Odd guided TE modes

The field inside the slab, $|x| < d$, for odd guided waves (E_y is an odd function of x) is given by

$$E_y = A \sin Kx \tag{2.2.16}$$

$$H_z = \frac{jK}{\omega\mu_0} A \cos Kx \tag{2.2.17}$$

$$H_x = \frac{-\beta}{\omega\mu_0} A \sin Kx \tag{2.2.18}$$

The field outside the slab, $|x| > d$, is given by

$$E_y = \frac{x}{|x|} A \sin Kd \, e^{-\gamma(|x| - d)} \tag{2.2.19}$$

$$H_z = \frac{-j\gamma}{\omega\mu_0} A \sin Kd \, e^{-\gamma(|x| - d)} \tag{2.2.20}$$

$$H_x = \frac{-\beta}{\omega\mu_0} A \sin Kd \, e^{-\gamma(|x| - d)} \qquad (2.2.21)$$

The constants K and γ are given by (2.2.9) and (2.2.13). By applying the boundary condition for E_y and H_z at $x = \pm d$, the eigenvalue equation is obtained

$$\tan Kd = -\frac{K}{\gamma} \qquad (2.2.22)$$

2.2.2. TM Modes

Similar to TE modes, the TM modes are obtained by setting $H_z = 0$, in which case the only non-vanishing field components are E_x, E_z and H_y. The two electric field components can be expressed in terms of the H_y component as

$$E_x = \frac{j}{\omega\varepsilon} \frac{\partial H_y}{\partial z} \qquad (2.2.23)$$

$$E_z = \frac{-j}{\omega\varepsilon} \frac{\partial H_y}{\partial x} \qquad (2.2.24)$$

The H_y component is obtained as a solution of the reduced wave equation

$$\frac{\partial^2 H_y}{\partial x^2} + (\varepsilon_r k_0^2 - \beta^2) H_y = 0 \qquad (2.2.25)$$

The solution for H_y is determined separately for the region inside the slab and the surrounding medium. The resulting field components must satisfy the boundary condition which requires the continuity of the tangential field components at the interface between the two media. This condition will lead to the eigenvalue equation of TM surface wave mode.

Even TM modes

The even TM modes (H_y is an even function of x) inside the slab $|x| < d$, have the following field solutions

$$H_y = B \cos Kx \tag{2.2.26}$$

$$E_z = \frac{jK}{\omega\varepsilon_r\varepsilon_0} B \sin Kx \tag{2.2.27}$$

$$E_x = \frac{\beta}{\omega\varepsilon_r\varepsilon_0} B \cos Kx \tag{2.2.28}$$

where K is the same constant given by (2.2.9).

The field components outside the slab $|x| > d$, are

$$H_y = B \cos Kd \, e^{-\gamma(|x| - d)} \tag{2.2.29}$$

$$E_z = \frac{x}{|x|} \frac{j\gamma}{\omega\varepsilon_0} B \cos Kd \, e^{-\gamma(|x| - d)} \tag{2.2.30}$$

$$E_x = \frac{\beta}{\omega\varepsilon_0} B \cos Kd \, e^{-\gamma(|x| - d)} \tag{2.2.31}$$

By applying the boundary condition at $x = \pm d$, the eigenvalue equation is obtained as

$$\tan Kd = \frac{\varepsilon_r\gamma}{K} \tag{2.2.32}$$

Odd TM modes

The field of the odd TM modes (H_y is an odd function of x) inside the slab is (2.2.33)

$$H_y = B \sin Kx$$

$$E_z = \frac{-jk}{\omega\varepsilon_r\varepsilon_0} B \cos Kx$$

$$E_x = \frac{\beta}{\omega\varepsilon_r\varepsilon_0} B \sin Kx \tag{2.2.35}$$

The field outside the slab is given by

$$H_y = \frac{x}{|x|} B \sin Kd \, e^{-\gamma(|x| - d)} \tag{2.2.36}$$

$$E_z = \frac{j\gamma}{\omega\varepsilon_0} B \sin Kd \, e^{-\gamma(|x| - d)} \tag{2.2.37}$$

$$E_x = \frac{\beta}{\omega\varepsilon_0} B \sin Kd \, e^{-\gamma(|x| - d)} \tag{2.2.38}$$

The eigenvalue equation is obtained, after applying the boundary condition at $x = \pm d$, as

$$\tan Kd = \frac{-K}{\varepsilon_r \gamma} \tag{2.2.39}$$

From these eigenvalue equations (2.2.15), (2.2.22), (2.2.32) and (2.2.39), the propagation constants for each surface wave mode can be determined.

Some interesting features about surface wave modes which should be mentioned are the non-existence of an infinite number of discrete modes of propagation and the concept of cut-off frequency. Because of the first property, the surface wave modes alone do not form a complete system which can represent any arbitrary field. The concept of cut-off frequency has a somewhat different interpretation from that of metal (closed boundary) guides. Above the cut-off frequency, the dielectric slab guide propagates unattenuated modes, *i.e.*, β is real. Below the cut-off frequency, there is attenuated propagation, *i.e.*, β is a complex quantity. The phase constant of an unattenuated mode lies between the intrinsic phase constant of the dielectric and that of air, that is,

$$k_0 < \beta < k_d \quad ; \quad (k_d = k_0 \sqrt{\varepsilon_r}) \tag{2.2.40}$$

For the TE case the power carried by the surface wave mode is given by

$$P = -\frac{1}{2} \int_{-\infty}^{\infty} E_y H_x^* \, dx$$

$$= \frac{\beta}{\omega \mu_0} \int_0^{\infty} |E_y|^2 \, dx \tag{2.2.41}$$

while for the TM case it is given by

$$P = \frac{\beta}{\omega} \int_0^{\infty} \frac{1}{\varepsilon} |H_y|^2 \, dx$$

$$= \frac{\beta}{\omega\varepsilon_0\varepsilon_r} \int_0^d |H_y|^2 \, dx + \frac{\beta}{\omega\varepsilon_0} \int_d^\infty |H_y|^2 \, dx \qquad (2.2.42)$$

2.3 RADIATION MODES OF THE SLAB WAVEGUIDE

Since the discrete surface wave modes do not form a complete system, the radiation phenomena which occur at the discontinuities along the guide cannot be described by these modes alone. To account for the radiation, a system of "quasisurface wave modes" with a continuous spectrum is added to a system of discrete surface wave modes which together form a complete system [18, 34]. These quasisurface (radiation) modes also satisfy Maxwell's equations but instead of satisfying the stringent condition of surface wave modes that the field must vanish at infinity, they satisfy a weaker condition that the field only be finite at infinity [18, 34].

2.3.1. Even TE Radiation Modes

The field inside the slab $|x| < d$, is given by

$$E_y = C \cos \sigma x \qquad (2.3.1)$$

$$H_z = \frac{-j\sigma}{\omega\mu_0} C \sin \sigma x \qquad (2.3.2)$$

$$H_x = \frac{-\beta}{\omega\mu_0} C \cos \sigma x \qquad (2.3.3)$$

where $$\sigma^2 = \varepsilon_r k_0^2 - \beta^2 \qquad (2.3.4)$$

while the field outside slab $|x| > d$ is given by

$$E_y = D\, e^{-j\rho|x|} + F\, e^{j\rho|x|} \qquad (2.3.5)$$

$$H_z = \frac{x}{|x|} \frac{\rho}{\omega\mu_0} \left(D\, e^{-j\rho|x|} - F\, e^{j\rho|x|}\right) \qquad (2.3.6)$$

$$H_x = \frac{-\beta}{\omega\mu_0} \left(D\, e^{-j\rho|x|} + F\, e^{j\rho|x|}\right) \qquad (2.3.7)$$

where $\rho^2 = k_0^2 - \beta^2$ (2.3.8)

Applying the boundary conditions requiring continuity of E_y and H_z at $x = \pm d$ lead to (only $x = d$ is considered since the conditions at $x = -d$ are identical)

$$D = \frac{C}{2} e^{j\rho d} (\cos \sigma d - j \frac{\sigma}{\rho} \sin \sigma d) \quad (2.3.9)$$

$$F = D^* \quad (2.3.10)$$

where the star superscript denotes the complex conjugate.

2.3.2 Odd TE Radiation Modes

The field inside the slab $|x| < d$ is given by

$$E_y = C_0 \sin \sigma x \quad (2.3.11)$$

$$H_z = \frac{j\sigma}{\omega\mu_0} C_0 \cos \sigma x \quad (2.3.12)$$

$$H_x = \frac{-\beta}{\omega\mu_0} C_0 \sin \sigma x \quad (2.3.13)$$

while outside the slab it is given by

$$E_y = \frac{x}{|x|} (D_0 e^{-j\rho|x|} + F_0 e^{j\rho|x|}) \quad (2.3.14)$$

$$H_z = \frac{\rho}{\omega\mu_0} (D_0 e^{-j\rho|x|} - F_0 e^{j\rho|x|}) \quad (2.3.15)$$

$$H_x = \frac{-\beta}{\omega\mu_0} \frac{x}{|x|} (D_0 e^{-j\rho|x|} + F_0 e^{j\rho|x|}) \quad (2.3.16)$$

After applying the boundary conditions at $x = d$, the relation between the constants C_0, D_0 and F_0 is given by

$$D_0 = \frac{C_0}{2} e^{j\rho d} (\sin \sigma d + j \frac{\sigma}{\rho} \cos \sigma d) \quad (2.3.17)$$

$$F_0 = D_0^* \quad (2.3.18)$$

2.3.3. Even TM Radiation Modes

The field inside the slab $|x| < d$ is

$$H_y = L \cos \sigma x \tag{2.3.19}$$

$$E_z = \frac{j\sigma}{\omega \varepsilon_r \varepsilon_0} L \sin \sigma x \tag{2.3.20}$$

$$E_x = \frac{\beta}{\omega \varepsilon_r \varepsilon_0} L \cos \sigma x \tag{2.3.21}$$

while the field outside the slab $|x| > d$ is

$$H_y = M e^{-j\rho|x|} + N e^{j\rho|x|} \tag{2.3.22}$$

$$E_z = - \frac{x}{|x|} \frac{\rho}{\omega \varepsilon_0} (M e^{-j\rho|x|} - N e^{j\rho|x|}) \tag{2.3.23}$$

The relation between the constants L, M and N is given by

$$M = \frac{L}{2} e^{j\rho d} (\cos \sigma d - j \frac{\sigma}{\varepsilon_r \rho} \sin \sigma d) \tag{2.3.24}$$

$$N = M^* \tag{2.3.25}$$

2.3.4. Odd TM Radiation Modes

The field inside the slab $|x| < d$ is

$$H_y = L_0 \sin \sigma x \tag{2.3.26}$$

$$E_z = \frac{-j\sigma}{\omega \varepsilon_r \varepsilon_0} L_0 \cos \sigma x \tag{2.3.27}$$

$$E_x = \frac{\beta}{\omega \varepsilon_r \varepsilon_0} L_0 \sin \sigma x \tag{2.3.28}$$

while outside the slab the field is given by

$$H_y = \frac{x}{|x|} (M_0 e^{-j\rho|x|} + N_0 e^{j\rho|x|}) \tag{2.3.29}$$

$$E_z = \frac{-\rho}{\omega \varepsilon_0} (M_0 e^{-j\rho|x|} - N_0 e^{j\rho|x|}) \tag{2.3.30}$$

$$E_x = \frac{\beta}{\omega\varepsilon_0} \frac{x}{|x|} \left(M_0 e^{-j\rho|x|} + N_0 e^{j\rho|x|}\right) \qquad (2.3.31)$$

The relation between constants L_o, M_o and N_o is given by

$$M_0 = \frac{L_0}{2} e^{j\rho d} \left(\sin \sigma d + j \frac{\sigma}{\varepsilon_r \rho} \cos \sigma d\right) \qquad (2.3.32)$$

$$N_0 = M_0^* \qquad (2.3.33)$$

2.4 DISCONTINUITY ON THE SLAB WAVEGUIDE

The configuration of the discontinuity on the slab waveguide under consideration is shown in figure 2.3 which shows an abrupt termination of one dielectric waveguide into another guide with different value of dielectric constant. The thickness of the two guides can either be the same or different with $d_1 > d_2$ or $d_1 < d_2$.

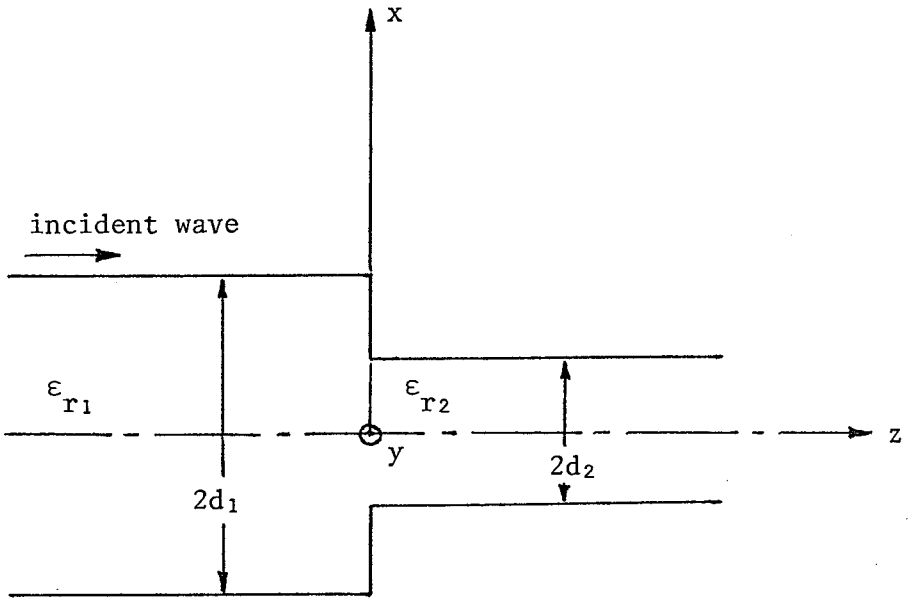

Figure 2.3 Step discontinuity on a planar dielectric slab waveguide

2.4.1 Transmission Coefficient by Lorentz Reciprocity Theorem

By applying the Lorentz reciprocity theorem, it was shown by Barlow and Brown [16] that

$$T = \frac{1}{16 P_1 P_2} \left| \int_S [\bar{E}_1 \times \bar{H}_2 - \bar{E}_2 \times \bar{H}_1] \cdot \hat{n} \, ds \right|^2 \qquad (2.4.1)$$

where T is the transmission coefficient defined as the ratio of transmitted to incident power, S denotes the cross-sectional plane at $z = 0$, P_1 and P_2 are the incident surface wave power traveling on the left and right hand sides of the surface S, respectively. $\bar{E}_1$, $\bar{H}_1$ and $\bar{E}_2$, $\bar{H}_2$ are the fields created over S when the surface wave is incident from the left and right hand sides of S, respectively.

Though equation (2.4.1) has been developed for the problem of discontinuity of surface wave supported by an impedance surface, it can also be applied to the problem of the slab waveguide with the same solutions for all parameters. Equation (2.4.1) will give the exact solution provided that all the fields $\bar{E}_1$, $\bar{H}_1$, $\bar{E}_2$ and $\bar{H}_2$ are known exactly. In our problem the fields are approximated by incident surface wave fields. For TE case we have, for $d_1 > d_2$,

$$T = \frac{(\beta_2 + \beta_1)^2 F_0^2 N_0^2}{4 \beta_1 \beta_2 \{(\varepsilon_{r_2} - \varepsilon_{r_1}) k_0^2 - \beta_2^2 + \beta_1^2\}^2 \{(\varepsilon_{r_1} - 1) k_0^2 + \beta_2^2 - \beta_1^2\}^2 (\beta_2^2 - \beta_1^2)^2} \qquad (2.4.2)$$

while for $d_2 \geq d_1$

$$T = \frac{(\beta_2 + \beta_1)^2 F_0^2 M_0^2}{4 \beta_1 \beta_2 \{(\varepsilon_{r_2} - \varepsilon_{r_1}) k_0^2 - \beta_2^2 + \beta_1^2\}^2 \{(\varepsilon_{r_2} - 1) k_0^2 - \beta_2^2 + \beta_1^2\}^2 (\beta_2^2 - \beta_1^2)^2} \qquad (2.4.3)$$

where F_0, N_0 and M_0 are given in Appendix D.

For TM case we have for $d_1 \geq d_2$,

$$T = \frac{1}{4\ \beta_1\beta_2} \left| R_o \left[\frac{v_1(\beta_1/\varepsilon_{r_1} + \beta_2/\varepsilon_{r_2}) + v_2(\beta_1/\varepsilon_{r_1} + \beta_2) + v_3(\beta_1 + \beta_2)}{(k_2^2 - k_1^2)\ (\gamma_2^2 + k_1^2)\ (\gamma_2^2 - \gamma_1^2)} \right] \right|^2 \tag{2.4.4}$$

where

$$v_1 = (k_2 \sin k_2d_2 \cos k_1d_2 - k_1 \cos k_2d_2 \sin k_1d_2)\ (\gamma_2^2 - \gamma_1^2)\ (\gamma_2^2 + k_1^2) \tag{2.4.5}$$

$$v_2 = (\gamma_2^2 - \gamma_1^2)\ (k_2^2 - k_1^2) \cos k_2d_2\ \{(k_1 \sin k_1d_1 - \gamma_2 \cos k_1d_1)e^{-\gamma_2(d_1 - d_2)} + (\gamma_2 \cos k_1d_2 - k_1 \sin k_1d_2)\} \tag{2.4.6}$$

$$v_3 = (k_2^2 - k_1^2)\ (\gamma_2^2 + k_1^2)\ (\gamma_2 - \gamma_1) \cos k_1d_1 \cos k_2d_2\ e^{-\gamma_2(d_1 - d_2)} \tag{2.4.7}$$

while for $d_2 \geq d_1$,

$$T = \frac{1}{4\ \beta_1\beta_2} \left| R_0 \left[\frac{v_1'(\beta_2/\varepsilon_{r_2} + \beta_1/\varepsilon_{r_1}) + v_2'(\beta_2/\varepsilon_{r_2} + \beta_1) + v_3'(\beta_2 + \beta_1)}{(k_2^2 - k_1^2)(\gamma_1^2 + k_2^2)(\gamma_2^2 - \gamma_1^2)} \right] \right|^2 \tag{2.4.8}$$

where

$$v_1' = (\gamma_2^2 - \gamma_1^2)\ (\gamma_1^2 + k_2^2)\ (k_2 \sin k_2d_1 \cos k_1d_1 - k_1 \cos k_2d_1 \sin k_1d_1) \tag{2.4.9}$$

$$v_2' = (\gamma_2^2 - \gamma_1^2)\ (k_2^2 - k_1^2) \cos k_1d_1\{(k_2 \sin k_2d_2 - \gamma_1 \cos k_2d_2)e^{-\gamma_1(d_2 - d_1)} - (k_2 \sin k_2d_1 - \gamma_1 \cos k_2d_1)\} \tag{2.4.10}$$

$$v_3' = (k_2^2 - k_1^2)\ (\gamma_1^2 + k_2^2)\ (\gamma_2 - \gamma_1) \cos k_1d_1 \cos k_2d_2\ e^{-\gamma_1(d_2 - d_1)} \tag{2.4.11}$$

2.4.2 Application of Kay's Analysis

Kay [20] analyzed the problem of scattering at the junction of two surface reactances for TM incidence and obtained the exact solution by the Wiener-Hopf technique. As it is known that under a restricted condition the problem of the slab waveguide can also be reduced to the reactance surface problem, yet no one has applied Kay's result to this problem. Though Kay's result gives a very accurate solution under a restricted condition, it can give some insights into the problem. In this section, it will be shown how this can be done. It is interesting to note that though Kay analyzed the TM case, with certain modifications his result can still be applied for TE incidence. Also, by comparison with the residue-calculus technique of Chapter 4, though the condition, given later, is violated, Kay's formula still provides an acceptable approximation.

Representation of a dielectric slab by surface impedance

The surface impedance is defined as the ratio of the tangential component of the electric field to the tangential component of the magnetic field in the direction perpendicular to the chosen electric field [22]. This ratio is evaluated at the surface which forms the boundary of the guiding structure. Before going directly into the dielectric slab problem, a conducting plane coated with a thin layer of dielectric will be first considered, following Collin [31].

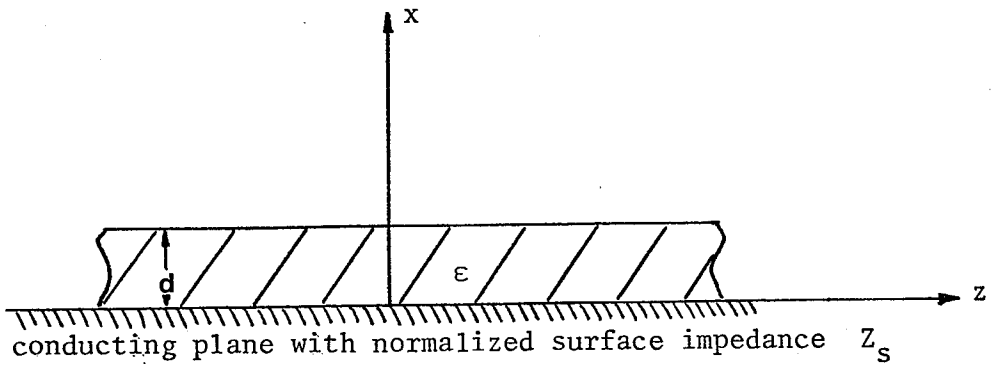

Figure 2.4 A dielectric coated conducting plane

The TM excitation is first considered. In a free space region, the magnetic field H_y can be written as

$$H_y = A \exp(jh_1 x - j\beta z) \qquad x > d \tag{2.4.12}$$

where $h_1^2 + \beta^2 = k_0^2$. In the dielectric, the field consists of two waves propagating in the positive and negative x direction, and hence has the form,

$$H_y = [B \exp(jh_2 x) + C \exp(-jh_2 x)]\, e^{-j\beta z} \qquad 0 \leq x \leq d \tag{2.4.13}$$

where $h_2^2 + \beta^2 = \varepsilon_r k_0^2$. The wave numbers h_1 and h_2 and the propagation constant β may be found by equating the surface impedance looking into dielectric at the dielectric-free space interface. Because the mathematical relation between E_z and H_y is similar to that of voltage and current in the transmission line equations, the following equivalent transmission line circuit is applicable.

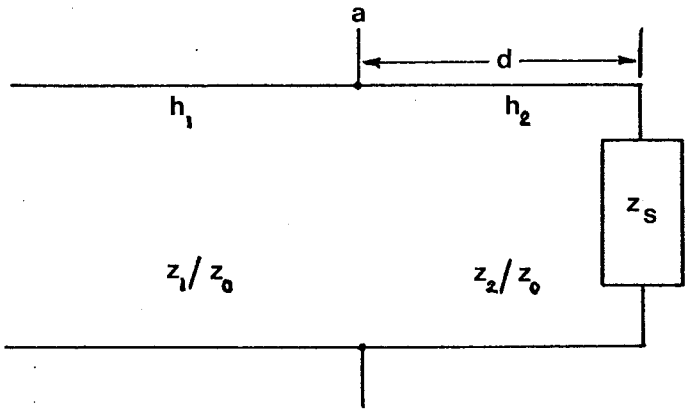

Figure 2.5 Equivalent transmission line circuit for a dielectric coated conducting plane

From the equation for the input impedance in a transmission line we have

$$\frac{z_1}{z_0} = z_{in} = \frac{z_2}{z_0}\left[\frac{z_s + j(z_2/z_0)\tan h_2 d}{(z_2/z_0) + jz_s \tan h_2 d}\right] \tag{2.4.14}$$

where $z_0 = \sqrt{\mu_0/\varepsilon_0}$ (2.4.15)

$$z_1 = \frac{z_0 h_1}{k_0} \tag{2.4.16}$$

$$z_2 = \frac{z_0 h_2}{\varepsilon_r k_0} \tag{2.4.17}$$

For TE excitation, by following the same procedure we have

$$\frac{z_1}{z_0} = z_{in} = \frac{z_2}{z_0}\left[\frac{z_s + j(z_2/z_0)\tan h_2 d}{(z_2/z_0) + jz_s \tan h_2 d}\right] \tag{2.4.18}$$

where $z_1 = \omega\mu_0/h_1$ (2.4.19)

$z_2 = \omega\mu_0/h_2$ (2.4.20)

Now consider the slab waveguide excited in TM mode (our problem is only concerned with the symmetrical (even) mode).

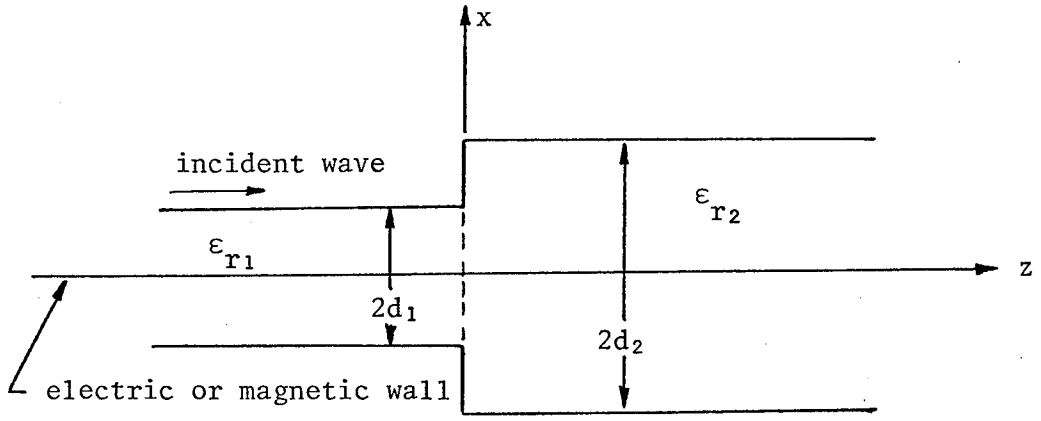

Figure 2.6 Surface wave incidence at a discontinuity junction on a planar dielectric slab waveguide

With the symmetrical mode, we have H_y varying symmetrically about the plane $x = 0$, thus

$$E_z \propto \frac{\partial H_y}{\partial x} = 0 \qquad \text{on} \qquad x = 0$$

This implies that an electric wall (E tangential = 0) may be placed along $x = 0$, hence the dielectric slab above and below $x = 0$ is reduced to the conducting plane coated with a dielectric layer mentioned above. Its surface impedance can then be obtained from (2.4.14) with $z_s = 0$. Under the condition that $h_2 d << 1$, it can be written as

$$z_{in} = \frac{h_1}{k_0} \simeq j \frac{(\varepsilon_r - 1)}{\varepsilon_r} k_0 d \qquad (2.4.21)$$

And for even TE mode, by using (2.4.18) with $z_s = \infty$, it can be reduced to

$$z_{in} = \frac{\omega \mu_0}{z_0 h_1} \simeq \frac{-j}{(\varepsilon_r - 1) k_0 d} \qquad (2.4.22)$$

It should be noted that without the approximation above (2.4.14) and (2.4.18) are equivalent to eigenvalue equations of surface wave modes for TM and TE modes, respectively.

Following Kay's analysis, it is required that the surface reactance be independent of wave number h_2, from (2.4.21) and (2.4.22) the slab waveguide will satisfy this requirement if $h_2 d << 1$.

From Barlow and Brown [16], the reflected power, P_{rf} is given by

$$P_{rf} = \frac{\gamma_1^2 (\gamma_1 - \gamma_2)^2}{\beta_1^2 (\beta_1 + \beta_2)^2} \qquad (2.4.23)$$

while the transmitted power, P_t, is

$$P_t = \frac{4 \gamma_1 \gamma_2}{(\gamma_1 + \gamma_2)^2} \qquad (2.4.24)$$

The radiated power is then obtained as

$$P_r = 1 - P_{rf} - P_t \qquad (2.4.25)$$

2.5 NUMERICAL RESULTS

The transmitted powers caused by symmetrical steps with $\varepsilon_{r_1} = 2.56$, $\varepsilon_{r_2} = 5.12$ for different ratios of d_2/d_1 are shown in figures 2.7 and 2.8 against kd_1 for TE and TM incidence, respectively. The open circle notation represents the results obtained by applying the reciprocity theorem using equations (2.4.2) if $d_1 > d_2$, (2.4.3) if $d_1 < d_2$ for TE incidence and equations (2.4.4) if $d_1 > d_2$, (2.4.8) if $d_1 < d_2$ for TM incidence. The solid circles represent the results obtained by applying Kay's technique equation (2.4.24) for both TE and TM incidence. The radiation losses of the same cases are plotted against Kd_1 in figures 2.9 and 2.10 for TE and TM incidence, respectively, using equations (2.4.23), (2.4.24) and (2.4.25). Because it is not possible to obtain the radiated power from the reciprocity theorem since the reflected power is unknown, only the results from Kay's technique are shown in figures 2.9 and 2.10.

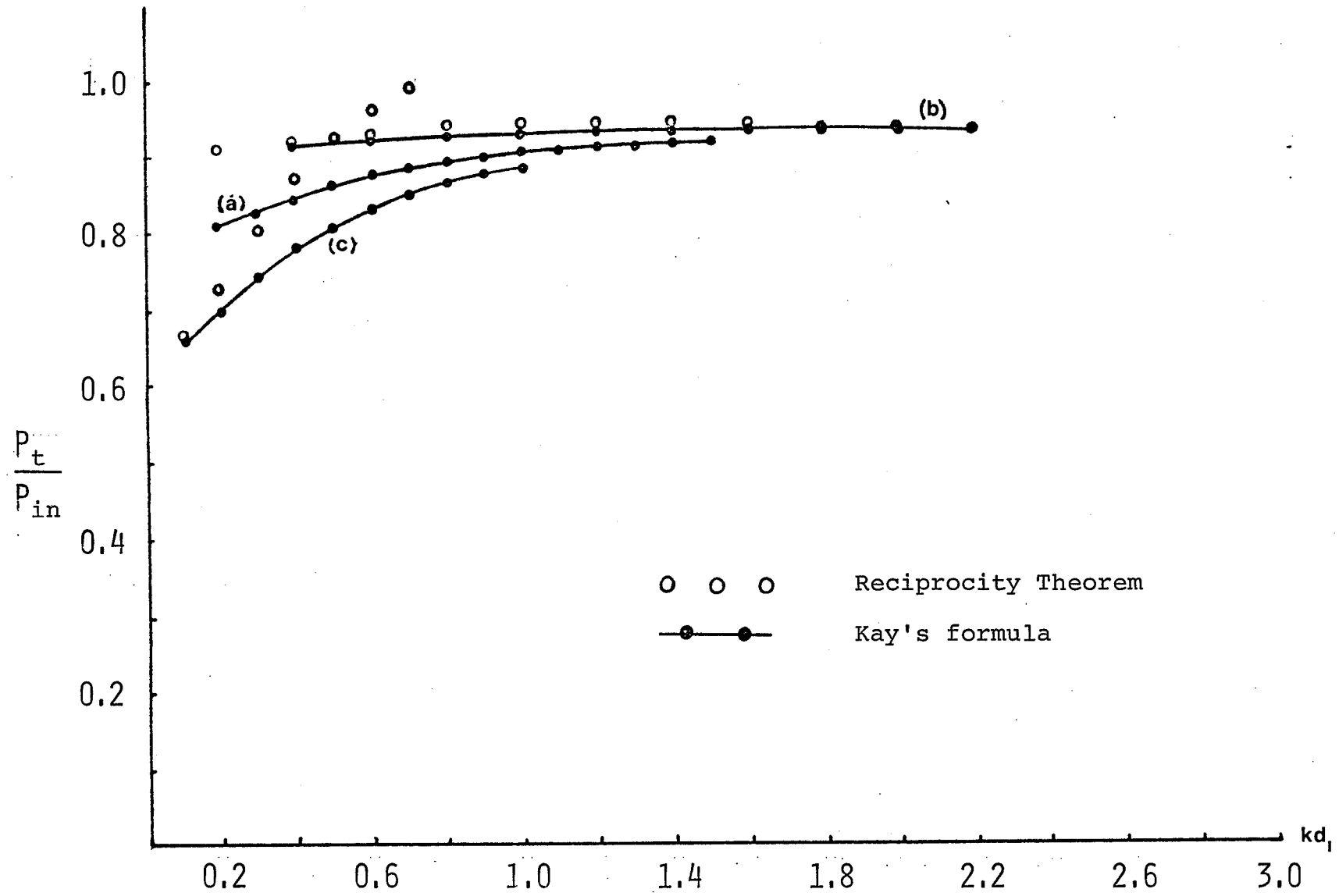

Figure 2.7 Transmitted power for TE incidence with $\varepsilon_{r_1} = 2.56$ and $\varepsilon_{r_2} = 5.12$

(a) $d_2/d_1 = 1.0$ (b) $d_2/d_1 = 0.7$ (c) $d_2/d_1 = 1.5$

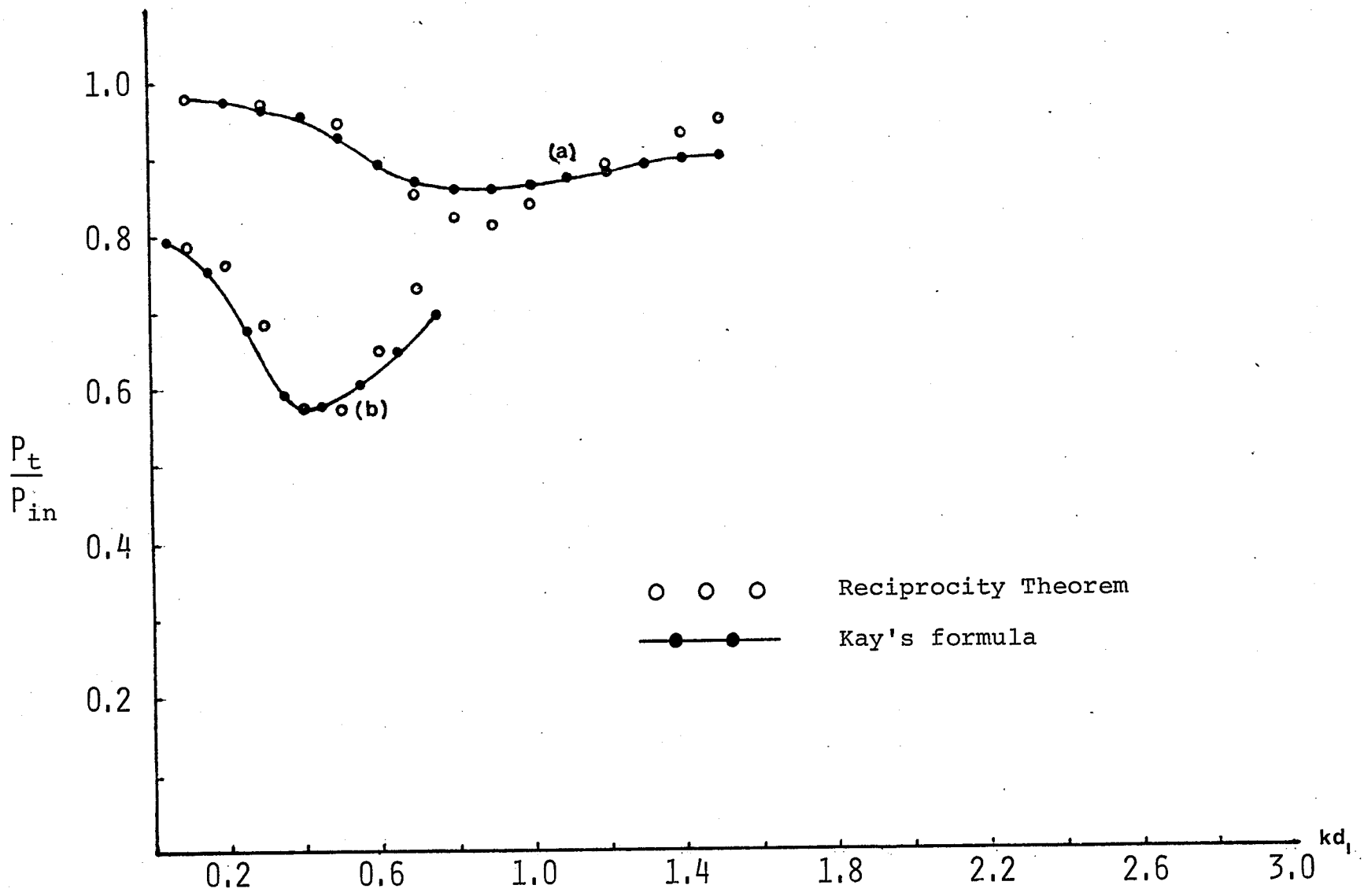

Figure 2.8 Transmitted power for TM incidence with $\varepsilon_{r_1} = 2.56$ and $\varepsilon_{r_2} = 5.12$

(a) $d_2/d_1 = 1.0$ (b) $d_2/d_1 = 2.0$

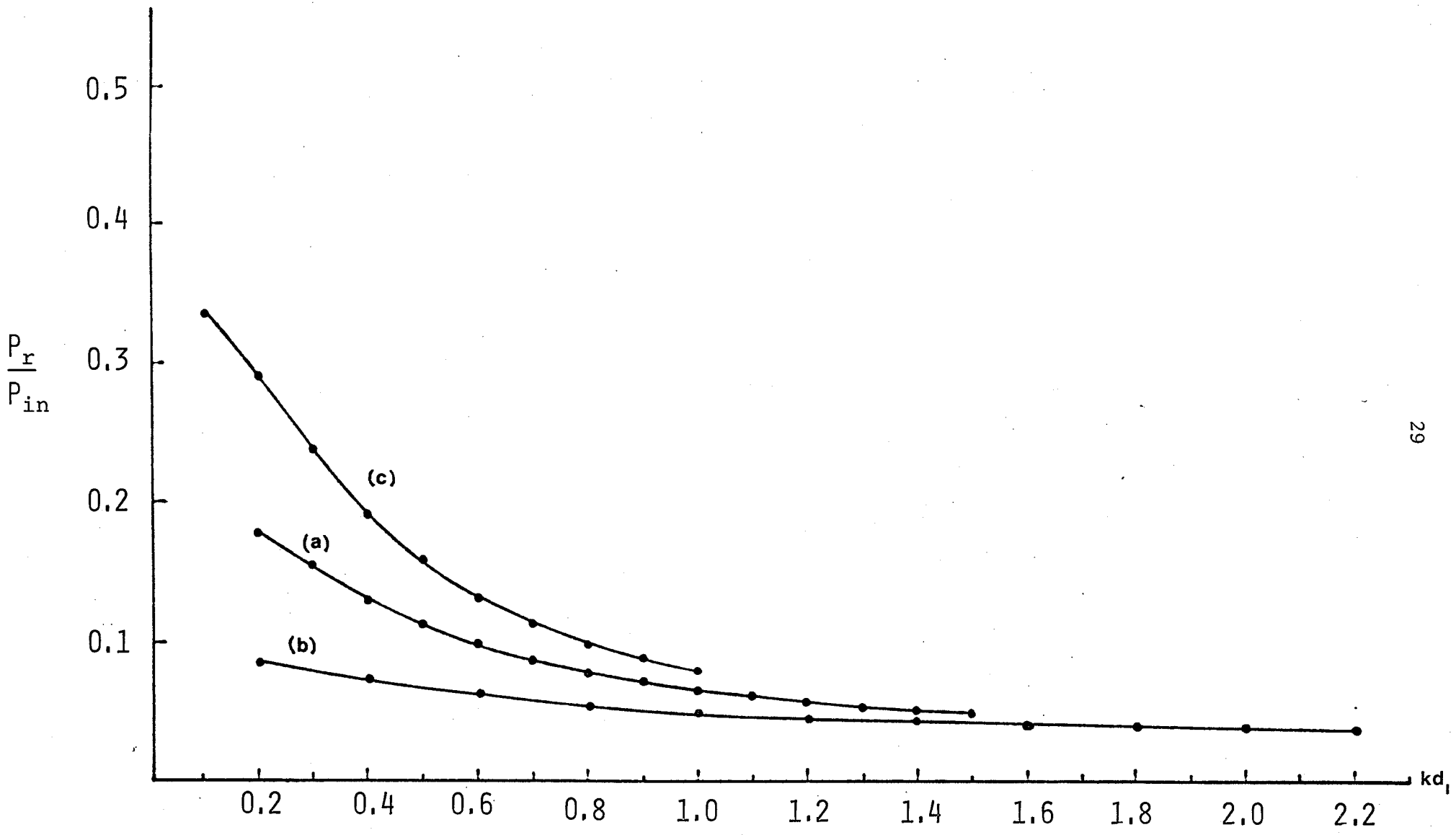

Figure 2.9 Radiation loss for TE incidence with the same parameters as for Fig. 2.7

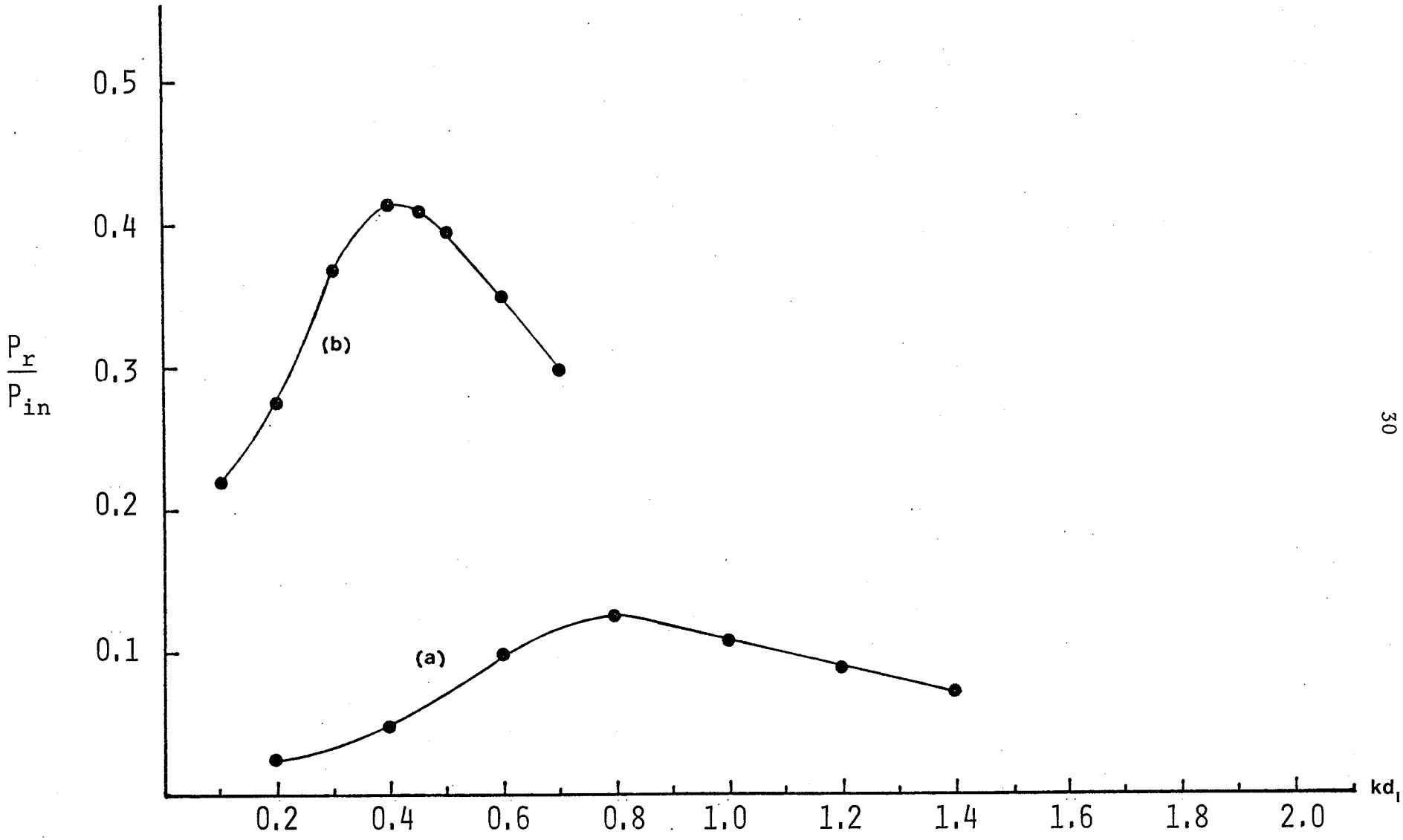

Figure 2.10 Radiation loss for TM incidence with the same parameters as for Fig. 2.8

CHAPTER 3

APPLICATION OF THE WIENER-HOPF TECHNIQUE

3.1 INTRODUCTION

Waveguide discontinuities such as bends, obstacles, etc., or changes in the material properties of the guide will always disturb the guidance of surface waves over the guiding structure. At these discontinuities the incident surface wave modes are coupled with other surface wave modes, thus leading to reflected, transmitted and radiation waves. These effects are important in the applications of dielectric waveguides in optical fiber communications where the reflection, transmission and radiation at the discontinuities are important in designing and estimating the performance of the system, and also in the design of surface wave antennas, whereby the discontinuities are introduced on the structure to yield the desired radiation.

The discontinuity considered in this chapter is confined to the junction of plane dielectric waveguides of the same thickness but different values of dielectric constants. The general approach to this type of problem is to expand the fields on both sides of the junction in terms of discrete surface wave modes together with a continuous mode spectrum or pseudomodes as called by Shevchenko [18]. The fields are then matched at the junction of the discontinuity and with the aid of the orthogonality property of the fields and certain approximations, the required mode amplitudes are found. The Wiener-Hopf technique was applied by Kay to study the scattering at the junction of two surface reactances [20]. Because of the configuration of his problem, he was able to obtain the

exact solution. The geometry considered here is different from that of Kay because it also involves the thickness of the slab, but it is still in that class of the problems which can be solved by the Wiener-Hopf technique [38],[39],[44],[45]. To obtain the Wiener-Hopf equation, the Fourier transform together with the boundary and edge conditions are applied. The key step in deriving the Wiener-Hopf equation is the factorization and decomposition which cannot be found in closed form for our case, and the techniques as given by Noble [38], Mittra and Lee [39] are therefore applied. The final solution contains unknown constants which can be determined from infinite-dimensional simultaneous linear equations. This implies that the exact solution for this type of problem cannot be found by this method.

3.2 FORMULATION OF THE PROBLEM

The configuration of the dielectric slab waveguide under consideration is shown in figure 3.1. It is assumed that the y-dimension is extended to infinity and all the field components are independent of the y-coordinate, *i.e.*, $\frac{\partial}{\partial y} = 0$. By using the subscripts 1 and 2 to denote the left and right sides of the junction, the dielectric constants for the left and right sides are shown as ε_{r_1} and ε_{r_2}, respectively. The slab thickness is denoted by $2d$ while the time dependence is $e^{j\omega t}$ which is suppressed throughout. The incident field at the junction will be either a TE or TM surface wave mode. The formulation for each case will be given separately and will be restricted to a single mode operation.

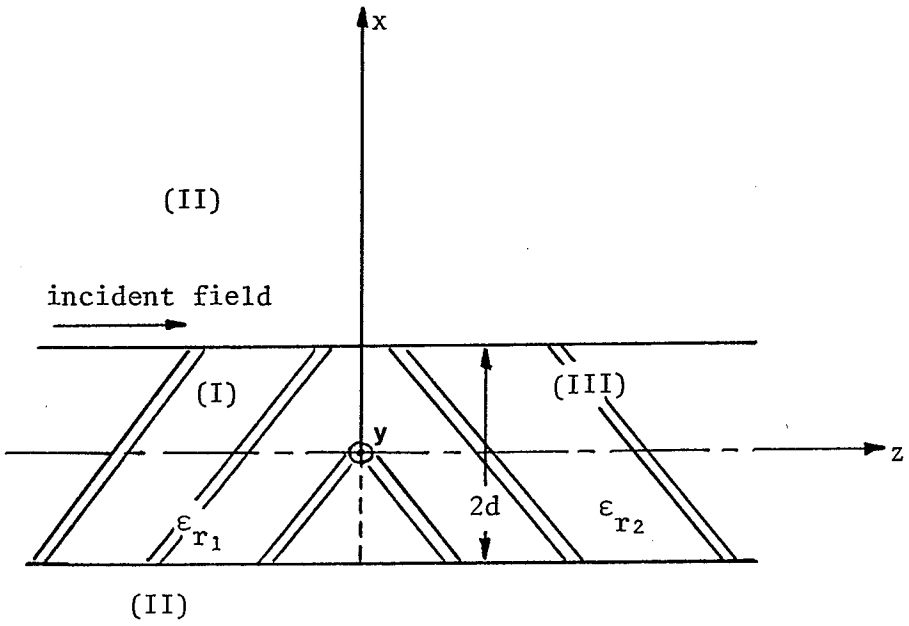

Figure 3.1 Schematic diagram of a dielectric slab waveguide

The geometry is subdivided into three regions as shown in figure 3.1. Consideration will be confined to even mode excitation, *i.e.*, E_y (TE) and H_y (TM) components are symmetrical with respect to z-coordinate. For the purpose of formulation, the free space wave number k_0 in region II is considered a complex quantity with very small but finite imaginary part denoted by k_0'', *i.e.*,

$$k_0 = k_0' - j\, k_0'' \quad ; \quad (k_0' > 0 \quad , \quad k_0'' > 0) \tag{3.2.1}$$

By letting k_0'' tend to zero, the final solution will be reduced to the solution of the original problem. The solution of the unknown field components is obtained by solving the two dimensional scalar wave equation,

$$\frac{\partial^2 \phi}{\partial x^2} + \frac{\partial^2 \phi}{\partial z^2} + k^2 \phi = 0 \tag{3.2.2}$$

where for TE incidence we have

$$E_y = \phi \tag{3.2.3a}$$

$$H_x = \left(\frac{-j}{\omega\mu_0}\right) \frac{\partial \phi}{\partial z} \tag{3.2.3b}$$

$$H_z = \left(\frac{j}{\omega\mu_0}\right) \frac{\partial \phi}{\partial x} \tag{3.2.3c}$$

while for TM incidence we have

$$H_y = \phi \tag{3.2.4a}$$

$$E_x = \left(\frac{j}{\omega\varepsilon}\right) \frac{\partial \phi}{\partial z} \tag{3.2.4b}$$

$$E_z = \left(\frac{-j}{\omega\varepsilon}\right) \frac{\partial \phi}{\partial x} \tag{3.2.4c}$$

The solution is to be obtained subject to the following boundary conditions:

(I) the tangential field components must be continuous at the $z = 0$ plane and at the $x = \pm d$ plane.

(II) as $|z| \to \infty$, asymptotic value of ϕ is the propagating surface wave mode.

(III) the field is assumed to have algebraic behaviour at the edge.

The last condition follows from the analysis of Collin [40] for an array of thin dielectric sheets. This is because the exact field behaviour for the general dynamic case remains unsolved [41]. If we use the static case to determine the field behaviour at the dielectric edge, following Anderson and Solodukhov [41], the field will have algebraic behaviour.

The formulation will be separately derived for TE and TM incidence. The TE mode incidence is considered first.

3.2.1 TE Mode Incidence

In this case, the incident field is E_y which is incident upon the junction of figure 3.1 from the left. The field in the three regions, as shown in figure 3.1, are then given by

Region I; $-d \leq x \leq d \quad , \quad z \leq 0$

The total field ϕ_t^I is given by

$$\phi_t^I = \phi^I + \phi_i^I \tag{3.2.5}$$

where the incident field ϕ_i^I (or E_y^i) is given by

$$\phi_i^I (x,z) = A_i \cos (k_1^2 - \beta_1^2)^{1/2} x \, e^{-j\beta_1 z} \tag{3.2.6}$$

Hence, it can be shown that $\phi^I(x,z)$ is the solution of

$$\frac{\partial^2 \phi^I}{\partial x^2} + \frac{\partial^2 \phi^I}{\partial z^2} + k_1^2 \phi^I = 0 \tag{3.2.7}$$

Region II; $|x| \geq d \quad , \quad -\infty < z < \infty$

The total field $\phi_t^{II}(x,z)$ is

$$\phi_t^{II}(x,z) = \phi^{II}(x,z) + \phi_i^{II}(x,z) \tag{3.2.8}$$

where the incident field $\phi_i^{II}(x,z)$ is given by

$$\phi_i^{II}(x,z) = A_i \, e^{(\beta_1^2 - k_0^2)^{1/2} d} \cos(k_1^2 - \beta_1^2)^{1/2} d \, e^{-(\beta_1^2 - k_0^2)^{1/2} |x|} e^{-j\beta_1 z} \tag{3.2.9}$$

Hence, it can be shown that $\phi^{II}(x,z)$ is the solution of

$$\frac{\partial^2 \phi^{II}}{\partial x^2} + \frac{\partial^2 \phi^{II}}{\partial z^2} + k_0^2 \phi^{II} = 0 \tag{3.2.10}$$

Region III; $-d \leq x \leq d \quad , \quad z \geq 0$

The total field $\phi_t^{III}(x,z)$ is

$$\phi_t^{III}(x,z) = \phi^{III}(x,z) \tag{3.2.11}$$

where $\phi^{III}(x,z)$ satisfies the two dimensional wave equation

$$\frac{\partial^2\phi^{III}}{\partial x^2} + \frac{\partial^2\phi^{III}}{\partial z^2} + k_2^2\,\phi^{III} = 0 \qquad (3.2.12)$$

In the equations (3.2.5) to (3.2.12), we define

A_i = amplitude of the incident wave

$k_1 = \sqrt{\varepsilon_{r_1}} \cdot k_0$

$k_2 = \sqrt{\varepsilon_{r_2}} \cdot k_0$

β_1 = propagation constant of the surface mode along the z-coordinate satisfying the eigenvalue equation for the slab waveguide on the left side of the junction, *i.e.*,

$$\tan(k_1^2 - \beta_1^2)^{1/2} d = \frac{(\beta_1^2 - k_0^2)^{1/2}}{(k_1^2 - \beta_1^2)^{1/2}} \qquad (3.2.13)$$

Define $\alpha = \sigma + j\tau$ (3.2.14)

Fourier transforming (3.2.7), (3.2.10) and (3.2.12) yields

$$\frac{d^2}{dx^2}\,\Phi_-^I(\alpha,x) - (\alpha^2 - k_1^2)\,\Phi_-^I(\alpha,x) = -\frac{1}{\sqrt{2\pi}}\left[\left(\frac{\partial\phi^I}{\partial z}\right)_{z=0} - j\alpha(\phi^I)_{z=0}\right] \qquad (3.2.15)$$

$$\frac{d^2}{dx^2}\,\Phi^{II}(\alpha,x) - (\alpha^2 - k_0^2)\,\Phi^{II}(\alpha,x) = 0 \qquad (3.2.16)$$

$$\frac{d^2}{dx^2}\,\Phi_+^{III}(\alpha,x) - (\alpha^2 - k_2^2)\,\Phi_+^{III}(\alpha,x) = \frac{1}{\sqrt{2\pi}}\left[\left(\frac{\partial\phi^{III}}{\partial z}\right)_{z=0} - j\alpha(\phi^{III})_{z=0}\right] \qquad (3.2.17)$$

From the behaviour of $\phi^I(x,z)$, $\phi^{II}(x,z)$ and $\phi^{III}(x,z)$ for any given x as $|z| \to \infty$, we can deduce that $\Phi_-^I(\alpha,x)$ is analytic for $\tau < b_1$ ($b_1 = -\mathrm{Im}(\beta_1)$), and $\Phi_+^{III}(\alpha,x)$ is analytic for $\tau > -b_2$ ($b_2 = -\mathrm{Im}(\beta_2)$). Because $\phi^{II}(x,z) \sim \phi^I(x,z)$ as $z \to -\infty$ and $\phi^{II}(x,z) \sim \phi^{III}(x,z)$ as

$z \to +\infty$, hence $\Phi^{II}(\alpha,x)$ is analytic in the strip $-b_2 < \tau < b_1$.

The solution of (3.2.16) can be found as

$$\Phi^{II}(\alpha,x) = A(\alpha)\, e^{-\lambda x} + B(\alpha)\, e^{\lambda x} \qquad (3.2.18)$$

where $\lambda = (\alpha^2 - k_0^2)^{1/2}$ which indicates that the solution possesses branch points at $\alpha = \pm k_0$.

If $\Phi^{II}(\alpha,x)$ is the solution of the wave equation representing the electromagnetic fields, it is required that, for any given x and for every α in the strip $-b_2 < \tau < b_1$, $\Phi^{II}(\alpha,x)$ is bounded. This requirement can be met by letting $B(\alpha) = 0$ and selecting the branch such that $Re(\lambda) > 0$ for any α as shown in figure 3.2. Hence, (3.2.18) is reduced to

$$\phi^{II}(\alpha,x) = A(\alpha)\, e^{-\lambda x} \qquad (3.2.19)$$

which is analytic in the strip $-k_0'' < \tau < k_0''$.

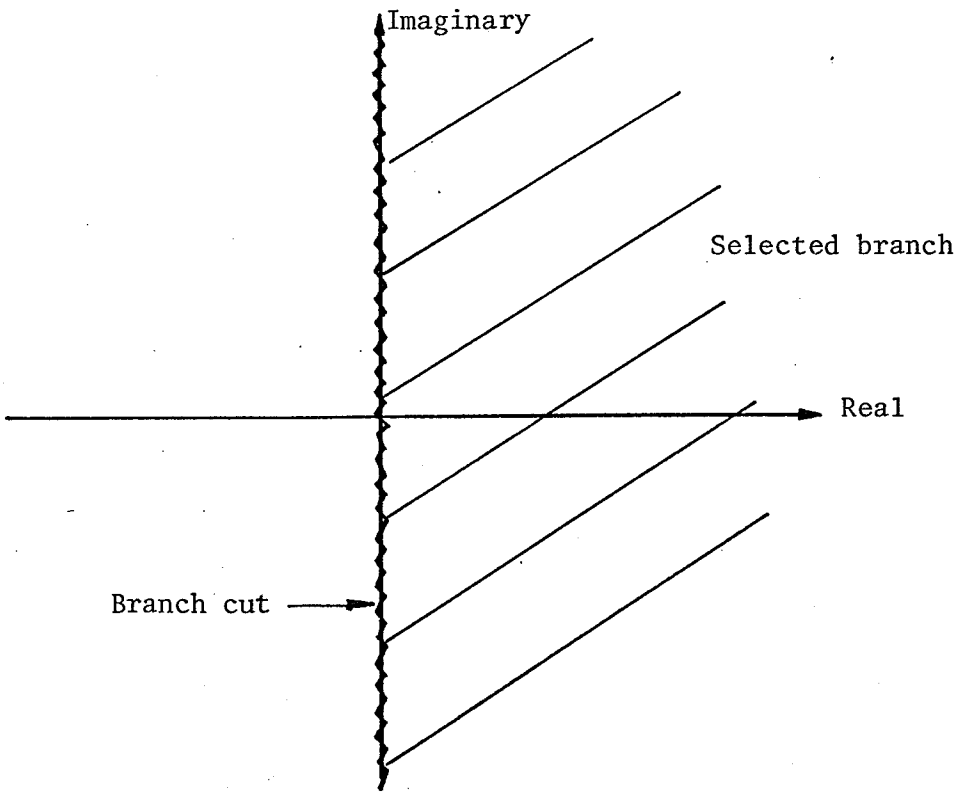

(a) λ-plane

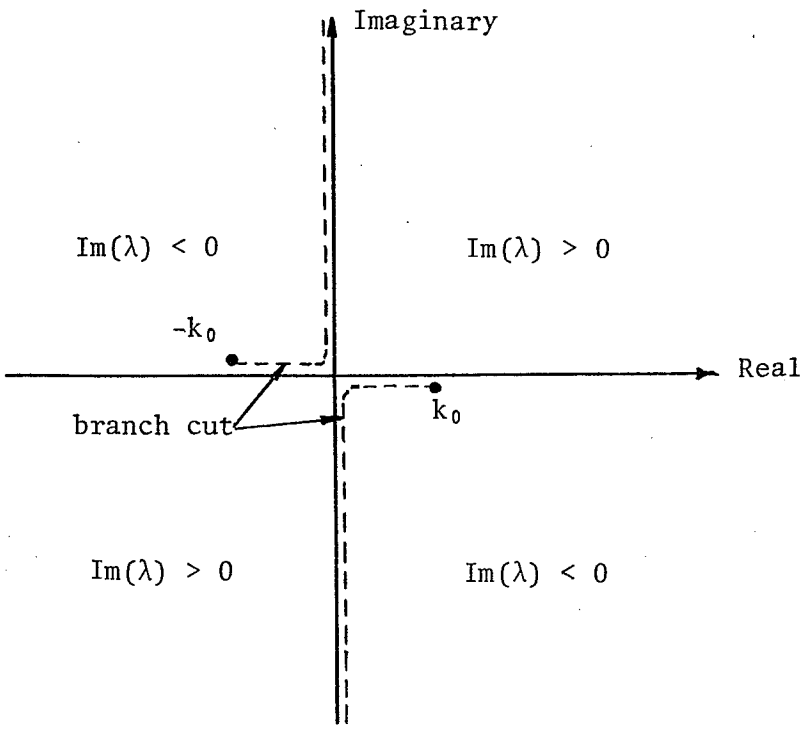

(b) α-plane

Figure 3.2 The selected Riemann sheet of (a) λ-plane (b) α-plane

By applying the boundary conditions that E_y and H_x must be continuous at the $z = 0$ plane, it can be shown that

$$(\phi^{III})_{z=0} = (\phi^{I})_{z=0} + A_i \cos(k_1^2 - \beta_1^2)^{1/2}x \qquad (3.2.20)$$

$$(\frac{\partial\phi^{III}}{\partial z})_{z=0} = (\frac{\partial\phi^{I}}{\partial z})_{z=0} - j\beta_1 A_i \cos(k_1^2 - \beta_1^2)^{1/2}x \qquad (3.2.21)$$

Substituting (3.2.20) and (3.2.21) in (3.2.17) yields

$$\frac{d^2}{dx^2}\Phi_+^{III}(\alpha,x) - (\alpha^2 - k_2^2)\Phi_+^{III}(\alpha,x) = \frac{1}{\sqrt{2\pi}}\left[(\frac{\partial\phi^{I}}{\partial z})_{z=0} - j\alpha(\phi^{I})_{z=0}\right]$$

$$\frac{-j}{\sqrt{2\pi}}(\beta_1 + \alpha) A_i \cos(k_1^2 - \beta_1^2)^{1/2}x \qquad (3.2.22)$$

Before attempting to solve (3.2.15) and (3.2.22), it is known that

(I) $\phi^I(x,z)$ and $\frac{\partial \phi^I}{\partial z}(x,z)$ are even continuous functions of x

(II) $\int_0^d [\phi^I(x,z)]'^2_{z=0}\, dx$ and $\int_0^d [\frac{\partial \phi^I}{\partial z}(x,z)]'^2_{z=0}\, dx$ are finite

Thus $[\phi^I(x,z)]_{z=0}$ and $[\frac{\partial \phi^I}{\partial z}(x,z)]_{z=0}$ can be expanded by the Fourier cosine series [42], *i.e.*,

$$-\frac{1}{\sqrt{2\pi}}\left[\left(\frac{\partial \phi^I}{\partial z}\right)_{z=0} - j\alpha(\phi^I)_{z=0}\right] = \frac{2}{d}\sum_{n=0}^{\infty}{}' \varepsilon_n' (f_n^A + j\alpha f_n^B)\cos(\frac{n\pi}{d}x) \quad (3.2.23)$$

where

$$f_n^A = \frac{-1}{\sqrt{2\pi}}\int_0^d \left(\frac{\partial \phi^I}{\partial z}\right)_{z=0} \cos(\frac{n\pi}{d}x)\, dx \quad (3.2.24)$$

$$f_n^B = \frac{1}{\sqrt{2\pi}}\int_0^d (\phi^I)_{z=0} \cos(\frac{n\pi}{d}x)\, dx \quad (3.2.25)$$

$\varepsilon_n' = 1$ for $n \geq 1$; $\varepsilon_0' = \frac{1}{2}$ for $n = 0$

Using (3.2.23), the solutions for (3.2.15) and (3.2.22) can be found as

$$\Phi_-^I(\alpha,x) = \frac{\cosh(\alpha^2 - k_1^2)^{\frac{1}{2}}x\ \Phi_-^{I'}(\alpha,d)}{(\alpha^2 - k_1^2)^{\frac{1}{2}}\sinh(\alpha^2 - k_1^2)^{\frac{1}{2}}d} - \frac{2}{d}\sum_{n=0}^{\infty}{}' \frac{\varepsilon_n'(f_n^A + j\alpha f_n^B)}{[\alpha^2 - k_1^2 + (\frac{n\pi}{d})^2]}\cos(\frac{n\pi}{d}x) \quad (3.2.26)$$

$$\Phi_+^{III}(\alpha,x) = \left[\Phi_+^{III'}(\alpha,d) + j\frac{A_i(\alpha+\beta_1)(k_1^2 - \beta_1^2)^{\frac{1}{2}}\sin(k_1^2 - \beta_1^2)^{\frac{1}{2}}d}{\sqrt{2\pi}(\alpha^2 - k_2^2 + k_1^2 - \beta_1^2)}\right]$$
$$\frac{\cosh(\alpha^2 - k_2^2)^{\frac{1}{2}}x}{(\alpha^2 - k_2^2)^{\frac{1}{2}}\sinh(\alpha^2 - k_2^2)^{\frac{1}{2}}d} + \frac{2}{d}\sum_{n=0}^{\infty}{}' \frac{\varepsilon_n'(f_n^A + j\alpha f_n^B)}{[\alpha^2 - k_2^2 + (\frac{n\pi}{d})^2]}$$
$$\cos(\frac{n\pi}{d}x) + j\frac{A_i(\alpha+\beta_1)\cos(k_1^2 - \beta_1^2)^{\frac{1}{2}}x}{\sqrt{2\pi}(\alpha^2 - k_2^2 + k_1^2 - \beta_1^2)} \quad (3.2.27)$$

where the primes on $\Phi_-^I(\alpha,d)$ and $\Phi_+^{III}(\alpha,d)$ denote the partial derivatives with respect to x evaluated at $x = d$.

At $x = d$, (3.2.26) and (3.2.27) are reduced to

$$\Phi_-^I(\alpha,d) = \frac{\cosh\,(\alpha^2 - k_1^2)^{\frac{1}{2}}d\ \Phi_-^{I'}(\alpha,d)}{(\alpha^2 - k_1^2)^{\frac{1}{2}}\sinh\,(\alpha^2 - k_1^2)^{\frac{1}{2}}d} - \frac{2}{d}\sum_{n=0}^{\infty}\frac{\varepsilon_n'(f_n^A + j\alpha f_n^B)}{[\alpha^2 - k_1^2 + (\frac{n\pi}{d})^2]}\cos(n\pi) \tag{3.2.28}$$

$$\Phi_+^{III}(\alpha,d) = \left[\Phi_+^{III'}(\alpha,d) + j\frac{A_i(\alpha+\beta_1)(k_1^2 - \beta_1^2)^{\frac{1}{2}}\sin(k_1^2 - \beta_1^2)^{\frac{1}{2}}d}{\sqrt{2\pi}\,(\alpha^2 - k_2^2 + k_1^2 - \beta_1^2)}\right]$$

$$\frac{\cosh\,(\alpha^2 - k_2^2)^{\frac{1}{2}}d}{(\alpha^2 - k_2^2)^{\frac{1}{2}}\sinh\,(\alpha^2 - k_2^2)^{\frac{1}{2}}d} + \frac{2}{d}\sum_{n=0}^{\infty}\frac{\varepsilon_n'(f_n^A + j\alpha f_n^B)}{[\alpha^2 - k_2^2 + (\frac{n\pi}{d})^2]}$$

$$\cos(n\pi) + j\frac{A_i(\alpha+\beta_1)\cos(k_1^2 - \beta_1^2)^{\frac{1}{2}}d}{\sqrt{2\pi}\,(\alpha^2 - k_2^2 + k_1^2 - \beta_1^2)} \tag{3.2.29}$$

From the property of the functions on the right-hand side of (3.2.28) and (3.2.29), (*i.e.*, that they must be regular in the lower and upper half planes, respectively) it can be shown that (See Appendix A):

$$\varepsilon_0'\,f_0^A = \frac{k_2\,\Phi_-^{I'}(k_1,d) - k_1\,\Phi_+^{III'}(-k_2,d)}{2(k_1+k_2)} + j\frac{A_i k_1(k_2-\beta_1)\sin(k_1^2 - \beta_1^2)^{\frac{1}{2}}d}{2\sqrt{2\pi}\,(k_1+k_2)(k_1^2 - \beta_1^2)^{\frac{1}{2}}} \tag{3.2.30}$$

$$\varepsilon_0'\,f_0^B = \frac{\Phi_-^{I'}(k_1,d) + \Phi_+^{III'}(-k_2,d)}{2j(k_1+k_2)} - \frac{A_i(k_2-\beta_1)\sin(k_1^2 - \beta_1^2)^{\frac{1}{2}}d}{2\sqrt{2\pi}\,(k_1+k_2)(k_1^2 - \beta_1^2)^{\frac{1}{2}}} \tag{3.2.31}$$

For $n \geq 1$, we have

$$\varepsilon_n'\,f_n^A\cos(n\pi) = \frac{\gamma_n'\,\Phi_-^{I'}(-j\gamma_n,d) - \gamma_n\Phi_+^{III'}(j\gamma_n',d)}{(\gamma_n + \gamma_n')} +$$

$$j\frac{A_i\gamma_n\,(\beta_1 + j\gamma_n')(k_1^2 - \beta_1^2)^{\frac{1}{2}}\sin(k_1^2 - \beta_1^2)^{\frac{1}{2}}d}{\sqrt{2\pi}\left[\beta_1^2 + (\frac{n\pi}{d})^2 - k_1^2\right](\gamma_n + \gamma_n')} \tag{3.2.32}$$

$$\varepsilon_n' f_n^B \cos(n\pi) = \frac{\Phi_-^{I'}(-j\gamma_n, d) + \Phi_+^{III'}(j\gamma_n', d)}{(\gamma_n + \gamma_n')} -$$

$$j \frac{A_i(\beta_1 + j\gamma_n')(k_1^2 - \beta_1^2)^{\frac{1}{2}} \sin(k_1^2 - \beta_1^2)^{\frac{1}{2}} d}{\sqrt{2\pi}\,(\gamma_n + \gamma_n')\,[\beta_1^2 + (\frac{n\pi}{d})^2 - k_1^2]} \qquad (3.2.33)$$

where

$$\gamma_n = \left[(\frac{n\pi}{d})^2 - k_1^2 \right]^{\frac{1}{2}} \qquad (3.2.34a)$$

$$\gamma_n' = \left[(\frac{n\pi}{d})^2 - k_2^2 \right]^{\frac{1}{2}} \qquad (3.2.34b)$$

Differentiating (3.2.19) with respect to x and letting $x = d$, it can be shown that

$$A(\alpha) = \frac{(-1)}{(\alpha^2 - k_0^2)^{\frac{1}{2}}} \left[\Phi_-^{II'}(\alpha, d) + \Phi_+^{II'}(\alpha, d) \right] e^{(\alpha^2 - k_0^2)^{\frac{1}{2}} d} \qquad (3.2.35)$$

Hence, (3.2.19) can be rewritten as

$$\Phi_-^{II}(\alpha, d) = \frac{(-1)}{(\alpha^2 - k_0^2)^{\frac{1}{2}}} \left[\Phi_-^{II'}(\alpha, d) + \Phi_+^{II'}(\alpha, d) \right] - \Phi_+^{II}(\alpha, d) \qquad (3.2.36)$$

3.2.2 Derivation of the Wiener-Hopf Equation

The Wiener-Hopf equation can be obtained from (3.2.28), (3.2.29) and (3.2.36) by applying the following boundary conditions:

(I) E_y is continuous at the $x = d$ plane. Thus, we have

$$\Phi_-^{I}(\alpha, d) = \Phi_-^{II}(\alpha, d)$$

$$= \frac{(-1)}{(\alpha^2 - k_0^2)^{\frac{1}{2}}} \left[\Phi_-^{II'}(\alpha, d) + \Phi_+^{II'}(\alpha, d) \right] - \Phi_+^{II}(\alpha, d) \qquad (3.2.37)$$

and

$$\Phi_+^{III}(\alpha,d) = \Phi_+^{II}(\alpha,d) + j\frac{A_i \cos(k_1^2 - \beta_1^2)^{\frac{1}{2}}d}{\sqrt{2\pi}\,(\alpha - \beta_1)} \tag{3.2.38}$$

(II) H_z is continuous at the $x = d$ plane. Thus, we have

$$\Phi_-^{I'}(\alpha,d) = \Phi_-^{II'}(\alpha,d) \tag{3.2.39}$$

and

$$\Phi_+^{III'}(\alpha,d) = \Phi_+^{II'}(\alpha,d) - j\frac{A_i(\beta_1^2 - k_0^2)^{\frac{1}{2}} \cos(k_1^2 - \beta_1^2)^{\frac{1}{2}}d}{\sqrt{2\pi}\,(\alpha - \beta_1)} \tag{3.2.40}$$

From (3.2.37) to (3.2.40), it can be shown that

$$\Phi_-^{I}(\alpha,d) = \frac{(-1)}{(\alpha^2 - k_0^2)^{\frac{1}{2}}}\left[\Phi_-^{I'}(\alpha,d) + \Phi_+^{III'}(\alpha,d) + j\frac{A_i(\beta_1^2 - k_0^2)^{\frac{1}{2}}\cos(k_1^2 - \beta_1^2)^{\frac{1}{2}}d}{\sqrt{2\pi}\,(\alpha - \beta_1)}\right]$$

$$- \Phi_+^{III}(\alpha,d) + j\frac{A_i \cos(k_1^2 - \beta_1^2)^{\frac{1}{2}}d}{\sqrt{2\pi}\,(\alpha - \beta_1)} \tag{3.2.41}$$

Equating (3.2.28) to (3.2.41) and substituting for $\Phi_+^{III}(\alpha,d)$ from (3.2.29) leads, after some algebraic manipulation, to the relation

$$N(\alpha)\,\Phi_-^{I'}(\alpha,d) = \frac{2}{d}\sum_{n=0}^{\infty}(f_n^A + j\alpha f_n^B)\,H_n(\alpha)\,\varepsilon_n' \cos(n\pi)$$

$$- M(\alpha)\,\Phi_+^{III'}(\alpha,d) + j\frac{A_i \cos(k_1^2 - \beta_1^2)^{\frac{1}{2}}d}{\sqrt{2\pi}\,(\alpha - \beta_1)}\left[1 - \frac{(\beta_1^2 - k_0^2)^{\frac{1}{2}}}{(\alpha^2 - k_0^2)^{\frac{1}{2}}}\right]$$

$$- j\frac{A_i\,(\beta_1 + \alpha)}{\sqrt{2\pi}(\alpha^2 - k_2^2 + k_1^2 - \beta_1^2)}\left[\frac{(k_1^2 - \beta_1^2)^{\frac{1}{2}}\sin(k_1^2 - \beta_1^2)^{\frac{1}{2}}d\coth(\alpha^2 - k_2^2)^{\frac{1}{2}}d}{(\alpha^2 - k_2^2)^{\frac{1}{2}}}\right.$$

$$\left. + \cos(k_1^2 - \beta_1^2)^{\frac{1}{2}}d\right] \tag{3.2.42}$$

Where

$$M(\alpha) = \frac{(\alpha^2 - k_2^2)^{\frac{1}{2}}\sinh(\alpha^2 - k_2^2)^{\frac{1}{2}}d + (\alpha^2 - k_0^2)^{\frac{1}{2}}\cosh(\alpha^2 - k_2^2)^{\frac{1}{2}}d}{(\alpha^2 - k_0^2)^{\frac{1}{2}}(\alpha^2 - k_2^2)^{\frac{1}{2}}\sinh(\alpha^2 - k_2^2)^{\frac{1}{2}}d} \tag{3.2.43}$$

$$H_n(\alpha) = \frac{1}{\alpha^2 - k_1^2 + (\frac{n\pi}{d})^2} - \frac{1}{\alpha^2 - k_2^2 + (\frac{n\pi}{d})^2} \qquad (3.2.44)$$

while $N(\alpha)$ is given by (3.2.43) with k_2 replaced by k_1. Because of the complexity of $M(\alpha)$ and $N(\alpha)$, the factorizations cannot be found in closed forms, the technique given by Mittra and Lee [39], (Appendix B), is applied. After factorization (3.2.42) can be rearranged as

$$\begin{aligned}\frac{N_-(\alpha)}{M_-(\alpha)}\ \Phi_-^{I'}(\alpha,d) &= \frac{2}{d}\ \frac{1}{N_+(\alpha)\ M_-(\alpha)}\ \sum_{n=0}^{\infty} H_n(\alpha)\ \varepsilon_n'\ f_n^A \cos(n\pi) \\ &+ \frac{2}{d}\ \frac{j\alpha}{N_+(\alpha)\ M_-(\alpha)}\ \sum_{n=0}^{\infty} H_n(\alpha)\ \varepsilon_n'\ f_n^B \cos(n\pi) \\ &+ j\ \frac{A_i \cos(k_1^2 - \beta_1^2)^{\frac{1}{2}} d}{\sqrt{2\pi}\ N_+(\alpha)\ M_-(\alpha)} \left[\frac{1}{(\alpha - \beta_1)} - \frac{(\beta_1^2 - k_0^2)^{\frac{1}{2}}}{(\alpha^2 - k_0^2)^{\frac{1}{2}}(\alpha - \beta_1)}\right. \\ &- \frac{(\beta_1 + \alpha)(\beta_1^2 - k_0^2)^{\frac{1}{2}} \coth(\alpha^2 - k_2^2)^{\frac{1}{2}} d}{(\alpha^2 - k_2^2 + k_1^2 - \beta_1^2)\ (\alpha^2 - k_2^2)^{\frac{1}{2}}} \\ &\left. - \frac{(\beta_1 + \alpha)}{(\alpha^2 - k_2^2 + k_1^2 - \beta_1^2)}\right] - \frac{M_+(\alpha)}{N_+(\alpha)}\ \Phi_+^{III'}(\alpha,d) \qquad (3.2.45)\end{aligned}$$

where $N_+(\alpha)$, $N_-(\alpha)$, $M_+(\alpha)$ and $M_-(\alpha)$ are given in Appendix C.

Defining

$$R(\alpha) = R_+(\alpha) + R_-(\alpha) = \frac{1}{N_+(\alpha)\ M_-(\alpha)} \left[\frac{1}{(\alpha - \beta_1)} - \frac{(\beta_1^2 - k_0^2)^{\frac{1}{2}}}{(\alpha^2 - k_0^2)^{\frac{1}{2}}(\alpha - \beta_1)}\right] \qquad (3.2.46)$$

$$\begin{aligned}S(\alpha) = S_+(\alpha) + S_-(\alpha) = \frac{1}{N_+(\alpha)\ M_-(\alpha)} &\left[\frac{(\beta_1 + \alpha)(\beta_1^2 - k_0^2)^{\frac{1}{2}} \coth(\alpha^2 - k_2^2)^{\frac{1}{2}} d}{(\alpha^2 - k_2^2 + k_1^2 - \beta_1^2)(\alpha^2 - k_2^2)^{\frac{1}{2}}}\right. \\ &\left. + \frac{(\beta_1 + \alpha)}{(\alpha^2 - k_2^2 + k_1^2 - \beta_1^2)}\right] \qquad (3.2.47)\end{aligned}$$

$$T_1^n(\alpha) = T_{1-}^n(\alpha) + T_{1+}^n(\alpha) = \frac{1}{N_+(\alpha)\, M_-(\alpha)} \left[\frac{1}{\alpha^2 - k_1^2 + (\frac{n\pi}{d})^2} \right] \quad (3.2.48)$$

$$\bar{T}_1^n(\alpha) = \bar{T}_{1-}^n(\alpha) + \bar{T}_{1+}^n(\alpha) = \frac{j\alpha}{N_+(\alpha)\, M_-(\alpha)} \left[\frac{1}{\alpha^2 - k_1^2 + (\frac{n\pi}{d})^2} \right] \quad (3.2.49)$$

$$T_2^n(\alpha) = T_{2-}^n(\alpha) + T_{2+}^n(\alpha) = \frac{1}{N_+(\alpha)\, M_-(\alpha)} \left[\frac{1}{\alpha^2 - k_2^2 + (\frac{n\pi}{d})^2} \right] \quad (3.2.50)$$

$$\bar{T}_2^n(\alpha) = \bar{T}_{2-}^n(\alpha) + \bar{T}_{2+}^n(\alpha) = \frac{j\alpha}{N_+(\alpha)\, M_-(\alpha)} \left[\frac{1}{\alpha^2 - k_2^2 + (\frac{n\pi}{d})^2} \right] \quad (3.2.51)$$

The above decompositions are obtained by applying a theorem given by Noble [38]. Again because of the complexity, they cannot be determined in closed forms. Substituting (3.2.46) to (3.2.51) into (3.2.45) and applying the Wiener-Hopf technique, both sides can then be set equal to zero from the condition at infinity (*i.e.*, $|\alpha| \to \infty$), obtainable from the edge condition. Thus, we have

$$\frac{N_-(\alpha)}{M_-(\alpha)} \Phi_-^{I'}(\alpha,d) - \frac{2}{d} [T_{1-}^0(\alpha) - T_{2-}^0(\alpha)] \varepsilon_0' f_0^A - \frac{2}{d} [\bar{T}_{1-}^0 - \bar{T}_{2-}^0(\alpha)] \varepsilon_0' f_0^B -$$

$$\frac{2}{d} \sum_{n=1}^{\infty} [T_{1-}^n(\alpha) - T_{2-}^n(\alpha)] \varepsilon_n' f_n^A \cos(n\pi) - \frac{2}{d} \sum_{n=1}^{\infty} [\bar{T}_{1-}^n(\alpha) - \bar{T}_{2-}^n(\alpha)] \varepsilon_n' f_n^B \cos(n\pi)$$

$$= j \frac{A_i \cos(k_1^2 - \beta_1^2)^{\frac{1}{2}} d}{\sqrt{2\pi}} [R_-(\alpha) - S_-(\alpha)] \quad (3.2.52)$$

and

$$\frac{M_+(\alpha)}{N_+(\alpha)} \Phi_+^{III'}(\alpha,d) - \frac{2}{d} [T_{1+}^0(\alpha) - T_{2+}^0(\alpha)] \varepsilon_0' f_0^A - \frac{2}{d} [\bar{T}_{1+}^0 - \bar{T}_{2+}^0(\alpha)] \varepsilon_0' f_0^B -$$

$$\frac{2}{d} \sum_{n=1}^{\infty} (T_{1+}^n(\alpha) - T_{2+}^n(\alpha)) \varepsilon_n' f_n^A \cos(n\pi) - \frac{2}{d} \sum_{n=1}^{\infty} (\bar{T}_{1+}^n(\alpha) - \bar{T}_{2+}^n(\alpha)) \varepsilon_n' f_n^B \cos(n\pi)$$

$$= j \frac{A_i \cos(k_1^2 - \beta_1^2)^{\frac{1}{2}} d}{\sqrt{2\pi}} [R_+(\alpha) - S_+(\alpha)] \quad (3.2.53)$$

Defining

$$C_-^n(\alpha) = \frac{2}{d}\left[T_{1-}^n(\alpha) - T_{2-}^n(\alpha)\right] \quad ; \quad n = 0, 1, 2, \ldots \tag{3.2.54}$$

$$\bar{C}_-^n(\alpha) = \frac{2}{d}\left[\bar{T}_{1-}^n(\alpha) - \bar{T}_{2-}^n(\alpha)\right] \quad ; \quad n = 0, 1, 2, \ldots \tag{3.2.55}$$

$$C_+^n(\alpha) = \frac{2}{d}\left[T_{1+}^n(\alpha) - T_{2+}^n(\alpha)\right] \quad ; \quad n = 0, 1, 2, \ldots \tag{3.2.56}$$

$$\bar{C}_+^n(\alpha) = \frac{2}{d}\left[\bar{T}_{1+}^n(\alpha) - \bar{T}_{2+}^n(\alpha)\right] \quad ; \quad n = 0, 1, 2, \ldots \tag{3.2.57}$$

and substituting (3.2.30) to (3.2.33) into (3.2.52) and (3.2.53) yields

$$\frac{N_-(\alpha)}{M_-(\alpha)}\,\Phi_-^{I'}(\alpha,d) - \left[(k_2 C_-^0(\alpha) - j\bar{C}_-^0(\alpha))\,\Phi_-^{I'}(k_1,d) - (k_1 C_-^0(\alpha) + j\,\bar{C}_-^0(\alpha))\,\Phi_+^{III'}(-k_2,d)\right]$$

$$\cdot\,\frac{1}{2(k_1+k_2)} - \sum_{n=1}^{\infty}\left[(C_-^n(\alpha)\gamma_n' + \bar{C}_-^n(\alpha))\,\Phi_-^{I'}(-j\gamma_n,d) - (C_-^n(\alpha)\gamma_n - \bar{C}_-^n(\alpha))\,\Phi_+^{III'}(j\gamma_n',d)\right]$$

$$\cdot\,\frac{1}{(\gamma_n+\gamma_n')} = j\,\frac{A_i}{\sqrt{2\pi}}\left[\frac{(k_1 C_-^0(\alpha) + j\,\bar{C}_-^0(\alpha)\,(k_2-\beta_1)\sin(k_1^2-\beta_1^2)^{\frac{1}{2}}d}{2(k_1+k_2)\,(k_1^2-\beta_1^2)^{\frac{1}{2}}} + \right.$$

$$\cos(k_1^2-\beta_1^2)^{\frac{1}{2}}d\,(R_-(\alpha) - S_-(\alpha)) + \sum_{n=1}^{\infty}\frac{(C_-^n(\alpha)\,\gamma_n - \bar{C}_-(\alpha))}{(\gamma_n+\gamma_n')}\cdot$$

$$\left.\frac{(\beta_1 + j\gamma_n')\,(k_1^2-\beta_1^2)^{\frac{1}{2}}\sin(k_1^2-\beta_1^2)^{\frac{1}{2}}d}{(\beta_1^2 + (\frac{n\pi}{d})^2 - k_1^2)}\right] \tag{3.2.58}$$

and

$$\frac{M_+(\alpha)}{N_+(\alpha)}\,\Phi_+^{III'}(\alpha,d) - \left[k_2 C_+^0(\alpha) - j\bar{C}_+^0(\alpha)\,\Phi_-^{I'}(k_1,d) - (k_1 C_+^0(\alpha) + j\bar{C}_+^0(\alpha))\,\Phi_+^{III'}(-k_2,d)\right]$$

$$\cdot\,\frac{1}{2(k_1+k_2)} - \sum_{n=1}^{\infty}\left[(C_+^n(\alpha)\gamma_n' + \bar{C}_+^n(\alpha))\,\Phi_-^{I'}(-j\gamma_n,d) - (C_+^n(\alpha)\gamma_n - \bar{C}_+^n(\alpha))\Phi_+^{III'}(j\gamma_n',d)\right]$$

$$\cdot\,\frac{1}{(\gamma_n+\gamma_n')} = j\,\frac{A_i}{\sqrt{2\pi}}\left[\cos(k_1^2-\beta_1^2)^{\frac{1}{2}}d(R_+(\alpha) - S_+(\alpha)) + \frac{(k_1 C_+^0(\alpha) + j\bar{C}_+^0(\alpha))}{2(k_1+k_2)}\right.$$

$$\cdot \frac{(k_2 - \beta_1)\sin(k_1^2 - \beta_1^2)^{\frac{1}{2}}d}{(k_1^2 - \beta_1^2)^{\frac{1}{2}}} + \sum_{n=1}^{\infty} \frac{(C_+^n(\alpha)\gamma_n - \bar{C}_+^n(\alpha))\ (\beta_1 + j\gamma_n')}{(\gamma_n + \gamma_n')}$$

$$\frac{(k_1^2 - \beta_1^2)^{\frac{1}{2}}\sin(k_1^2 - \beta_1^2)^{\frac{1}{2}}d}{(\beta_1^2 + (\frac{n\pi}{d})^2 - k_1^2)}\Bigg] \qquad (3.2.59)$$

Equations (3.2.58) and (3.2.59) will be further simplified as

$$\frac{N_-(\alpha)}{M_-(\alpha)}\ \Phi_-^{I'}(\alpha,d) - F_-^0(\alpha)\ \Phi_-^{I'}(k_1,d) + G_-^0(\alpha)\ \Phi_+^{III'}(-k_2,d) -$$

$$\sum_{n=1}^{\infty} [F_-^n(\alpha)\ \Phi_-^{I'}(-j\gamma_n,d) - G_-^n(\alpha)\ \Phi_+^{III'}(j\gamma_n',d)] = P_-(\alpha) + \sum_{n=1}^{\infty} Q_-^n(\alpha) \qquad (3.2.60)$$

and

$$\frac{M_+(\alpha)}{N_+(\alpha)}\ \Phi_+^{III'}(\alpha,d) - F_+^0(\alpha)\ \Phi_-^{I'}(k_1,d) + G_+^0(\alpha)\ \Phi_+^{III'}(-k_2,d) -$$

$$\sum_{n=1}^{\infty} [F_+^n(\alpha)\ \Phi_-^{I'}(-j\gamma_n,d) - G_+^n(\alpha)\ \Phi_+^{III'}(j\gamma_n',d)] = P_+(\alpha) + \sum_{n=1}^{\infty} Q_+^n(\alpha) \qquad (3.2.61)$$

where

$$F_+^0(\alpha) = \frac{(k_2C_+^0(\alpha) - j\bar{C}_+^0(\alpha))}{2(k_1 + k_2)} \qquad (3.2.62)$$

$$F_-^0(\alpha) = \frac{(k_2C_-^0(\alpha) - j\bar{C}_-^0(\alpha))}{2(k_1 + k_2)} \qquad (3.2.63)$$

$$G_+^0(\alpha) = \frac{(k_1C_+^0(\alpha) + j\bar{C}_+^0(\alpha))}{2(k_1 + k_2)} \qquad (3.2.64)$$

$$G_-^0(\alpha) = \frac{(k_1C_-^0(\alpha) + j\bar{C}_-^0(\alpha))}{2(k_1 + k_2)} \qquad (3.2.65)$$

$$P_+(\alpha) = j\frac{A_i}{\sqrt{2\pi}}\Bigg[\cos(k_1^2 - \beta_1^2)^{\frac{1}{2}}d\ (R_+(\alpha) - S_+(\alpha)) +$$

$$\frac{(k_1C_+^0(\alpha) + j\bar{C}_+^0(\alpha))(k_2 - \beta_1)\sin(k_1^2 - \beta_1^2)^{\frac{1}{2}}d}{2(k_1 + k_2)\ (k_1^2 - \beta_1^2)^{\frac{1}{2}}}\Bigg] \qquad (3.2.66)$$

$$P_-(\alpha) = j\frac{A_i}{\sqrt{2\pi}}\left[\cos(k_1^2 - \beta_1^2)^{\frac{1}{2}}d\,(R_-(\alpha) - S_-(\alpha)) + \frac{(k_1 C_-^0(\alpha) + j\bar{C}_-^0(\alpha))(k_2 - \beta_1)\sin(k_1^2 - \beta_1^2)^{\frac{1}{2}}d}{2(k_1 + k_2)\,(k_1^2 - \beta_1^2)^{\frac{1}{2}}}\right] \quad (3.2.67)$$

$$F_+^n(\alpha) = \frac{(C_+^n(\alpha)\gamma_n' + \bar{C}_+^n(\alpha))}{(\gamma_n + \gamma_n')} \quad (3.2.68)$$

$$F_-^n(\alpha) = \frac{(C_-^n(\alpha)\gamma_n' + \bar{C}_-^n(\alpha))}{(\gamma_n + \gamma_n')} \quad (3.2.69)$$

$$G_+^n(\alpha) = \frac{(C_+^n(\alpha)\gamma_n - \bar{C}_+^n(\alpha))}{(\gamma_n + \gamma_n')} \quad (3.2.70)$$

$$G_-^n(\alpha) = \frac{(C_-^n(\alpha)\gamma_n - \bar{C}_-^n(\alpha))}{(\gamma_n + \gamma_n')} \quad (3.2.71)$$

$$Q_+^n(\alpha) = j\,A_i\,\frac{(C_+^n(\alpha)\gamma_n - \bar{C}_+^n(\alpha))(\beta_1 + j\gamma_n')(k_1^2 - \beta_1^2)^{\frac{1}{2}}\sin(k_1^2 - \beta_1^2)^{\frac{1}{2}}d}{\sqrt{2\pi}\,(\gamma_n + \gamma_n')\,(\beta_1^2 + (\frac{n\pi}{d})^2 - k_1^2)} \quad (3.2.72)$$

$$Q_-^n(\alpha) = j\,A_i\,\frac{(C_-^n(\alpha)\gamma_n - \bar{C}_-^n(\alpha))(\beta_1 + j\gamma_n')(k_1^2 - \beta_1^2)^{\frac{1}{2}}\sin(k_1^2 - \beta_1^2)^{\frac{1}{2}}d}{\sqrt{2\pi}\,(\gamma_n + \gamma_n')\,(\beta_1^2 + (\frac{n\pi}{d})^2 - k_1^2)} \quad (3.2.73)$$

From (3.2.60) and (3.2.61), it is evident that the solution of the problem involves the constants, $\Phi_-^{I'}(k_1,d)$, $\Phi_-^{I'}(-j\gamma_n,d)$, $\Phi_+^{III'}(-k_2,d)$ and $\Phi_+^{III'}(j\gamma_n',d)$, n = 1, 2, 3, ... The solution is complete when these constants are determined.

3.2.3 Solution of the Problem

The unknowns, $\Phi_-^{I'}(k_1,d)$, $\Phi_-^{I'}(-j\gamma_n,d)$, $\Phi_+^{III'}(-k_2,d)$ and $\Phi_+^{III'}(j\gamma_n',d)$, n = 1, 2, 3, ... in (3.2.60) and (3.2.61) can be determined approximately by first truncating the infinite sum in (3,2.60) and (3.2.61) to "N", *i.e.*, n = 1, 2, 3, ..., N. A set of simultaneous

linear algebraic equations is then obtained by substituting $\alpha = k_1$, $-j\gamma_n$, $n = 1, 2, 3, \ldots, N$ in (3.2.60) and by substituting $\alpha = -k_2$, $j\gamma'_n$, $n = 1, 2, 3, \ldots, N$ in (3.2.61). This leads to

$$\left[\frac{N_-(k_1)}{M_-(k_1)} - F_-^0(k_1)\right] \Phi_-^{I'}(k_1,d) + G_-^0(k_1)\, \Phi_+^{III'}(-k_2,d) - \sum_{n=1}^{N} \left[F_-^n(k_1) \cdot \Phi_-^{I'}(-j\gamma_n,d) - G_-^n(k_1)\, \Phi_+^{III'}(j\gamma'_n,d) \right] = P_-(k_1) + \sum_{n=1}^{N} Q_-^n(k_1) \qquad (3.2.74a)$$

$$\frac{N_-(-j\gamma_r)}{M_-(-j\gamma_r)}\, \Phi_-^{I'}(-j\gamma_r,d) - F_-^0(-j\gamma_r)\, \Phi_-^{I'}(k_1,d) + G_-^0(-j\gamma_r)\, \Phi_+^{III'}(-k_2,d) - \sum_{n=1}^{N} \left[F_-^n(-j\gamma_r)\, \Phi_-^{I'}(-j\gamma_n,d) - G_-^n(-j\gamma_r)\, \Phi_+^{III'}(j\gamma'_n,d) \right] = P_-(-j\gamma_r) + \sum_{n=1}^{N} Q_-^n(-j\gamma_r) \qquad (3.2.74b)$$

$r = 1, 2, 3, \ldots, N.$

$$\left[\frac{M_+(-k_2)}{N_+(-k_2)} + G_+^0(-k_2)\right] \Phi_+^{III'}(-k_2,d) - F_+^0(-k_2)\, \Phi_-^{I'}(k_1,d) - \sum_{n=1}^{N} \left[F_+^n(-k_2) \cdot \Phi_-^{I'}(-j\gamma_n,d) - G_+^n(-k_2)\, \Phi_+^{III'}(j\gamma'_n,d) \right] = P_+(-k_2) + \sum_{n=1}^{N} Q_+^n(-k_2) \qquad (3.2.74c)$$

$$\frac{M_+(j\gamma'_r)}{N_+(j\gamma'_r)}\, \Phi_+^{III'}(j\gamma'_r,d) - F_+^0(j\gamma'_r)\, \Phi_-^{I'}(k_1,d) + G_+^0(j\gamma'_r)\, \Phi_+^{III'}(-k_2,d) - \sum_{n=1}^{N} \left[F_+^n(j\gamma'_r)\, \Phi_-^{I'}(-j\gamma_n,d) - G_+^n(j\gamma'_r)\, \Phi_+^{III'}(j\gamma'_n,d) \right] = P_+(j\gamma'_r) + \sum_{n=1}^{N} Q_+^n(j\gamma'_r) \qquad (3.2.74d)$$

$r = 1, 2, 3, \ldots, N.$

After the unknowns, $\Phi_-^{I'}(k_1,d)$, $\Phi_-^{I'}(-j\gamma_n,d)$, $\Phi_+^{III'}(-k_2,d)$ and $\Phi_+^{III'}(j\gamma'_n,d)$ are found by solving the above system of linear simultaneous equations, using (3.2.60) and (3.2.61) in

$$\Phi^{II}(\alpha,x) = -\frac{e^{(\alpha^2 - k_0^2)^{\frac{1}{2}}d}}{(\alpha^2 - k_0^2)^{\frac{1}{2}}} \left[\Phi_-^{I'}(\alpha,d) + \Phi_+^{III'}(\alpha,d) + j \frac{A_i(\beta_1^2 - k_0^2)^{\frac{1}{2}} \cos(k_1^2 - \beta_1^2)^{\frac{1}{2}} d}{\sqrt{2\pi}\ (\alpha - \beta_1)} \right] e^{-(\alpha^2 - k_0^2)^{\frac{1}{2}}x} \quad (3.2.75)$$

and applying the inverse Fourier transform

$$\phi^{II}(x,z) = \frac{1}{\sqrt{2\pi}} \int_{-\infty + j\tau_0}^{\infty + j\tau_0} \Phi^{II}(\alpha,x)\, e^{-j\alpha z}\, d\alpha \quad ; \quad |\tau_0| < k_0'' \quad (3.2.76)$$

After deforming the contour into the upper and lower half planes, the reflected and transmitted surface waves can, respectively, be represented by

$$\phi^{II}_{REF.}(x,z) = K_r \left[F_-^0(-\beta_1)\, \Phi_-^{I'}(k_1,d) - G_-^0(-\beta_1)\, \Phi_+^{III'}(-k_2,d) + \sum_{n=1}^{N} \left(F_-^n(-\beta_1)\, \Phi_-^{I'}(-j\gamma_n,d) - G_-^n(-\beta_1)\, \Phi_+^{III'}(j\gamma_n',d) \right) + P_-(-\beta_1) + \sum_{n=1}^{N} Q_-^n(-\beta_1) \right] \frac{(-\sqrt{2\pi})j}{\cos(k_1^2 - \beta_1^2)^{\frac{1}{2}}d\ (\beta_1^2 - k_0^2)^{\frac{1}{2}}} \cdot \cos(k_1^2 - \beta_1^2)^{\frac{1}{2}}d\ \ e^{(\beta_1^2 - k_0^2)^{\frac{1}{2}}d - (\beta_1^2 - k_0^2)^{\frac{1}{2}}x}\ \ e^{j\beta_1 z} \quad (3.2.77)$$

and

$$\phi^{II}_{TRANS.}(x,z) = K_t \left[F_+^0(\beta_2)\, \Phi_-^{I'}(k_1,d) - G_+^0(\beta_2)\, \Phi_+^{III'}(-k_2,d) + \sum_{n=1}^{N} \left(F_+^n(\beta_2)\, \Phi_-^{I'}(-j\gamma_n,d) - G_+^n(\beta_2)\, \Phi_+^{III'}(j\gamma_n',d) \right) + P_+(\beta_2) + \sum_{n=1}^{N} Q_+^n(\beta_2) \right] \frac{j\sqrt{2\pi}\cos(k_2^2 - \beta_2^2)^{\frac{1}{2}}d}{\cos(k_2^2 - \beta_2^2)^{\frac{1}{2}}d\ (\beta_2^2 - k_0^2)^{\frac{1}{2}}}\ e^{(\beta_2^2 - k_0^2)^{\frac{1}{2}}d}\ e^{-(\beta_2^2 - k_0^2)^{\frac{1}{2}}x}\ e^{-j\beta_2 z} \quad (3.2.78)$$

Where

$$K_r = \prod_{n=1}^{\infty} \left(1 + \frac{\beta_i}{j\gamma_n'}\right) e^{-j\frac{\beta_1 d}{n\pi}} \prod_{n=1}^{\infty} \left(1 + \frac{\beta_1}{j\gamma_n}\right) e^{j\frac{\beta_1 d}{n\pi}} \sqrt{\frac{H_1(0)k_2 \sin k_1 d}{H(0)k_1 \sin k_2 d}}$$

$$\left(\frac{k_1 - \beta_1}{k_2 - \beta_1}\right) \left(1 - \frac{\beta_1}{\beta_2}\right) \beta_1 \exp[q_1(\beta_1) - q_0(\beta_1)] \qquad (3.2.79)$$

$$K_t = \prod_{n=1}^{\infty} \left(1 + \frac{\beta_2}{j\gamma_n}\right) e^{-j\frac{\beta_2 d}{n\pi}} \prod_{n=1}^{\infty} \left(1 + \frac{\beta_2}{j\gamma_n'}\right) e^{j\frac{\beta_2 d}{n\pi}} \sqrt{\frac{H(0)k_1 \sin k_2 d}{H_1(0)k_2 \sin k_1 d}}$$

$$\left(\frac{\beta_2 - k_2}{\beta_2 - k_1}\right) (-\beta_2) \left(1 - \frac{\beta_2}{\beta_1}\right) \exp[q_0(\beta_2) - q_1(\beta_2)] \qquad (3.2.80)$$

while $H(0)$, $H_1(0)$, $q_0(\alpha)$ and $q_1(\alpha)$ are defined in Appendix C.

The far field is found from the inverse transform, from (3.2.76)

$$\Phi^{II}(x,z) = \int_{-\infty + j\tau_0}^{\infty + j\tau_0} F(\alpha)\, e^{-jk_x(x-d) - j\alpha z}\, d\alpha \quad ; \quad |\tau_0| < k_0'' \qquad (3.2.81)$$

where

$$F(\alpha) = \frac{(-1)}{\sqrt{2\pi}\,(\alpha^2 - k_0^2)^{\frac{1}{2}}} \left[\Phi_-^{I'}(\alpha,d) + \Phi_+^{III'}(\alpha,d) + \frac{jA_i(\beta_1^2 - k_0^2)^{\frac{1}{2}} \cos(k_1^2 - \beta_1^2)^{\frac{1}{2}} d}{\sqrt{2\pi}\,(\alpha - \beta_1)} \right] \qquad (3.2.82)$$

$$k_x = (k_0^2 - \alpha^2)^{\frac{1}{2}} \quad ; \quad [(\alpha^2 - k_0^2)^{\frac{1}{2}} = j\,(k_0^2 - \alpha^2)^{\frac{1}{2}}] \qquad (3.2.83)$$

By introducing the polar coordinates shown in figure 3.3 and using the transformation

$$\alpha = k_0 \sin\omega \quad ; \quad \omega = \zeta + j\eta$$
$$k_x = k_0 \cos\omega \qquad (3.2.84)$$

we obtain

$$\phi^{II}(r,\theta) = \int_P \bar{F}(\omega)\, e^{-jk_0 r \cos(\omega - \theta)}\, d\omega \qquad (3.2.85)$$

where the contour of integration in (3.2.81) maps into the contour P in the ω-plane.

where

$$\bar{F}(\omega) = k_0 \cos\omega F(\alpha) \tag{3.2.86}$$

For the far field $(k_0 r >> 1)$, we apply the method of steepest descent [56,43] to obtain

$$\phi^{II}(r,\theta) \sim \sqrt{\frac{2\pi}{k_0 r}}\ \bar{F}(\theta)\ e^{-j(k_0 r - \frac{\pi}{4})} \tag{3.2.87}$$

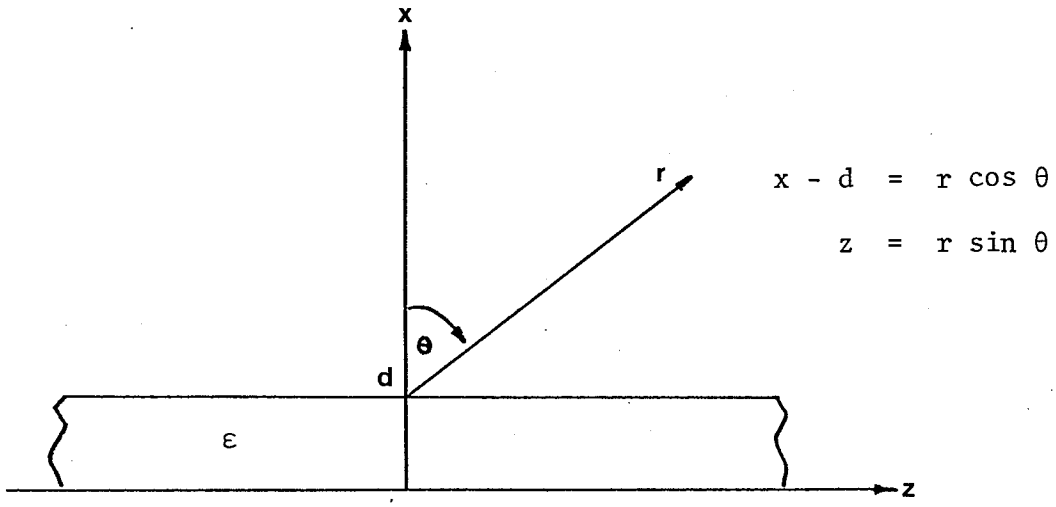

Figure 3.3 Polar-coordinates at a discontinuity junction on a dielectric slab waveguide

3.2.4 TM Mode Incidence

The problem is similar to the TE incidence case except that the incident field is H_y. We can follow the procedure of the TE case, which after applying the Wiener-Hopf technique leads to the following equations for $\Phi_-^{I'}(\alpha,d)$ and $\Phi_+^{III'}(\alpha,d)$:

$$\frac{L_-(\alpha)}{K_-(\alpha)}\ \Phi_-^{I'}(\alpha,d) + \frac{[j\bar{D}_-^0(\alpha)\ (\frac{\varepsilon_{r_1}}{\varepsilon_{r_2}}) - D_-^0(\alpha)\ k_2]}{2(\frac{\varepsilon_{r_2}}{\varepsilon_{r_1}})\ k_1 + k_2}\ \Phi_-^{I'}(k_1,d) +$$

$$\frac{[j\bar{D}_-^0(\alpha) + D_-^0(\alpha)\ k_1]}{2[(\frac{\varepsilon_{r_2}}{\varepsilon_{r_1}})\ k_1 + k_2']}\ \Phi_+^{III'}(-k_2,d) - \sum_{n=0}^{\infty} \frac{(\bar{D}_-^n(\alpha)(\frac{\varepsilon_{r_2}}{\varepsilon_{r_1}}) + D_-^n(\alpha)\gamma_n')}{[(\frac{\varepsilon_{r_2}}{\varepsilon_{r_1}})\ \gamma_n + \gamma_n']}\ \Phi_-^{I'}(-j\gamma_n,d)$$

$$- \sum_{n=0}^{\infty} \frac{(\bar{D}_-^n(\alpha) - D_-^n(\alpha)\gamma_n)}{[(\frac{\varepsilon_{r_2}}{\varepsilon_{r_1}})\ \gamma_n + \gamma_n']}\ \Phi_+^{III'}(j\gamma_n',d) = j\frac{A_i \cos(k_1^2 - \beta_1^2)^{\frac{1}{2}}d}{\sqrt{2\pi}}\ [U_-(\alpha) -$$

$$V_-(\alpha)] + \frac{A_i}{\sqrt{2\pi}}(\bar{D}_-^0(\alpha) - jD_-^0(\alpha)\ k_1)\ (\frac{\varepsilon_{r_2}\beta_1}{\varepsilon_{r_1}} - k_2)\ \frac{\sin(k_1^2 - \beta_1^2)^{\frac{1}{2}}\ d}{2[(\frac{\varepsilon_{r_2}}{\varepsilon_{r_1}})\ k_1 + k_2](k_1^2 - \beta_1^2)^{\frac{1}{2}}}$$

$$+ \sum_{n=0}^{\infty} j\frac{A_i}{\sqrt{2\pi}}(\bar{D}_-^n(\alpha) - D_-^n(\alpha)\ \gamma_n)\ (\frac{\varepsilon_{r_2}\beta_1}{\varepsilon_{r_1}} + j\gamma_n')\ \frac{(k_1^2 - \beta_1^2)^{\frac{1}{2}}\sin(k_1^2 - \beta_1^2)^{\frac{1}{2}}d}{[(\frac{\varepsilon_{r_2}}{\varepsilon_{r_1}})\gamma_n + \gamma_n']\ (k_1^2 - (\frac{n\pi}{d})^2 - \beta_1^2)}$$

(3.2.88)

and

$$\frac{K_+(\alpha)}{L_+(\alpha)}\ \Phi_+^{III'}(\alpha,d) + \frac{[j\bar{D}_+^0(\alpha)\ (\frac{\varepsilon_{r_2}}{\varepsilon_{r_1}}) - D_+^0(\alpha)\ k_2]}{2[(\frac{\varepsilon_{r_2}}{\varepsilon_{r_1}})\ k_1 + k_2]}\ \Phi_-^{I'}(k_1,d) +$$

$$\frac{[j\bar{D}_+^0(\alpha) + D_+^0(\alpha)\ k_1]}{2[\frac{\varepsilon_{r_2}}{\varepsilon_{r_1}})\ k_1 + k_2]}\ \Phi_+^{III'}(-k_2,d) - \sum_{n=0}^{\infty} \frac{(\bar{D}_+^n(\alpha)(\frac{\varepsilon_{r_2}}{\varepsilon_{r_1}}) + D_+^n(\alpha)\gamma_n')}{[(\frac{\varepsilon_{r_2}}{\varepsilon_{r_1}})\ \gamma_n + \gamma_n']}\ \Phi_-^{I'}(-j\gamma_n,d)$$

$$- \sum_{n=0}^{\infty} \frac{(\bar{D}_+^n(\alpha) - D_+^n(\alpha)\ \gamma_n)}{[(\frac{\varepsilon_{r_2}}{\varepsilon_{r_1}})\ \gamma_n + \gamma_n']}\ \Phi_+^{III'}(j\gamma_n',d) = j\frac{A_i \cos(k_1^2 - \beta_1^2)^{\frac{1}{2}}d}{\sqrt{2\pi}}\ [U_+(\alpha) - V_+(\alpha)]$$

$$+ \frac{A_i}{\sqrt{2\pi}}(\bar{D}_+^0(\alpha) - jD_+^0(\alpha)\ k_1)(\frac{\varepsilon_{r_2}\beta_1}{\varepsilon_{r_1}} - k_2)\ \frac{\sin(k_1^2 - \beta_1^2)^{\frac{1}{2}}d}{2[(\frac{\varepsilon_{r_2}}{\varepsilon_{r_1}})\ k_1 + k_2]\ (k_1^2 - \beta_1^2)^{\frac{1}{2}}}$$

$$+ \sum_{n=0}^{\infty} j \frac{A_i}{\sqrt{2\pi}} (\bar{D}_+^n(\alpha) - D_+^n(\alpha)\gamma_n)(\frac{\varepsilon_{r_1}\beta_1}{\varepsilon_{r_1}} + j\gamma_n') \frac{(k_1^2 - \beta_1^2)^{\frac{1}{2}} \sin(k_1^2 - \beta_1^2)^{\frac{1}{2}} d}{[(\frac{\varepsilon_{r_2}}{\varepsilon_{r_1}})\gamma_n + \gamma_n'](k_1^2 - (\frac{n\pi}{d})^2 - \beta_1^2)} \tag{3.2.89}$$

where

$$D_-^n(\alpha) = \frac{2}{d} [W_{1-}^n(\alpha) - (\frac{\varepsilon_{r_2}}{\varepsilon_{r_1}}) W_{2-}^n(\alpha)] \tag{3.2.90a}$$

$$D_+^n(\alpha) = \frac{2}{d} [W_{1+}^n(\alpha) - (\frac{\varepsilon_{r_2}}{\varepsilon_{r_1}}) W_{2+}^n(\alpha)] \tag{3.2.90b}$$

$$\bar{D}_-^n(\alpha) = \frac{2}{d} [\bar{W}_{1-}^n(\alpha) - \bar{W}_{2-}^n(\alpha)] \tag{3.2.90c}$$

$$\bar{D}_+^n(\alpha) = \frac{2}{d} [\bar{W}_{1+}^n(\alpha) - \bar{W}_{2+}^n(\alpha)] \tag{3.2.90d}$$

$n = 0, 1, 2, 3, \ldots\ldots$

while $L_+(\alpha)$, $L_-(\alpha)$, $K_+(\alpha)$, $K_-(\alpha)$, $U_+(\alpha)$, $U_-(\alpha)$, $V_+(\alpha)$, $V_-(\alpha)$, $W_{1-}^n(\alpha)$, $W_{1+}^n(\alpha)$, $W_{2-}^n(\alpha)$, $W_{2+}^n(\alpha)$, $\bar{W}_{1-}^n(\alpha)$, $\bar{W}_{1+}^n(\alpha)$, $\bar{W}_{2-}^n(\alpha)$ and $\bar{W}_{2+}^n(\alpha)$ are given in Appendix C.

From equations (3.2.88) and (3.2.89), it is evident that the unknown constants, $\Phi_-^{I'}(k_1,d)$, $\Phi_-^{I'}(-j\gamma_n,d)$; $n = 1, 2, 3, \ldots\ldots$, $\Phi_+^{III'}(-k_2,d)$ and $\Phi_+^{III'}(j\gamma_n',d)$, $n = 1, 2, 3, \ldots$ can be found by the same technique already applied for the TE case. Once these unknown constants are determined, we apply the inverse Fourier transform, with the proper contour deformations for the regions of $z < 0$ and $z > 0$, to the expression

$$\Phi^{II}(\alpha,d) = \frac{(-1)\, e^{(\alpha^2 - k_0^2)^{\frac{1}{2}} d}}{(\alpha^2 - k_0^2)^{\frac{1}{2}}} \left[\frac{\Phi_-^{I'}(\alpha,d)}{\varepsilon_{r1}} + \frac{\Phi_+^{III'}(\alpha,d)}{\varepsilon_{r_2}} + j \frac{A_i(\beta_1^2 - k_0^2)^{\frac{1}{2}}}{\sqrt{2\pi}} \right.$$

$$\left. \frac{\cos(k_1^2 - \beta_1^2)^{\frac{1}{2}}}{(\alpha - \beta_1)} \right] e^{-(\alpha^2 - k_0^2)^{\frac{1}{2}} x} \tag{3.2.91}$$

to find the following expressions for the reflected and transmitted waves

$$\phi^{II}_{REF.}(x,z) = \frac{\sqrt{2\pi}}{\varepsilon_{r_1}} j \, Res[\Phi_-^{I'}(\alpha,d) ; \alpha = -\beta_1] \left[\frac{(-1)}{(\beta_1^2 - k_0^2)^{\frac{1}{2}} \cos(k_1^2 - \beta_1^2)^{\frac{1}{2}} d}\right]$$

$$\cdot \cos(k_1^2 - \beta_1^2)^{\frac{1}{2}} d \; e^{(\beta_1^2 - k_0^2)^{\frac{1}{2}} d} \; e^{-(\beta_1^2 - k_0^2)^{\frac{1}{2}} x} \; e^{+j\beta_1 z} \tag{3.2.92}$$

and

$$\phi^{II}_{TRAN.}(x,z) = \frac{\sqrt{2\pi}}{\varepsilon_{r_2}} j \, Res[\Phi_+^{III'}(\alpha,d) ; \alpha = \beta_2] \left[\frac{(1)}{(\beta_2^2 - k_0^2)^{\frac{1}{2}} \cos(k_2^2 - \beta_2^2)^{\frac{1}{2}} d}\right]$$

$$\cdot \cos(k_2^2 - \beta_2^2)^{\frac{1}{2}} d \; e^{(\beta_2^2 - k_0^2)^{\frac{1}{2}} d} \; e^{-(\beta_2^2 - k_0^2)^{\frac{1}{2}} x} \; e^{-j\beta_2 z} \tag{3.2.93}$$

Where $Res[\Phi_-^{I'}(\alpha,d) ; \alpha = -\beta_1]$ and $Res[\Phi_+^{III'}(\alpha,d) ; \alpha = \beta_2]$ are the residues of $\Phi_-^{I'}(\alpha,d)$ at $-\beta_1$ and $\Phi_+^{III'}(\alpha,d)$ at β_2, respectively.

Applying the method of steepest descent as in TE case, the far field is given by

$$\phi^{II}(r,\theta) \sim \sqrt{\frac{2\pi}{k_0 r}} \; k_\phi \cos\theta \; G(k_0 \sin\theta) \; e^{-j(k_0 r - \frac{\pi}{4})} \tag{3.2.94}$$

where

$$G(\alpha) = \frac{(-1)}{\sqrt{2\pi}\,(\alpha^2 - k_0^2)^{\frac{1}{2}}} \left[\frac{\Phi_-^{I'}(\alpha,d)}{\varepsilon_{r_1}} + \frac{\Phi_+^{III'}(\alpha,d)}{\varepsilon_{r_2}} + j \frac{A_i (\beta_1^2 - k_0^2)^{\frac{1}{2}}}{\sqrt{2\pi}}\right.$$

$$\left. \cdot \frac{\cos(k_1^2 - \beta_1^2)^{\frac{1}{2}} d}{(\alpha - \beta_1)}\right] \tag{3.2.95}$$

3.3 Numerical Results

Figure 3.4 shows the magnitude of the reflection coefficient at the discontinuity junction as a function of kd_1. The solid circle notation represents the results obtained by the Wiener-Hopf technique proposed in this chapter while the solid line represents the results based on the residue-calculus technique as discussed in the next chapter. The dash

lines represent the asymptotic values as obtained from the consideration of a normal plane wave incident at the junction of two dielectric media [53],[54]. The Wiener-Hopf results are obtained by first solving (3.2.74) for the unknown constants. By substituting these constants in (3.2.77), the reflected surface wave and the reflection coefficient, which is defined as the ratio of the reflected surface wave to the incident surface wave, can be found. The ratio of transmitted power to incident power as a function of kd_1 is shown in figure 3.5 using the same notations as in figure 3.4, while the open circle notation represents the results by the reciprocity theorem. The Wiener-Hopf results are again obtained by first solving (3.2.74) for the unknown constants which are substituted into (3.2.78) to obtain the transmitted surface wave.

Tables (3.1) and (3.2) show the calculated values of the unknown constants for different kd_1. These unknown constants are values of the partial derivative w.r.t. x of field of region I in the lower half of α-plane at $k_1, -j\gamma_n$, $n = 1, 2, 3, \ldots\ldots$ (*i.e.*, $\Phi_-^{I'}(k_1,d)$, $\Phi_-^{I'}(-j\gamma_n,d)$) and the partial derivative w.r.t. x of field of region III in the upper half of α-plane at $-k_2, j\gamma_n'$, $n = 1, 2, 3, \ldots\ldots$ (*i.e.*, $\Phi_+^{III'}(-k_2,d)$, $\Phi_+^{III'}(j\gamma_n',d)$). They are found by solving equation (3.2.74).

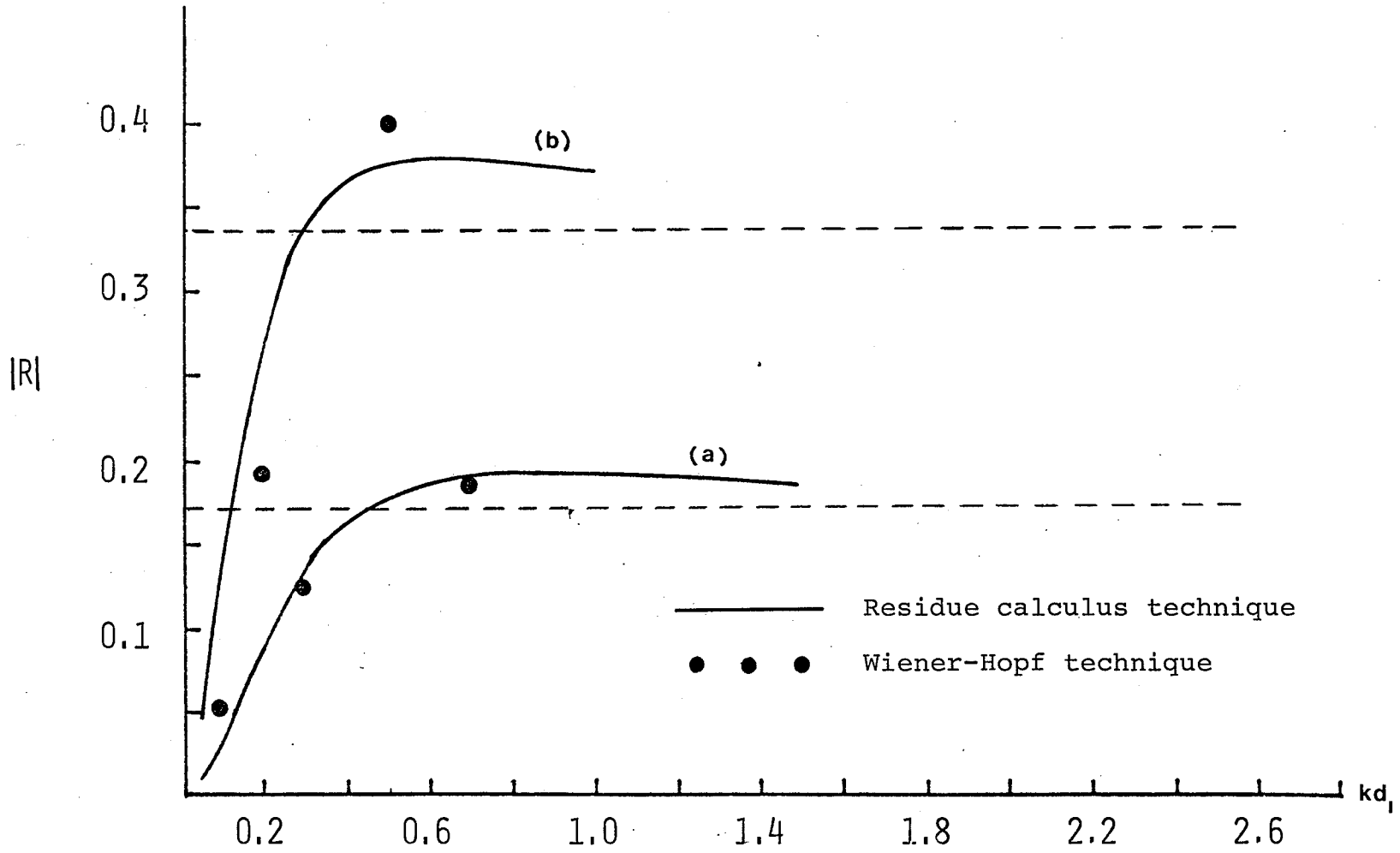

Figure 3.4 Reflection coefficient for TE incidence with $\varepsilon_{r_1} = 2.56$

(a) $\varepsilon_{r_2} = 5.12$ (b) $\varepsilon_{r_2} = 10.24$

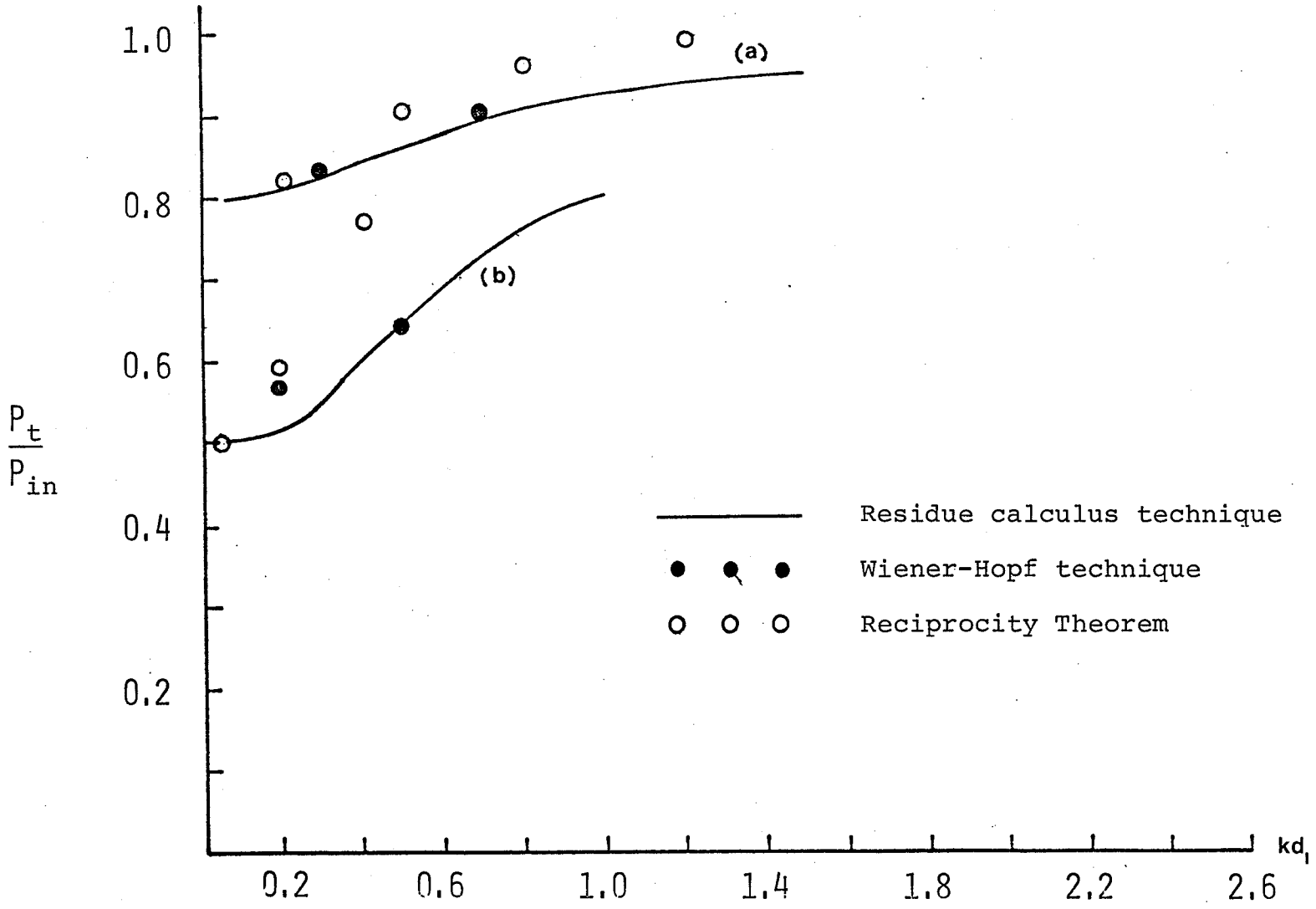

Figure 3.5 Transmitted power for TE incidence with the same parameters as for Fig. 3.4

TABLE 3.1

Calculated values of unknown constants for TE mode with

$\varepsilon_{r_1} = 2.56$; $\varepsilon_{r_2} = 5.12$

	$kd_1 = 0.3$		$kd_1 = 0.7$	
	REAL	IMAGINARY	REAL	IMAGINARY
$\Phi_-^{I'}(k_1,d)$	-0.1119×10^{-1}	0.1351×10^{-1}	0.1538×10^{-1}	-0.7617×10^{-3}
$\Phi_-^{I'}(-j\gamma_1,d)$	0.8117×10^{-3}	-0.3697×10^{-3}	0.8802×10^{-1}	0.8665×10^{-2}
$\Phi_-^{I'}(-j\gamma_2,d)$	-0.2106×10^{-3}	0.4296×10^{-4}	-0.2269×10^{-2}	-0.1080×10^{-2}
$\Phi_-^{I'}(-j\gamma_3,d)$	0.3115×10^{-3}	-0.1575×10^{-3}	0.2169×10^{-2}	-0.2132×10^{-2}
$\Phi_+^{III'}(-k_2,d)$	0.2661×10^{-1}	0.1281	0.4631×10^{-1}	0.1157
$\Phi_+^{III'}(j\gamma_1',d)$	-0.1879×10^{-1}	0.3558×10^{-2}	-0.8816×10^{-1}	0.1897×10^{-1}
$\Phi_+^{III'}(j\gamma_2',d)$	-0.8316×10^{-2}	0.9484×10^{-3}	-0.2777×10^{-1}	0.2001×10^{-2}
$\Phi_+^{III'}(j\gamma_3',d)$	-0.4691×10^{-2}	0.7937×10^{-4}	-0.2017×10^{-1}	0.2197×10^{-3}

TABLE 3.2

Calculated values of unknown constants for TE modes with

$\varepsilon_{r_1} = 2.56$; $\varepsilon_{r_2} = 10.24$

	$kd_1 = 0.2$		$kd_1 = 0.5$	
	REAL	IMAGINARY	REAL	IMAGINARY
$\Phi_-^{I'}(k_1,d)$	-0.2083×10^{-1}	0.3283×10^{-1}	0.6592×10^{-1}	0.2170×10^{-1}
$\Phi_-^{I'}(-j\gamma_1,d)$	-0.8640×10^{-1}	0.4562×10^{-1}	0.1209×10^{-1}	-0.1242×10^{1}
$\Phi_-^{I'}(-j\gamma_2,d)$	-0.3990×10^{-1}	0.1827×10^{-1}	0.5021×10^{-1}	-0.8448×10^{-3}
$\Phi_-^{I'}(-j\gamma_3,d)$	-0.8632×10^{-2}	0.4409×10^{-2}	0.8585×10^{-2}	-0.2739×10^{-2}
$\Phi_+^{III'}(-k_2,d)$	0.7032×10^{-2}	0.1151	-0.1459×10^{-1}	-0.5578×10^{-1}
$\Phi_+^{III'}(+j\gamma_1',d)$	0.1923×10^{1}	0.1198	0.1667×10^{1}	-0.4013
$\Phi_+^{III'}(j\gamma_2',d)$	-0.7179×10^{-1}	0.2336×10^{-1}	0.6309	-0.2751×10^{-1}
$\Phi_+^{III'}(j\gamma_3',d)$	0.1165×10^{-1}	-0.3470×10^{-2}	0.5045	-0.5291×10^{-1}

CHAPTER 4

APPLICATION OF THE RESIDUE-CALCULUS TECHNIQUE

4.1 INTRODUCTION

The Wiener-Hopf technique as applied in Chapter 3 for solving the problem of a discontinuity in a dielectric slab waveguide is very complicated when dealing with a structure with finite thickness. The solution, which always contains constants satisfying linear algebraic simultaneous equations, cannot be found in closed form. The problem becomes more complicated when the dielectric slab waveguide takes on a more general form, *i.e.*, different thickness on the left and right sides of the junction. It is the purpose of this chapter to present a new technique based on the residue-calculus method [46-49] to deal with this more complicated structure. It is found that the solution obtained by this technique, though approximate, is far simpler and more convenient to apply.

By the residue-calculus technique, the problem is formulated based on the mode matching technique similar to the procedure of Marcuse [4,23] leading to two simultaneous equations after applying the boundary condition at the junction. However, instead of following those techniques previously reported for solving these equations, the residue-calculus technique is applied. Essentially by this technique, a function is constructed such that its poles have the same locations and contributions as those of surface wave poles while its branch cut integral is equal to the contribution from the radiated field. This term-by-term comparison then permits the calculation of the unknown quantities. However, in constructing this function, the fundamental assumption is

made that the resulting mode amplitudes, when expanded asymptotically, have the proper algebraic behaviour as shown by Collin [40] for a different problem which also involves a dielectric slab. Consequently, the entire function involved in the constructed function is simply a constant which can be found from the incident field. In order to check for the accuracy of the results, the reciprocity theorem, as applied by Barlow and Brown [16] for the problem of discontinuity in surface impedance, is used. And by representing the slab waveguide by surface impedance, under certain conditions, a check based on the application of Kay's result [20] can also be made.

4.2 FORMULATION OF THE PROBLEM

The configuration of the dielectric slab waveguide under consideration is shown in figure 4.1. It is assumed that the y-dimension is extended to infinity and all field components are independent of y, *i.e.*, $\frac{\partial}{\partial y} = 0$. The subscripts 1 and 2 denote the left and right sides of the discontinuity, respectively, so that the slab thickness changes from $2d_1$ to $2d_2$ and the dielectric constant changes from ε_{r_1} to ε_{r_2}. The formulation is given in detail for the case $d_1 > d_2$ and a similar procedure can be used to derive the results for the case $d_2 > d_1$. Two cases of incident fields, TE and TM, are formulated separately assuming $e^{j\omega t}$ time dependence which is suppressed throughout.

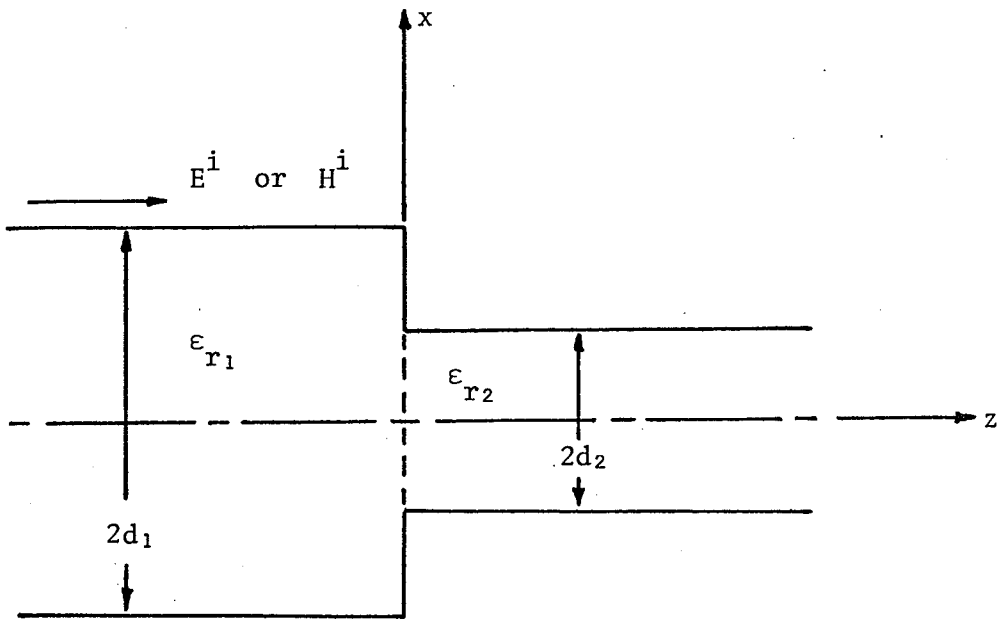

Figure 4.1 Schematic diagram of a stepped dielectric slab waveguide.

4.2.1 TE Incidence

By using a modal expansion (involving a single surface wave mode plus psuedosurface or radiation modes) of the electric field on each side of the junction and applying the boundary conditions, that the tangential electric and magnetic field components must be continuous at $z = 0$ plane, the two simultaneous equations for the unknown mode amplitudes are given by

$$E_y^i + E_y^r + \int_o^\infty E_y^r(\rho)\, d\rho = E_y^t + \int_o^\infty E_y^t(\rho')\, d\rho' \qquad (4.2.1)$$

$$-\beta_1 E_y^i + \beta_1 E_y^r + \int_o^\infty \beta E_y^r(\rho)\, d\rho = -\beta_2 E_y^t - \int_o^\infty \beta' E_y^t(\rho')\, d\rho' \qquad (4.2.2)$$

where $E_y^{i,r,t}$ represent the y-components of the incident, reflected

and transmitted field, respectively, which are given by

$$E_y^i = A_i \psi^i(x) = \begin{cases} A_i \cos(k_1 x) & , \quad |x| \leq d_1 \\ A_i \, e^{\gamma_1 d_1} \cos(k_1 d_1) \, e^{-\gamma_1 |x|} & , \quad |x| \geq d_1 \end{cases} \tag{4.2.3a}$$

$$E_y^r = A_r \psi^r(x) = \begin{cases} A_r \cos(k_1 x) & , \quad |x| \leq d_1 \\ A_r \, e^{\gamma_1 d_1} \cos(k_1 d_1) \, e^{-\gamma_1 |x|} & , \quad |x| \geq d_1 \end{cases} \tag{4.2.3b}$$

$$E_y^t = A_t \psi^t(x) = \begin{cases} A_t \cos(k_2 x) & , \quad |x| \leq d_2 \\ A_t \, e^{\gamma_2 d_2} \cos(k_2 d_2) \, e^{-\gamma_2 |x|} & , \quad |x| \geq d_2 \end{cases} \tag{4.2.3c}$$

where A_i, A_r and A_t are the amplitudes of the incident, reflected and transmitted surface wave modes, respectively. The propagation constant for the surface wave mode in the longitudinal direction is β while in the transverse direction it is denoted by k in the dielectric waveguide and γ in the surrounding medium. These constants are related to one another by the expressions

$$\begin{aligned} k_{1,2} &= (\varepsilon_{r_{1,2}} k_0^2 - \beta_{1,2}^2)^{\frac{1}{2}} \\ \gamma_{1,2} &= (\beta_{1,2}^2 - k_0^2)^{\frac{1}{2}} \\ k_0 &= \omega\sqrt{\mu_0 \varepsilon_0} = \frac{2\pi}{\lambda_0} \end{aligned} \tag{4.2.4}$$

and λ_0 is the free space wavelength. $E_y^r(\rho)$ and $E_y^t(\rho)$ are the radiation modes to the left (backward) and right (forward) sides of the junction, respectively, where

$$E_y^r(\rho) = q_r(\rho)\,\psi^r(\rho) = \begin{cases} q_r(\rho)\cos\sigma x & , \ |x| \leq d_1 \\ q_r(\rho)\,(\Delta_1 e^{j\rho|x|} + \Delta_1^* e^{-j\rho|x|}) & , \ |x| \geq d_1 \end{cases} \tag{4.2.5}$$

$$E_y^t(\rho') = q_t(\rho')\,\psi^t(\rho') = \begin{cases} q_t(\rho')\cos\sigma' x & , \ |x| \leq d_2 \\ q_t(\rho')\,(\Delta_2 e^{j\rho'|x|} + \Delta_2^* e^{-j\rho'|x|}) & , \ |x| \geq d_2 \end{cases} \tag{4.2.6}$$

Here $q_r(\rho)$ and $q_t(\rho')$ are the amplitudes of radiation modes in the backward and forward directions and

$$\Delta_1 = \frac{1}{2} e^{-j\rho d_1}\left(\cos\sigma d_1 + j\,\frac{\sigma}{\rho}\sin\sigma d_1\right) \tag{4.2.7}$$

$$\Delta_2 = \frac{1}{2} e^{-j\rho' d_2}\left(\cos\sigma' d_2 + j\,\frac{\sigma'}{\rho'}\sin\sigma' d_2\right) \tag{4.2.8}$$

and the star superscript denotes the complex conjugate. The propagation constants σ, ρ and β are related to one another by

$$\begin{aligned} \sigma &= (\varepsilon_{r_1} k_0^2 - \beta^2)^{\frac{1}{2}} \\ \rho &= (k_0^2 - \beta^2)^{\frac{1}{2}} \end{aligned} \tag{4.2.9}$$

while the relation between σ', ρ' and β' are still the same as given above, except that ε_{r_1} is replaced by ε_{r_2}.

Applying the orthogonality condition to (4.2.1) and (4.2.2) and normalizing the field expressions, *i.e.*,

$$\int_0^\infty |\psi|^2\, dx = 1 \tag{4.2.10}$$

we obtain after some algebraic manipulation,

$$F_0 A_i(\beta_2 - \beta_1)\int_0^\infty \psi^i\psi^{t*}\, dx + F_0 A_r(\beta_2 + \beta_1)\int_0^\infty \psi^r\psi^{t*}\, dx +$$

$$\int_0^\infty F_1 q_r(\rho)\ (\beta_2 + \beta) \int_0^\infty \psi^r(\rho)\ \psi^{t*}\ dx\ d\rho = 0 \qquad (4.2.11)$$

$$F_0 A_i (\beta_2 + \beta_1) \int_0^\infty \psi^i \psi^{t*}\ dx + F_0 A_r (\beta_2 - \beta_1) \int_0^\infty \psi^r \psi^{t*}\ dx +$$

$$\int_0^\infty F_1 q_r(\rho)\ (\beta_2 - \beta) \int_0^\infty \psi^r(\rho)\ \psi^{t*}\ dx\ d\rho = 2\beta_2\ A_t \qquad (4.2.12)$$

where F_0 and F_1 are given in Appendix D. After performing the integration with the aid of (4.2.3) to (4.2.9), equations (4.2.11) and (4.2.12) can be written, for $d_1 > d_2$, as

$$\frac{A_i}{(\beta_2 + \beta_1)} + \frac{A_r}{(\beta_2 - \beta_1)} + C_0 \int_0^\infty \frac{q_r(\rho)\ F_1 N_1\ d\rho}{\{(\varepsilon_{r_2} - \varepsilon_{r_1})k_0^2 - \beta_2^2 + \beta^2\}\{(\varepsilon_{r_1} - 1)k_0^2 + \beta_2^2 - \beta^2\}(\beta_2 - \beta)}$$

$$= 0 \qquad (4.2.13)$$

$$\frac{A_i}{(\beta_2 - \beta_1)} + \frac{A_r}{(\beta_2 + \beta_1)} + C_0 \int_0^\infty \frac{q_r(\rho)\ F_1 N_1\ d\rho}{\{(\varepsilon_{r_2} - \varepsilon_{r_1})k_0^2 - \beta_2^2 + \beta^2\}\{(\varepsilon_{r_1} - 1)k_0^2 + \beta_2^2 - \beta^2\}(\beta_2 + \beta)}$$

$$= 2\ C_0 \beta_2\ A_t \qquad (4.2.14)$$

while for $d_2 > d_1$

$$\frac{A_i}{(\beta_2 + \beta_1)} + \frac{A_r}{(\beta_2 - \beta_1)} + C_1 \int_0^\infty \frac{q_r(\rho)\ F_1 M_1\ d\rho}{\{(\varepsilon_{r_2} - \varepsilon_{r_1})k_0^2 - \beta_2^2 + \beta^2\}\{(\varepsilon_{r_2} - 1)k_0^2 - \beta_2^2 + \beta^2\}(\beta_2 - \beta)}$$

$$= 0 \qquad (4.2.15)$$

$$\frac{A_i}{(\beta_2 - \beta_1)} + \frac{A_r}{(\beta_2 + \beta_1)} + C_1 \int_0^\infty \frac{q_r(\rho)\ F_1 M_1\ d\rho}{\{(\varepsilon_{r_2} - \varepsilon_{r_1})k_0^2 - \beta_2^2 + \beta^2\}\{(\varepsilon_{r_2} - 1)k_0^2 - \beta_2^2 + \beta^2\}(\beta_2 + \beta)}$$

$$= 2\ C_1 \beta_2\ A_t \qquad (4.2.16)$$

4.2.2 TM Incidence

Similar to the TE case, the following equations are obtained at the junction for TM modes:

$$H_y^i + H_y^r + \int_o^\infty H_y^r(\rho)\, d\rho = H_y^t + \int_o^\infty H_y^t(\rho')\, d\rho' \tag{4.2.17}$$

$$\frac{\beta_1}{\varepsilon_{r_1}(x)} H_y^i - \frac{\beta_1}{\varepsilon_{r_1}(x)} H_y^r - \int_o^\infty \frac{\beta}{\varepsilon_{r_1}(x)} H_y^r(\rho)\, d\rho = \frac{\beta_2}{\varepsilon_{r_2}(x)} H_y^t + \int_o^\infty \frac{\beta'}{\varepsilon_{r_2}(x)} H_y^t(\rho')\, d\rho' \tag{4.2.18}$$

where

$$\varepsilon_{r_1}(x) = \begin{cases} \varepsilon_{r_1}, & |x| \leq d_1 \\ 1, & |x| > d_1 \end{cases} \tag{4.2.19}$$

$$\varepsilon_{r_2}(x) = \begin{cases} \varepsilon_{r_2}, & |x| \leq d_2 \\ 1, & x > d_2 \end{cases} \tag{4.2.20}$$

By applying the orthogonality property and following the same procedure as in the TE case, the integral equations containing the unknown mode amplitudes can be obtained from (4.2.17) and (4.2.18) as

a) for $d_1 > d_2$;

$$\frac{A_i R_0 (\beta_2 S_0 - \beta_1 S_1)}{\{(\varepsilon_{r_2} - \varepsilon_{r_1})k_0^2 - \beta_2^2 + \beta_1^2\}\{(\varepsilon_{r_1} - 1)k_0^2 + \beta_2^2 - \beta_1^2\}(\beta_2^2 - \beta_1^2)} +$$

$$\frac{A_r R_0 (\beta_2 S_0 + \beta_1 S_1)}{\{(\varepsilon_{r_2} - \varepsilon_{r_1})k_0^2 - \beta_2^2 + \beta_1^2\}\{(\varepsilon_{r_1} - 1)k_0^2 + \beta_2^2 - \beta_1^2\}(\beta_2^2 - \beta_1^2)} +$$

$$\int_0^\infty \frac{q_r(\rho)\, R_1(\beta_2 T_0 + \beta T_1)\, d\rho}{\{(\varepsilon_{r_2} - \varepsilon_{r_1})k_0^2 - \beta_2^2 + \beta^2\}\{(\varepsilon_{r_1} - 1)k_0^2 + \beta_2^2 - \beta^2\}(\beta_2^2 - \beta^2)}$$

$$= 0 \qquad (4.2.21)$$

$$\frac{A_i R_0\, (\beta_2 S_0 + \beta_1 S_1)}{\{(\varepsilon_{r_2} - \varepsilon_{r_1})k_0^2 - \beta_2^2 + \beta_1^2\}\{(\varepsilon_{r_1} - 1)k_0^2 + \beta_2^2 - \beta_1^2\}(\beta_2^2 - \beta_1^2)} +$$

$$\frac{A_r R_0\, (\beta_2 S_0 - \beta_1 S_1)}{\{(\varepsilon_{r_2} - \varepsilon_{r_1})k_0^2 - \beta_2^2 + \beta_1^2\}\{(\varepsilon_{r_1} - 1)k_0^2 + \beta_2^2 - \beta_1^2\}(\beta_2^2 - \beta_1^2)} +$$

$$\int_0^\infty \frac{q_r(\rho)\, R_1(\beta_2 T_0 - \beta T_1)\, d\rho}{\{(\varepsilon_{r_2} - \varepsilon_{r_1})k_0^2 - \beta_2^2 + \beta^2\}\{(\varepsilon_{r_1} - 1)k_0^2 + \beta_2^2 - \beta^2\}(\beta_2^2 - \beta^2)}$$

$$= 2\beta_2 A_t \qquad (4.2.22)$$

b) for $d_2 > d_1$;

$$\frac{A_i R_0\, (\beta_2 S_0' - \beta_1 S_1')}{\{(\varepsilon_{r_2} - \varepsilon_{r_1})k_0^2 - \beta_2^2 + \beta_1^2\}\{(\varepsilon_{r_2} - 1)k_0^2 - \beta_2^2 + \beta_1^2\}(\beta_2^2 - \beta_1^2)} +$$

$$\frac{A_r R_0\, (\beta_2 S_0' + \beta_1 S_1')}{\{(\varepsilon_{r_2} - \varepsilon_{r_1})k_0^2 - \beta_2^2 + \beta_1^2\}\{(\varepsilon_{r_2} - 1)k_0^2 - \beta_2^2 + \beta_1^2\}(\beta_2^2 - \beta_1^2)} +$$

$$\int_0^\infty \frac{q_r(\rho)\, R_1(\beta_2 T_0' + \beta T_1')\, d\rho}{\{(\varepsilon_{r_2} - \varepsilon_{r_1})k_0^2 - \beta_2^2 + \beta^2\}\{(\varepsilon_{r_2} - 1)k_0^2 - \beta_2^2 + \beta^2\}(\beta_2^2 - \beta^2)}$$

$$= 0 \qquad (4.2.23)$$

$$\frac{A_i R_0\, (\beta_2 S_0' + \beta_1 S_1')}{\{(\varepsilon_{r_2} - \varepsilon_{r_1})k_0^2 - \beta_2^2 + \beta_1^2\}\{(\varepsilon_{r_2} - 1)k_0^2 - \beta_2^2 + \beta_1^2\}(\beta_2^2 - \beta_1^2)} +$$

$$\frac{A_r R_0\, (\beta_2 S_0' - \beta_1 S_1')}{\{(\varepsilon_{r_2} - \varepsilon_{r_1})k_0^2 - \beta_2^2 + \beta_1^2\}\{(\varepsilon_{r_2} - 1)k_0^2 - \beta_2^2 + \beta_1^2\}(\beta_2^2 - \beta_1^2)} +$$

$$\int_0^\infty \frac{q_r(\rho)\, R_1(\beta_2 T_0' - \beta T_1')\, d\rho}{\{(\varepsilon_{r_2} - \varepsilon_{r_1})k_0^2 - \beta_2^2 + \beta^2\}\{(\varepsilon_{r_2} - 1)k_0^2 - \beta_2^2 + \beta^2\}(\beta_2^2 - \beta^2)}$$

$$= 2\beta_2 A_t \qquad (4.2.24)$$

where the expressions for R_0, R_1, S_0, S_1, T_0, T_1, S_0', S_1', T_0', T_1' are given in Appendix D.

4.3 SOLUTION FOR THE MODE AMPLITUDE

The unknown mode amplitudes $q_r(\rho)$ of equations (4.2.13), (4.2.15), (4.2.21) and (4.2.23) will be determined by applying the residue-calculus method. The main step in the residue-calculus method is to construct a complex function $f(\rho)$, which after being integrated over the contour in the complex plane, gives rise to an equation which is identical to the equation we are attempting to solve. It then becomes possible to identify the unknowns in the equation with the residues or value of $f(\rho)$, thereby extracting the desired solution. In order to construct the function $f(\rho)$ the general properties of $q_r(\rho)$, such as its asymptotic behaviour, its poles, etc., have to be known. This technique will give an exact solution provided that all the singularities of the unknown function, $q_r(\rho)$, are known.

From the observation of the previous problems involving surface wave propagation, it is clear that A_i and A_r are related to $q_r(\rho)$ by familiar relationships similar to those shown by Shevchenko [50], Hessel [56], Tamir [57] and Zucker [24] where the general field is expressed by an integral over the longitudinal wave number β. By closing the countour in the upper or lower half planes of β depending on the region of interest, and using Cauchy's theorem, such a field expansion may be separated into a surface wave field (arising from surface wave poles in the β-plane)

and a radiation field (branch cut integral in the β-plane) which is in the form of an integral over the transverse wave number ρ. Because this integration is always from $-\infty$ to ∞, the integrations in (4.2.13), (4.2.15), (4.2.21) and (4.2.23) will also be extended to that limit. This can be done by considering $q_r(\rho)$ as an even function since all the other quantities in the integrand are even functions of ρ.

4.3.1 Solution for TE Incidence

In order to solve (4.2.13) by the residue-calculus technique, the variables ρ and β are considered complex quantities related to each other by (4.2.9), *i.e.*, $\rho^2 = k_0^2 - \beta^2$. Equation (4.2.13) is rewritten as

$$\frac{A_i}{(\beta_2 + \beta_1)} + \frac{A_r}{(\beta_2 - \beta_1)} + \frac{C_0}{2} \int_{-\infty}^{\infty} \frac{q_r(\rho)\, F_1 N_1\, d\rho}{\{(\varepsilon_{r_2} - \varepsilon_{r_1})k_0^2 - \beta_2^2 + \beta^2\}\{(\varepsilon_{r_1} - 1)k_0^2 + \beta_2^2 - \beta^2\}(\beta_2 - \beta)}$$

$$= 0 \qquad (4.3.1)$$

The properties of $q_r(\rho)$ should be such that when the contour is deformed in the lower half of the ρ-plane, the contribution from the poles must cancel the first two terms and, because the right side of (4.3.1) is zero, the integral around the branch cut due to the term $(\beta_2 - \beta)$ must vanish. To satisfy these requirements, $q_r(\rho)$ must contain a term which permits removing the branch point singularity from the integrand. Another property of $q_r(\rho)$ is that it has an algebraic behaviour at infinity [40], *i.e.*, $q_r(\rho) \sim \rho^{-2}$ as $|\rho| \to \infty$. With this asymptotic behaviour of $q_r(\rho)$, the entire function, in the function to be constructed, is simply a constant which can be found from the incident field. For simplicity, we will start from the β-plane and consider

the contour integral

$$\oint_C \frac{f(\beta)}{\{(\varepsilon_{r_2} - \varepsilon_{r_1})k_0^2 - \beta_2^2 + \beta^2\}\{(\varepsilon_{r_1} - 1)k_0^2 + \beta_2^2 - \beta^2\}(\beta_2 - \beta)} \frac{\beta}{\rho} \, d\beta$$

This contour integral will then be transformed back to the ρ-plane with the bottom sheet of the ρ-plane (Im $\rho < 0$) being chosen. The β-plane corresponding to this sheet is shown in figure 4.2.

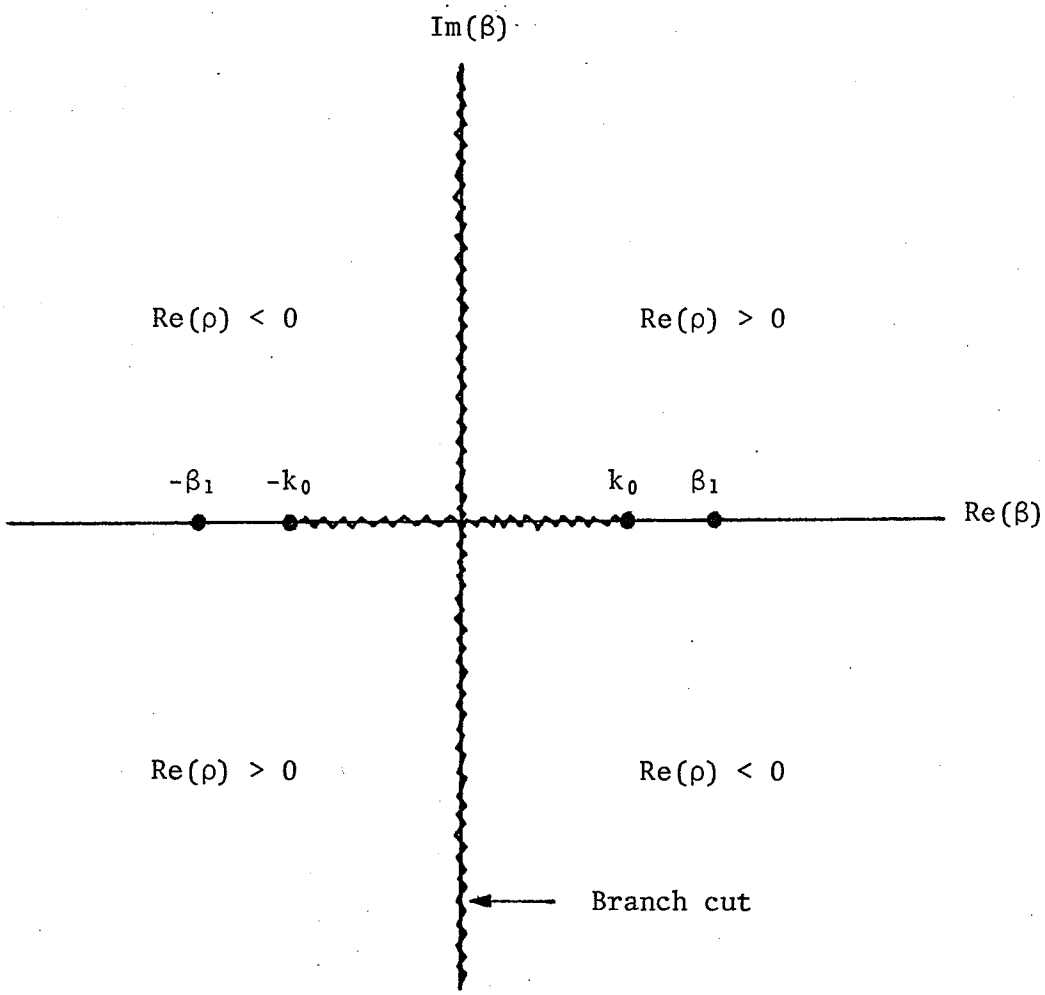

Figure 4.2 β-plane corresponding to Im(ρ) < 0

From the properties of $q_r(\rho)$, the function $f(\beta)$ is constructed in the form

$$f(\beta) = \frac{L_0(1 - \beta/\beta_2)(1 - \beta^2/((\varepsilon_{r_1} - 1)k_0^2 + \beta_2^2))(1 - \beta^2/(\beta_2^2 - (\varepsilon_{r_2} - \varepsilon_{r_1})k_0^2))}{(1 + \beta/\beta_1)(1 - \beta/\beta_1)} \tag{4.3.2}$$

where L_0 is a constant to be determined. After substituting for $f(\beta)$, choosing the contour in the lower half of the β-plane, and transforming the integration along the branch cut into an integral in the ρ-plane we obtain

$$\frac{-(C_0/2)[\text{Res}\{f(\beta);\ -\beta_1\}/\{(\varepsilon_{r_2} - \varepsilon_{r_1})k_0^2 - \beta_2^2 + \beta_1^2\}\{(\varepsilon_{r_1} - 1)k_0^2 + \beta_2^2 - \beta_1^2\}]\beta_1}{(\beta_2 + \beta_1)\ (j\gamma_1)} -$$

$$\frac{(C_0/2)[\text{Res}\{f(\beta);\ \beta_1\}/\{(\varepsilon_{r_2} - \varepsilon_{r_1})k_0^2 - \beta_2^2 + \beta_1^2\}\{(\varepsilon_{r_1} - 1)k_0^2 + \beta_2^2 - \beta_1^2\}](-\beta_1)}{(\beta_2 - \beta_1)\ (j\gamma_1)} +$$

$$\frac{C_0}{2\pi j}\int_{-\infty}^{\infty} \frac{f(\beta)}{\{(\varepsilon_{r_2} - \varepsilon_{r_1})k_0^2 - \beta_2^2 + \beta^2\}\{(\varepsilon_{r_1} - 1)k_0^2 + \beta_2^2 - \beta^2\}(\beta_2 - \beta)}\, d\rho = 0 \tag{4.3.3}$$

where

$$\text{Res}\{f(\beta);\ -\beta_1\} = \frac{[L_0(\beta_2 + \beta_1)\{(\varepsilon_{r_1} - 1)k_0^2 + \beta_2^2 - \beta_1^2\}\{\beta_2^2 - (\varepsilon_{r_2} - \varepsilon_{r_1})k_0^2 - \beta_1^2\}\beta_1]}{[2\beta_2\{(\varepsilon_{r_1} - 1)k_0^2 + \beta_2^2\}\{\beta_2^2 - (\varepsilon_{r_2} - \varepsilon_{r_1})k_0^2\}]} \tag{4.3.4a}$$

$$\text{Res}\{f(\beta);\ \beta_1\} = \frac{[-L_0(\beta_2 - \beta_1)\{(\varepsilon_{r_1} - 1)k_0^2 + \beta_2^2 - \beta_1^2\}\{\beta_2^2 - (\varepsilon_{r_2} - \varepsilon_{r_1})k_0^2 - \beta_1^2\}\beta_1]}{[2\beta_2\{(\varepsilon_{r_1} - 1)k_0^2 + \beta_2^2\}\{\beta_2^2 - (\varepsilon_{r_2} - \varepsilon_{r_1})k_0^2\}]} \tag{4.3.4b}$$

By comparing equations (4.3.3) with (4.3.1), it is found that the amplitudes of the incident and reflected fields can be obtained from the contribution of the poles at $-\beta_1$ and β_1, respectively. Hence, the following relations are obtained:

$$L_0 = \frac{4\, A_i (j\gamma_1)\beta_2 \{(\varepsilon_{r_1} - 1)k_0^2 + \beta_2^2\}\{\beta_2^2 - (\varepsilon_{r2} - \varepsilon_{r_1})k_0^2\}}{C_0(\beta_2 + \beta_1)\beta_1^2} \qquad (4.3.5)$$

$$A_r = \frac{(\beta_2 - \beta_1)}{(\beta_2 + \beta_1)} A_i \qquad (4.3.6)$$

$$q_r(\rho) = \frac{f(\beta)}{\pi j F_1 N_1}\Bigg|_{\beta = \sqrt{k_0^2 - \rho^2}} \qquad (4.3.7)$$

A_t can be found from equation (4.2.14), as

$$A_t = \frac{1}{2C_0\beta_2}\left(\frac{A_i}{\beta_2 - \beta_1} + \frac{A_r}{\beta_2 + \beta_1}\right) - \frac{A_i\gamma_1}{\pi\beta_2(\beta_2 + \beta_1)C_0}\int_{-\infty}^{\infty} \frac{\beta_2 - \beta_1}{(\beta_1^2 - \beta^2)(\beta_2 + \beta)}\, d\rho \qquad (4.3.8)$$

Using the same procedure, the following relations are obtained for the case $d_2 > d_1$,

$$A_r = \frac{(\beta_2 - \beta_1)}{(\beta_2 + \beta_1)} A_i \qquad (4.3.9)$$

$$A_t = \frac{A_i}{\beta_2 C_1}\left(\frac{\beta_2^2 + \beta_1^2}{(\beta_2 - \beta_1)(\beta_2 + \beta_1)^2}\right) - \frac{A_i\gamma_1}{\pi\beta_2(\beta_2 + \beta_1)C_1}\int_{-\infty}^{\infty} \frac{\beta_2 - \beta}{(\beta_1^2 - \beta^2)(\beta_2 + \beta)}\, d\rho \qquad (4.3.10)$$

4.3.2 Solution for TM Incidence

By using the same procedure as in the TE incidence case, the following relations are obtained for TM incidence with $d_1 > d_2$:

$$A_r = \frac{(\beta_2 S_0 - \beta_1 S_1)}{(\beta_2 S_0 + \beta_1 S_1)} A_i \qquad (4.3.11)$$

$$A_t = \frac{R_0 A_i [\{(\beta_2 S_0)^2 + (\beta_1 S_1)^2\}/\beta_2(\beta_2 S_0 + \beta_1 S_1)]}{\{(\varepsilon_{r_2} - \varepsilon_{r_1})k_0^2 - \beta_2^2 + \beta_1^2\}\{(\varepsilon_{r_1} - 1)k_0^2 + \beta_2^2 - \beta_1^2\}(\beta_2^2 - \beta_1^2)} -$$

$$\frac{\gamma_1 R_0 \ (\beta_2 S_0 - \beta_1 S_1) \ A_i}{\pi\beta_2(\beta_2^2 - \beta_1^2)\{(\varepsilon_{r_1} - 1)k_0^2 + \beta_2^2 - \beta_1^2\}\{(\varepsilon_{r_2} - \varepsilon_{r_1})k_0^2 - \beta_2^2 + \beta_1^2\}}$$

$$\int_{-\infty}^{\infty} \frac{(\beta_2 T_0/T_1 - \beta)}{(\beta_1^2 - \beta^2) \ (\beta_2 T_0/T_1 + \beta)} \ d\rho \qquad (4.3.12)$$

while for $d_2 > d_1$,

$$A_r = \frac{(\beta_2 S_0' - \beta_1 S_1')}{(\beta_2 S_0' + \beta_1 S_1')} \ A_i \qquad (4.3.13)$$

$$A_t = \frac{R_0 A_i [\{(\beta_2 S_0')^2 + (\beta_1 S_1')^2\}/\beta_2(\beta_2 S_0' + \beta_1 S_1')]}{\{(\varepsilon_{r_2} - \varepsilon_{r_1})k_0^2 - \beta_2^2 + \beta_1^2\}\{(\varepsilon_{r_2} - 1)k_0^2 - \beta_2^2 + \beta_1^2\}(\beta_2^2 - \beta_1^2)} -$$

$$\frac{\gamma_1 R_0 (\beta_2 S_0' - \beta_1 S_1') \ A_i}{\pi\beta_2\{(\varepsilon_{r_2} - \varepsilon_{r_1})k_0^2 - \beta_2^2 + \beta_1^2\}\{(\varepsilon_{r_2} - 1)k_0^2 - \beta_2^2 + \beta_1^2\}(\beta_2^2 - \beta_1^2)}$$

$$\int_{-\infty}^{\infty} \frac{(\beta_2 T_0'/T_1' - \beta)}{(\beta_1^2 - \beta^2) \ (\beta_2 T_0'/T_1' + \beta)} \ d\rho \qquad (4.3.14)$$

4.3.3 Solution for the Radiated Power

The reflected power P_{rf} and transmitted power P_t can be calculated once A_r and A_t are found by applying equation (2.2.41) for the TE case and equation (2.2.42) for the TM case, with the normalized fields as given by (4.2.10). The radiated power P_r can then be obtained as

$$P_r = P_{in} - P_{rf} - P_t \qquad (4.3.15)$$

where P_{in} denotes the incident power.

4.4 NUMERICAL RESULTS

The radiation losses caused by a symmetrical step with the ratio $d_2/d_1 = 0.5$ for the case $\varepsilon_r = 1.0201$ are plotted in figures 4.3 and 4.4 as a function of kd_1 for TE and TM excitations, respectively. The solid lines are the results obtained from the residue-calculus technique, based on equations (4.3.6), (4.3.8), (4.3.15) for the TE case and equations (4.3.11), (4.3.12), (4.3.15) for the TM case. The dotted lines are the results from applying Kay's solution, as explained in Chapter 2. Also shown in these figures are the results as obtained by Marcuse [23] using two different techniques, the perturbation technique and the method of approximation where a large step is approximated by infinitely many small steps. These results are given here for comparison purpose. The radiation loss of a symmetrical step as a function of d_2/d_1 for $\varepsilon_r = 1.0201$ and $kd_1 = 10.0$ for TE excitation is shown in figure 4.5. The solid line is obtained from the residue-calculus based on equations (4.3.6), (4.3.8), (4.3.15) while the open-circle symbol represents Marcuse's result.

The reflection coefficients at the junction discontinuity with $\varepsilon_{r_1} = 2.56$, $d_2/d_1 = 1.0$ for four different values of ε_{r_2} are plotted against kd_1 in figures 4.6 and 4.7 for TE and TM excitations, respectively. The results in figure 4.6 are based on equation (4.3.6) while figure 4.7 is based on equation (4.3.11). [It should also be noted at this point that as $d_2/d_1 = 1$, the same results can be obtained from equations (4.3.6) and (4.3.9) for the TE case and from equations (4.3.11) and (4.3.13) for the TM case.] For these same cases, the results for the radiation losses are shown in figures 4.8 for TE excitations and (4.9) for TM excitation. The results in figure 4.8 are based on equations

(4.3.6), (4.3.8), (4.3.15) or (4.3.9), (4.3.10), (4.3.15) while figure 4.9 is based on (4.3.11), (4.3.12) (4.3.15) or (4.3.13), (4.3.14), (4.3.15). The results for the transmitted power are shown in figure 4.10 for TE excitation based on equation (4.3.8) or (4.3.10) and figure 4.11 for TM excitation based on equation (4.3.12) or (4.3.14).

The reflection coefficients at the discontinuity junction with $\varepsilon_{r_1} = 2.56$ and $\varepsilon_{r_2} = 5.12$ for different ratios of d_2/d_1 are plotted against kd_1 in figures 4.12 and 4.13 for TE and TM excitations, respectively. The results in figure 4.12 are based on equations (4.3.6) when $d_2/d_1 < 1.0$ and on (4.3.9) when $d_2/d_1 > 1.0$, while figure 4.13 is based on (4.3.11) when $d_2/d_1 < 1.0$ and on (4.3.13) when $d_2/d_1 > 1.0$. For these same cases, the results for the radiation losses are shown in figures 4.14 for TE excitation and 4.15 for TM excitation. The results in figure 4.14 are based on equations (4.3.6), (4.3.8), (4.3.15) when $d_2/d_1 < 1.0$ and on (4.3.9), (4.3.10), (4.3.15) when $d_2/d_1 > 1.0$, while figure 4.15 is based on (4.3.11), (4.3.12), (4.3.15) when $d_2/d_1 < 1.0$ and on (4.3.13), (4.3.14), (4.3.15) when $d_2/d_1 > 1.0$. The results for the transmitted power are shown in figure 4.15, for TE excitation based on (4.3.8) and (4.3.10) when $d_2/d_1 \lesssim 1.0$, and figure 4.17, for TM excitation based on (4.3.12) and (4.3.14) when $d_2/d_1 \lesssim 1.0$.

The discussion of these results and conclusions are given in Chapter 5.

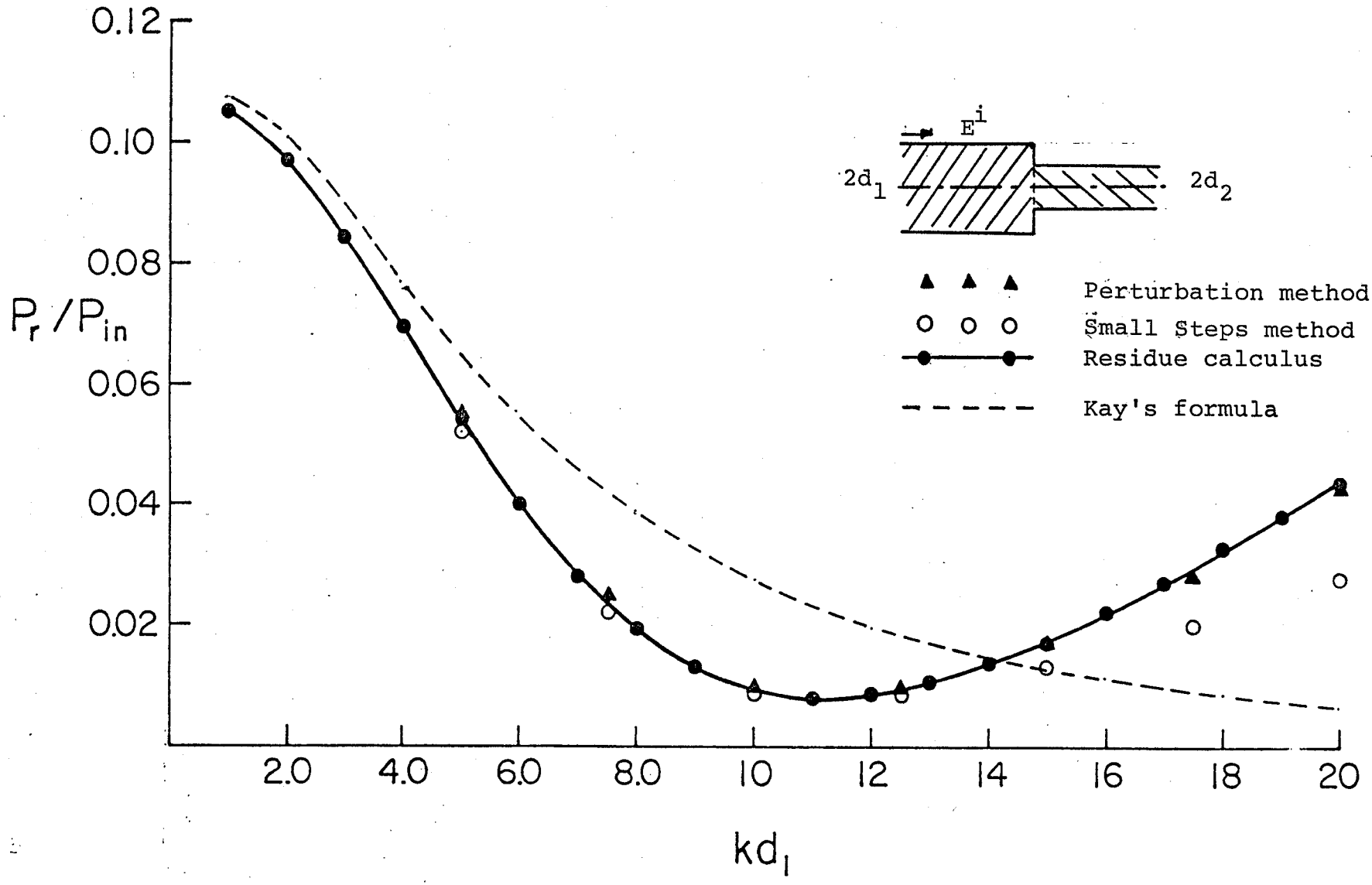

Figure 4.3 Radiation loss for TE incidence with $d_2/d_1 = 0.5$ and $\sqrt{\varepsilon_r} = 1.01$

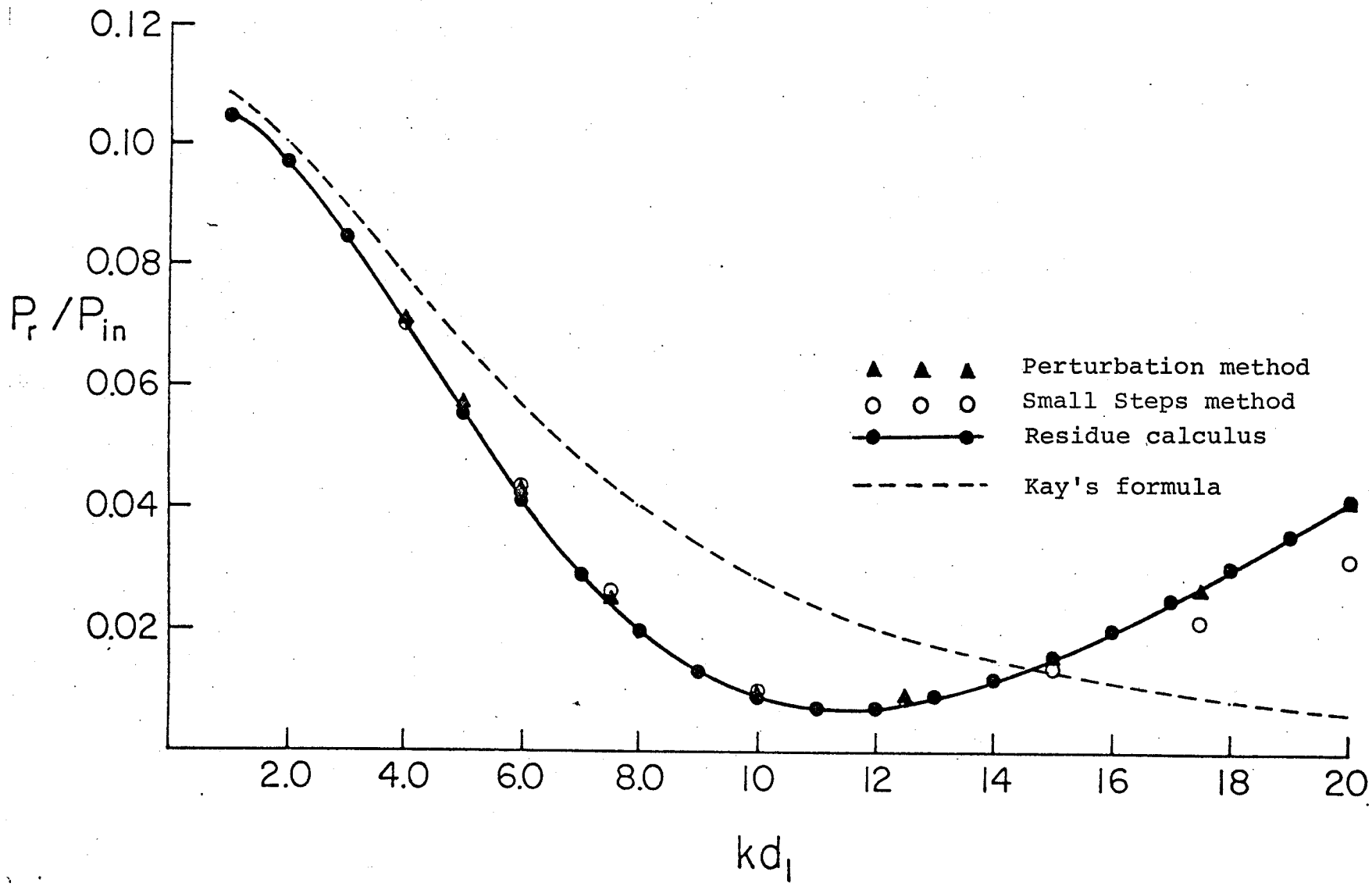

Figure 4.4 Radiation loss for TM incidence with $d_2/d_1=0.5$ and $\sqrt{\varepsilon_r}=1.01$

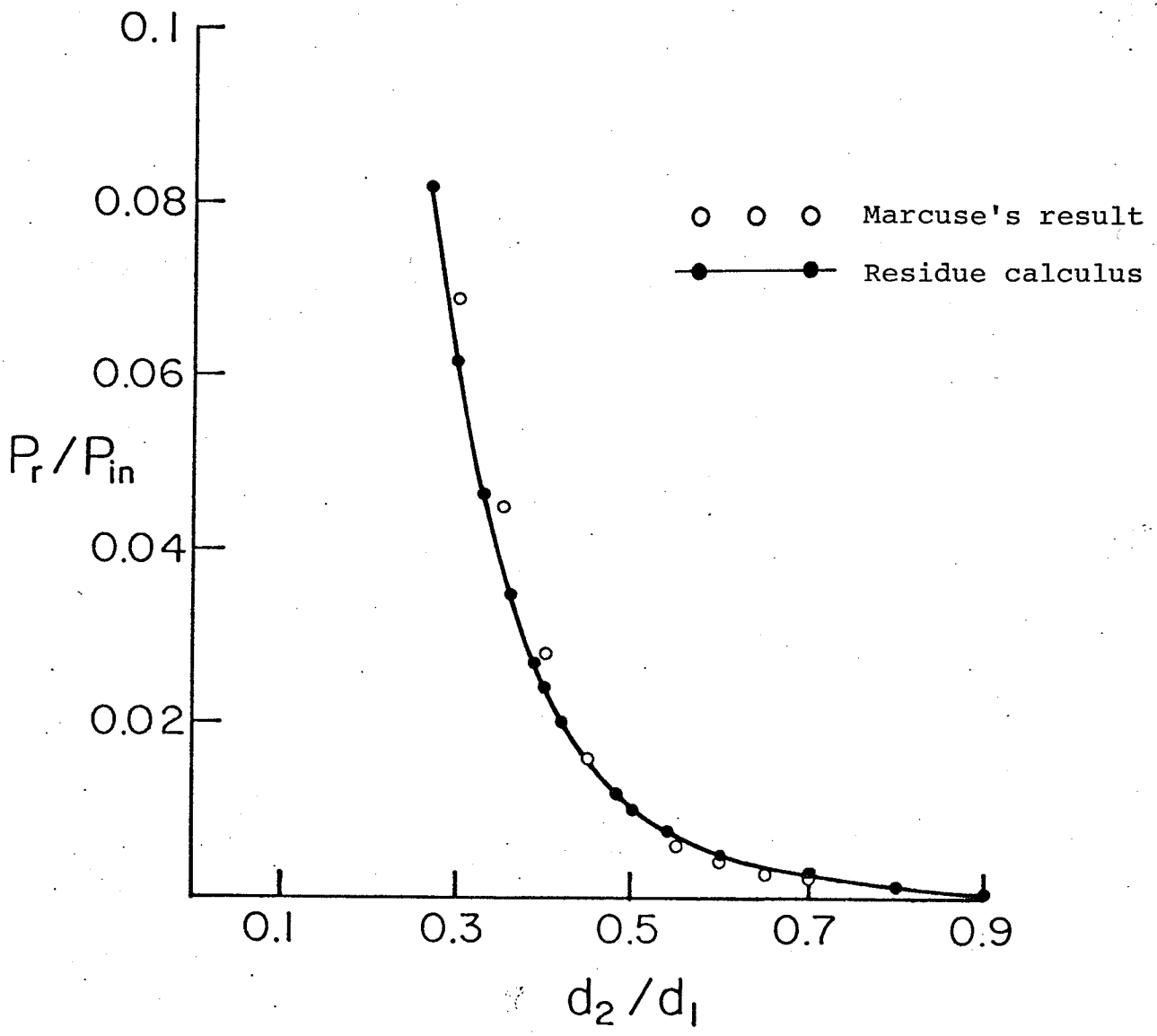

Figure 4.5 Radiation loss for TE incidence with $kd_1=10.0$ and $\sqrt{\varepsilon_r}=1.01$

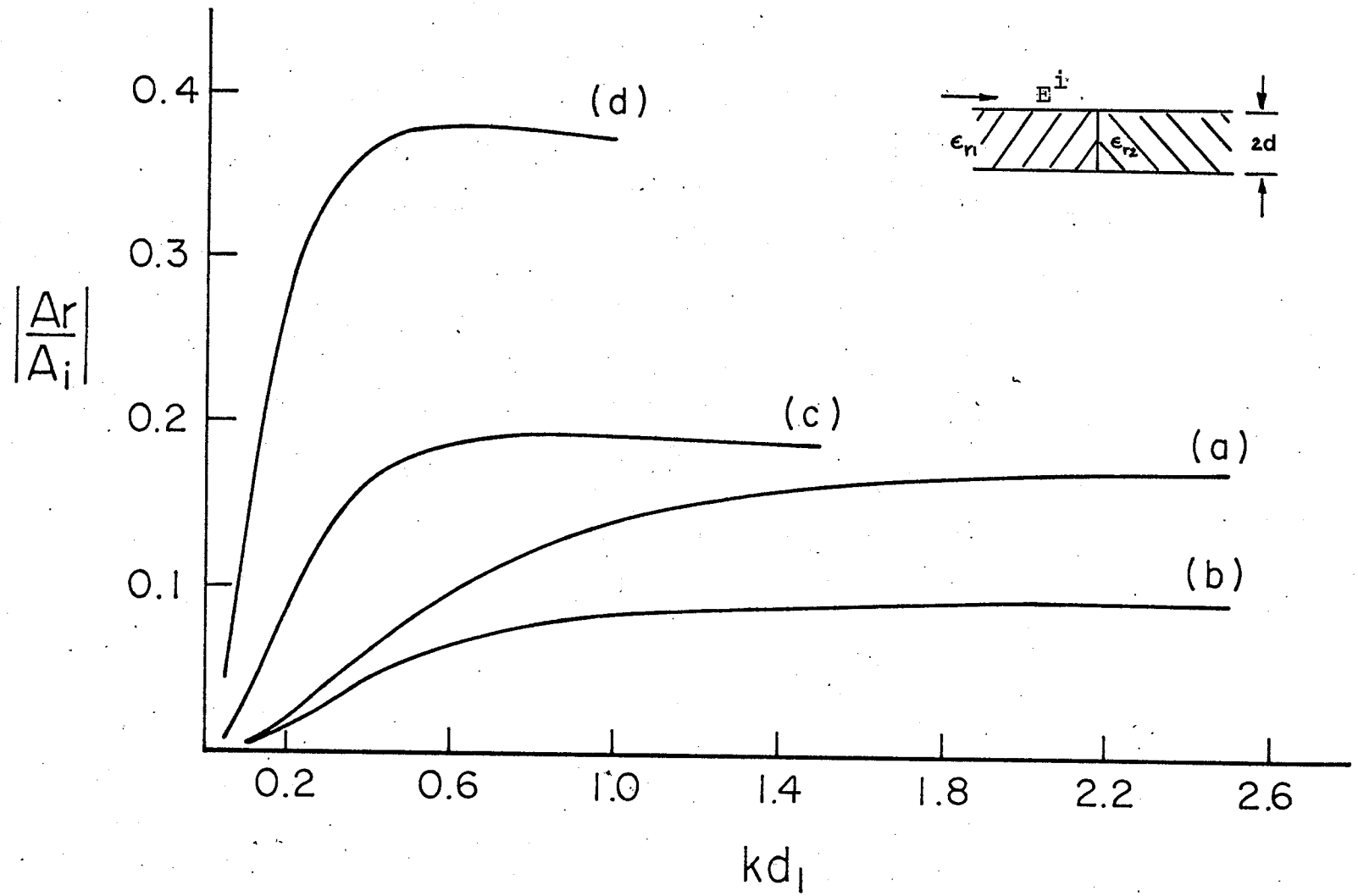

Figure 4.6 Reflection coefficient for TE incidence with $d_2/d_1=1.0$ and $\varepsilon_{r_1}=2.56$ (a) $\varepsilon_{r_2}=1.28$ (b) $\varepsilon_{r_2}=1.8$ (c) $\varepsilon_{r_2}=5.12$ (d) $\varepsilon_{r_2}=10.24$

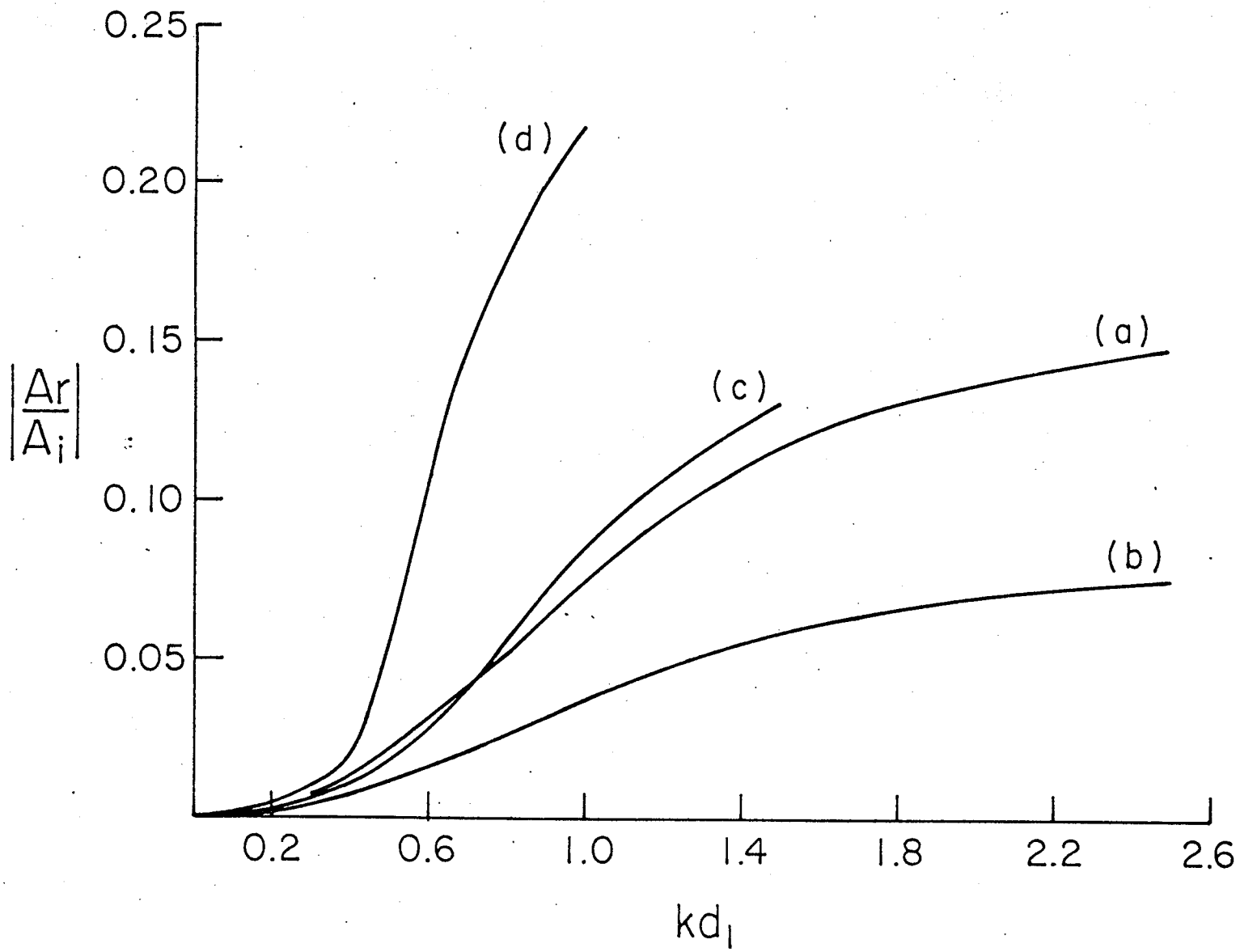

Figure 4.7 Reflection coefficient for TM incidence with the same parameters as for Fig. 4.6

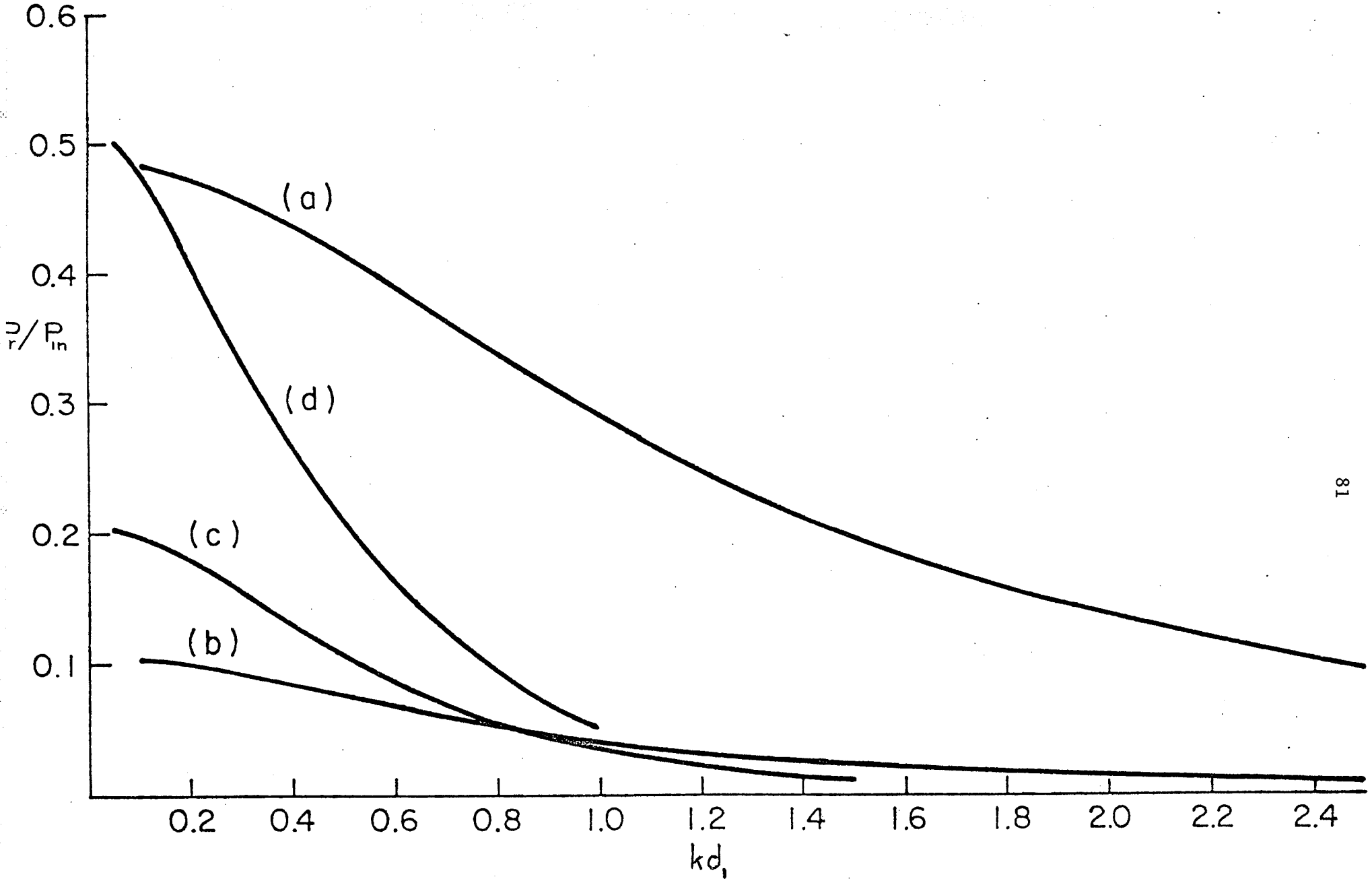

Figure 4.8 Radiation loss for TE incidence with the same parameters as for Fig. 4.6

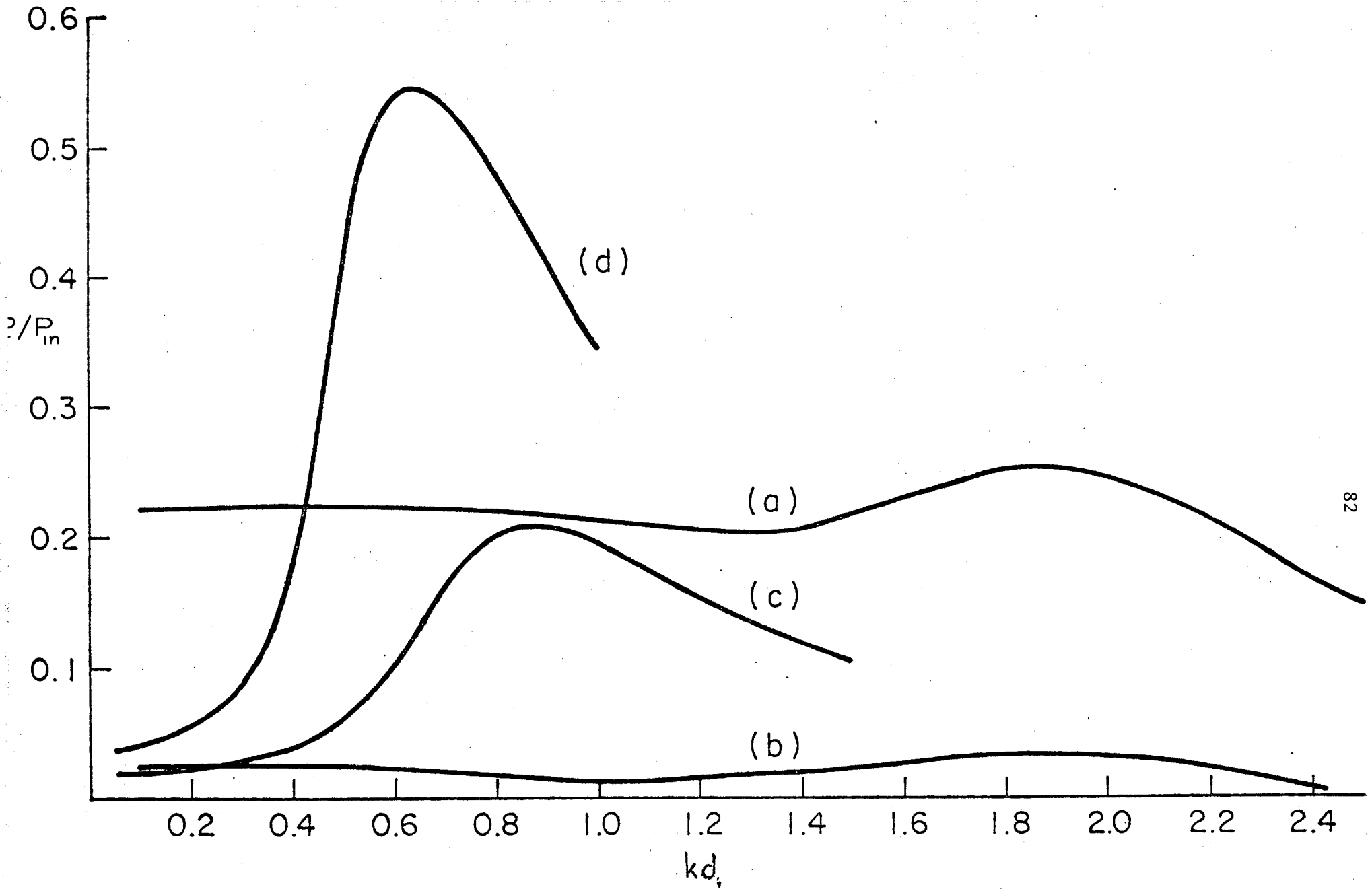

Figure 4.9 Radiation loss for TM incidence with the same parameters as for Fig. 4.6

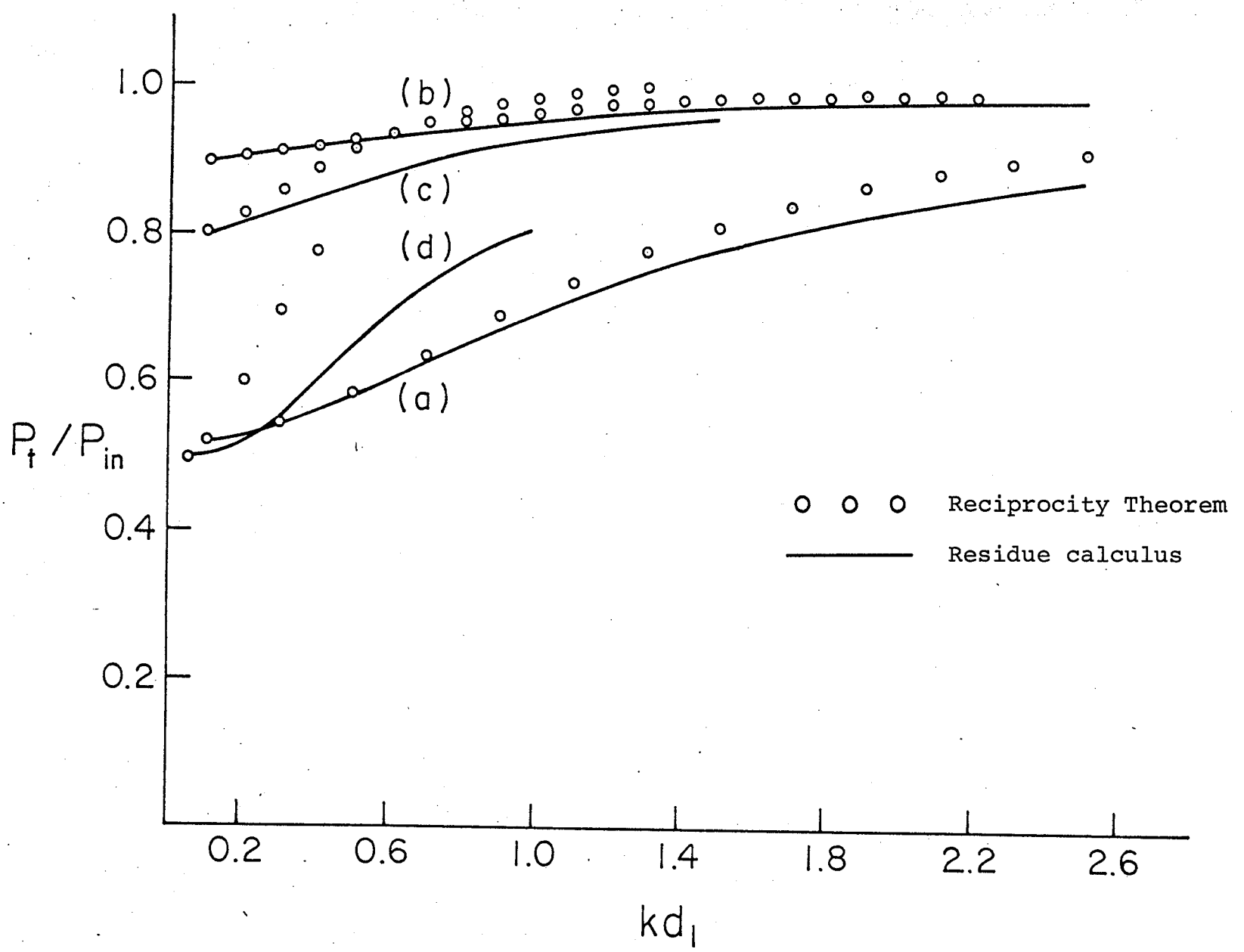

Figure 4.10 Transmitted power for TE incidence with the same parameters as for Fig. 4.6

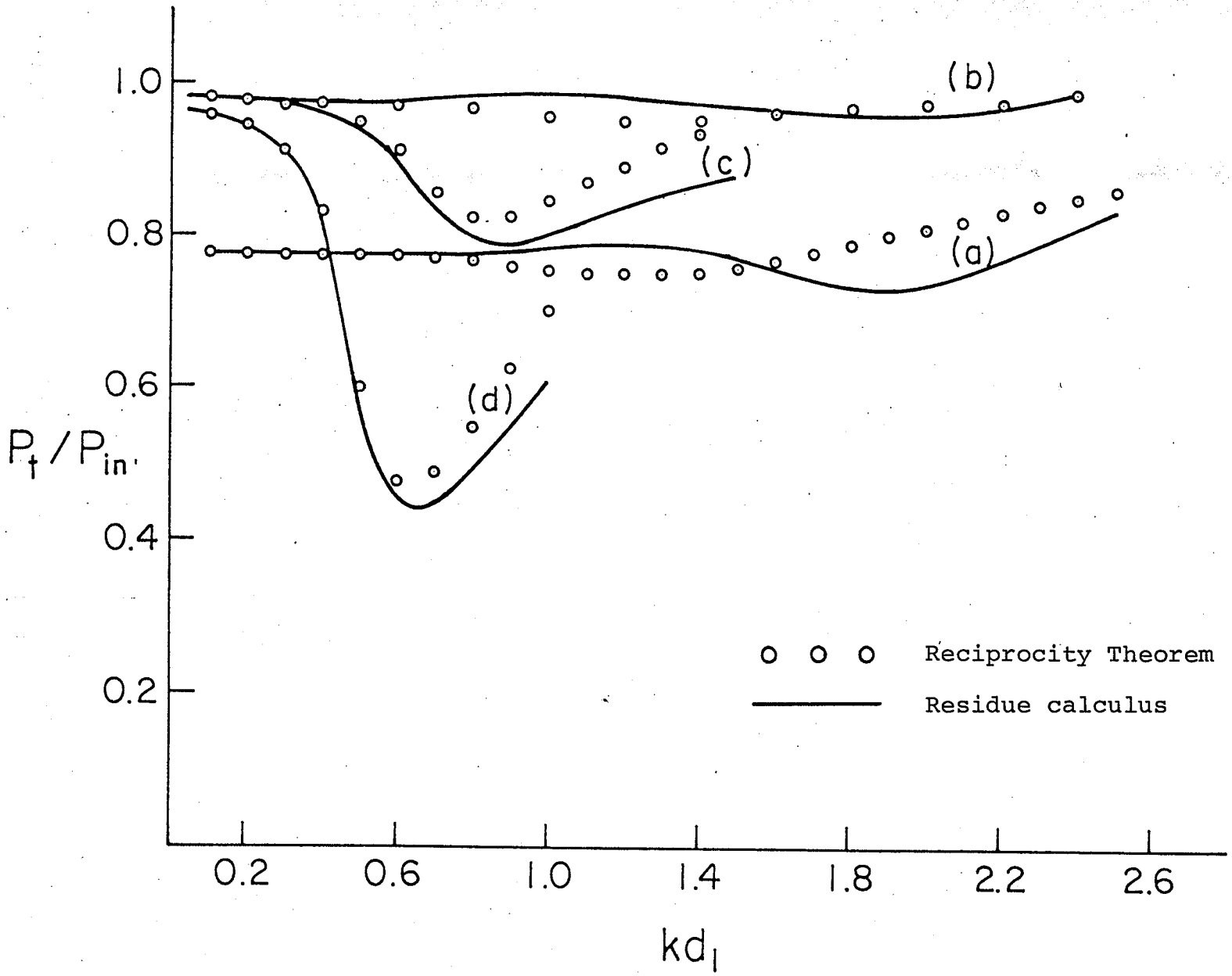

Figure 4.11 Transmitted power for TM incidence with the same parameters as for Fig. 4.6

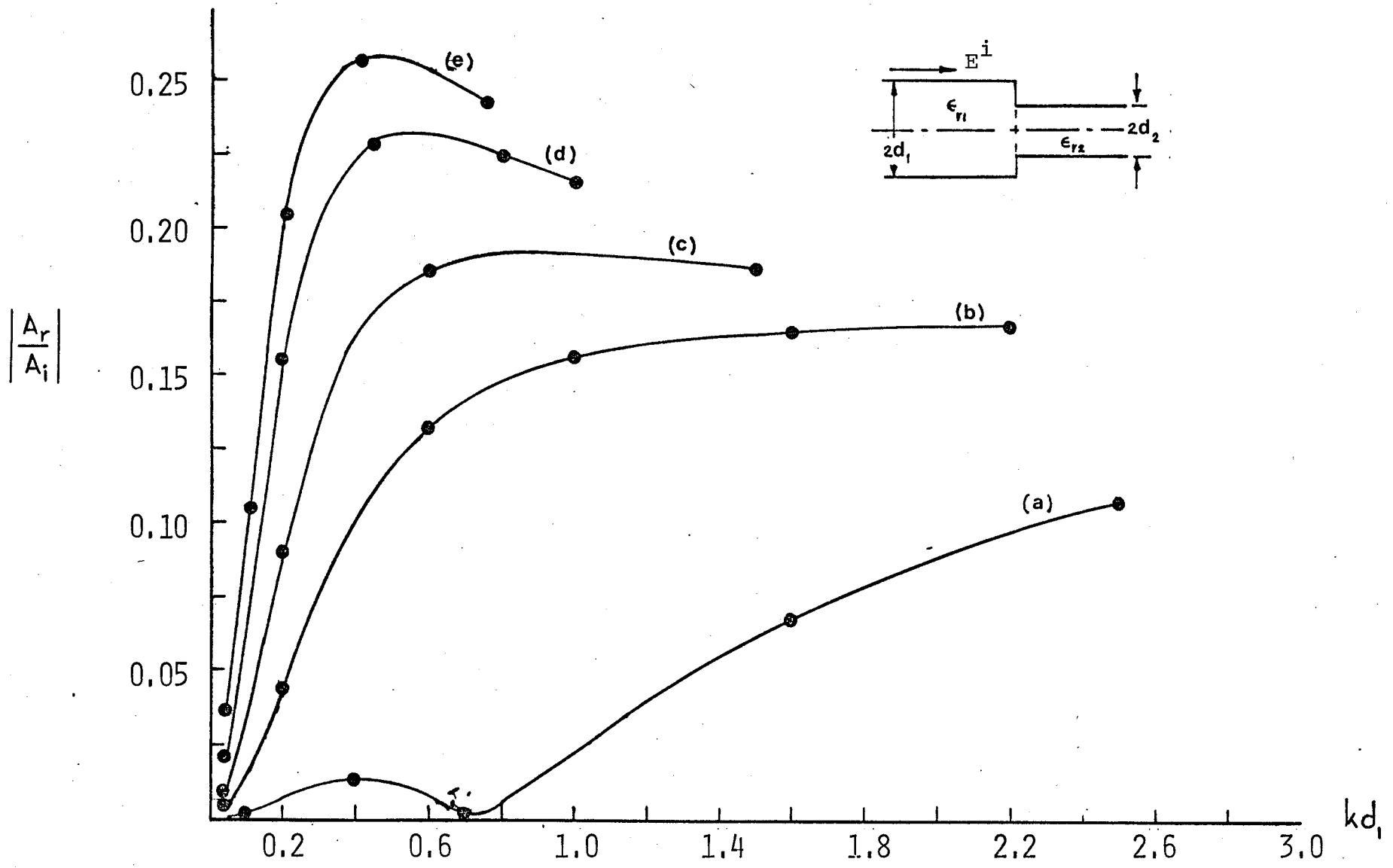

Figure 4.12 Reflection coefficient for TE incidence with $\varepsilon_{r_1}=2.56$ and $\varepsilon_{r_2}=5.12$
(a) $d_2/d_1=0.3$ (b) $d_2/d_1=0.7$ (c) $d_2/d_1=1.0$ (d) $d_2/d_1=1.5$
(e) $d_2/d_1=2.0$

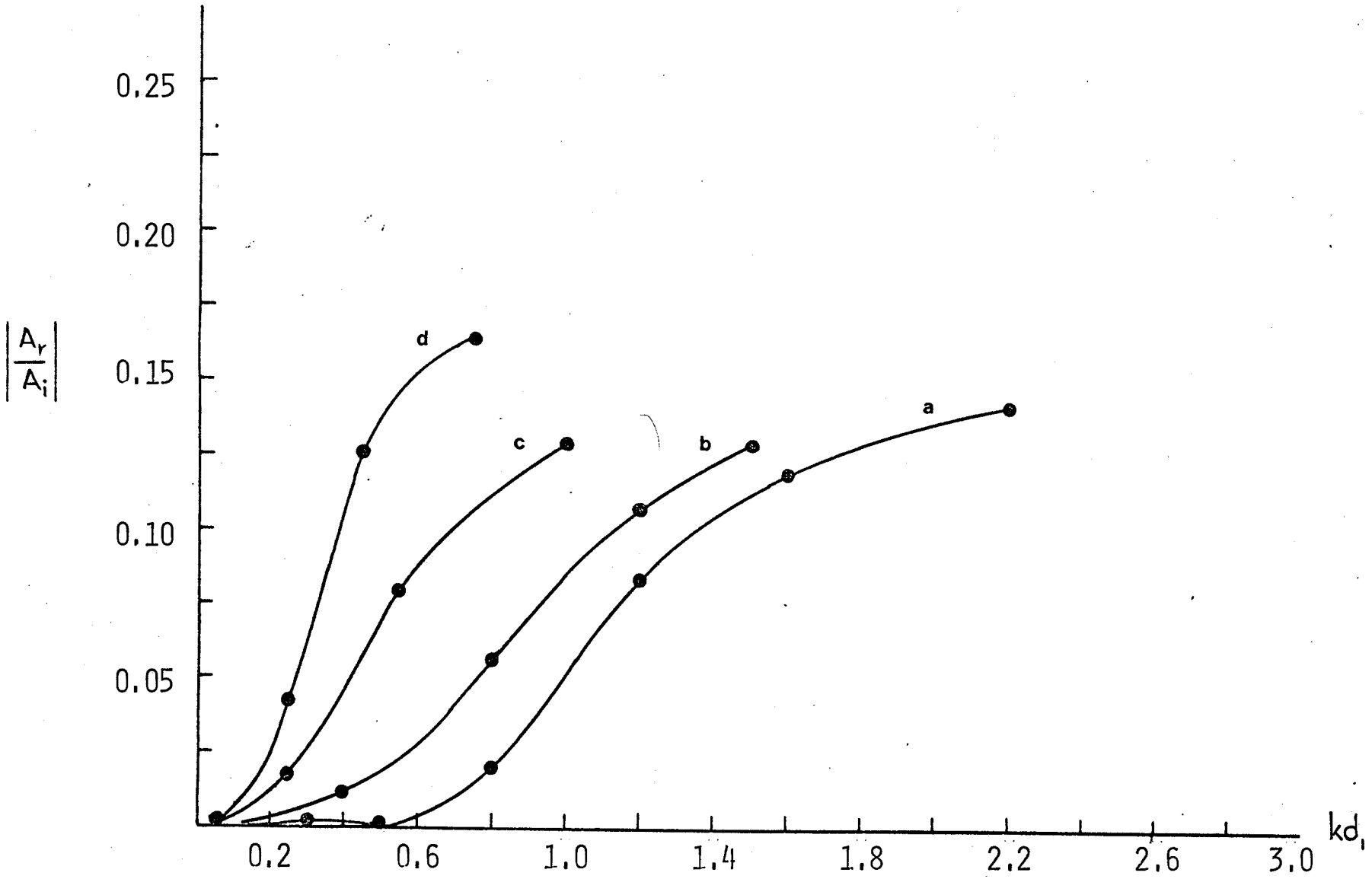

Figure 4.13 Reflection coefficient for TM incidence with $\varepsilon_{r_1}=2.56$ and $\varepsilon_{r_2}=5.12$
(a) $d_2/d_1=0.7$ (b) $d_2/d_1=1.0$ (c) $d_2/d_1=1.5$ (d) $d_2/d_1=2.0$

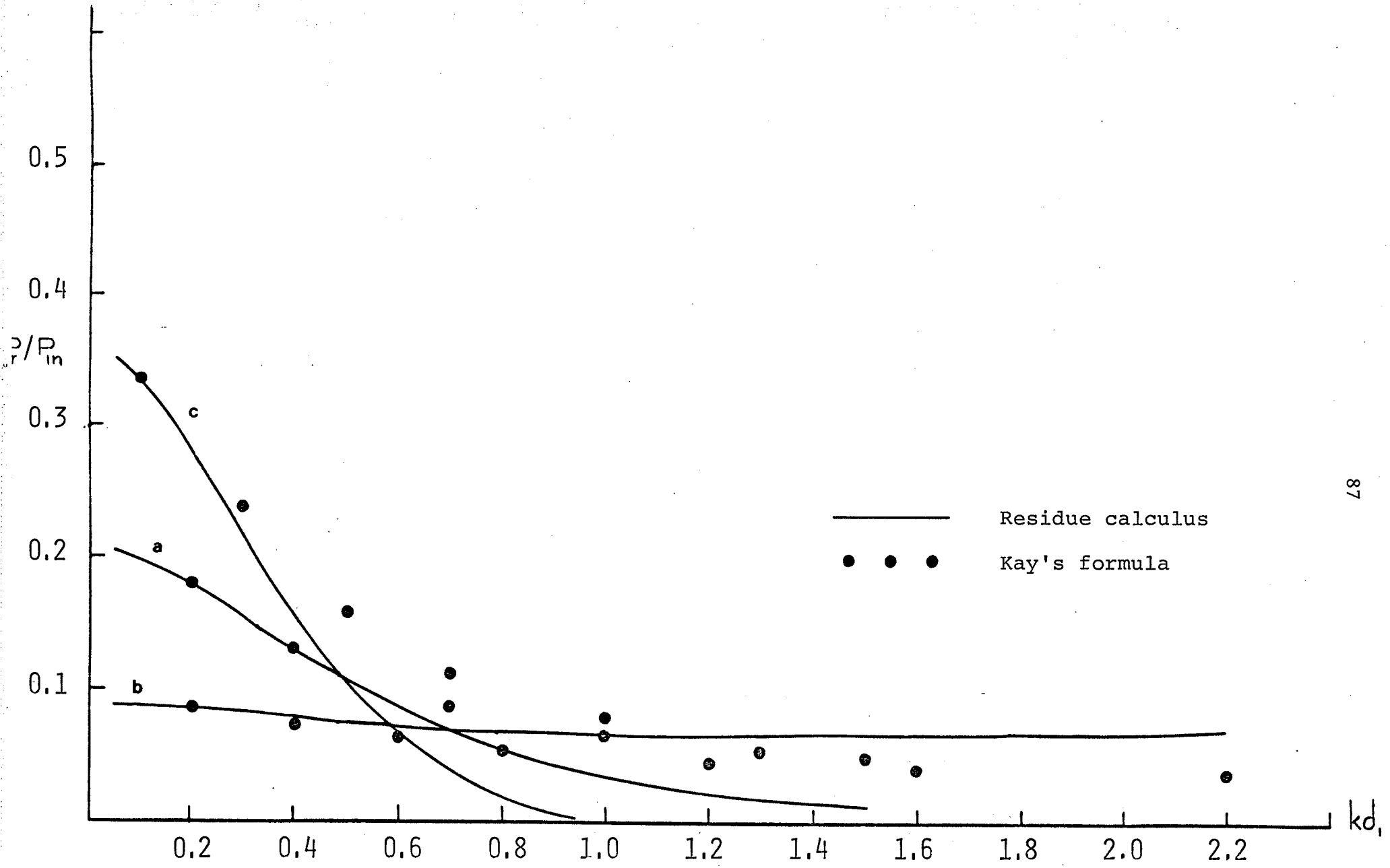

Figure 4.14 Radiation loss for TE incidence with $\varepsilon_{r_1}=2.56$ and $\varepsilon_{r_2}=5.12$ (a) $d_2/d_1=1.0$ (b) $d_2/d_1=0.7$ (c) $d_2/d_1=1.5$

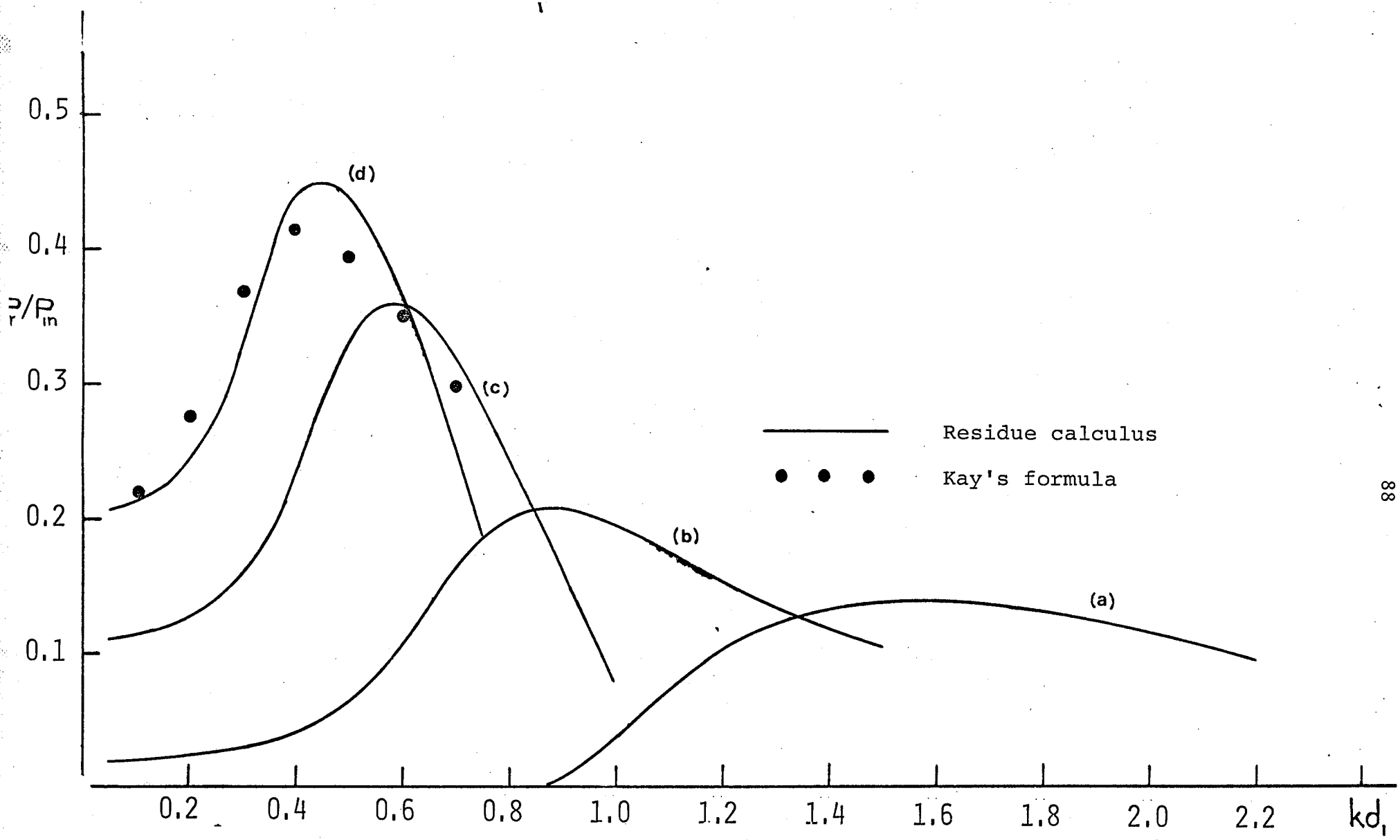

Figure 4.15 Radiation loss for TM incidence with the same parameters as for Fig.4.13

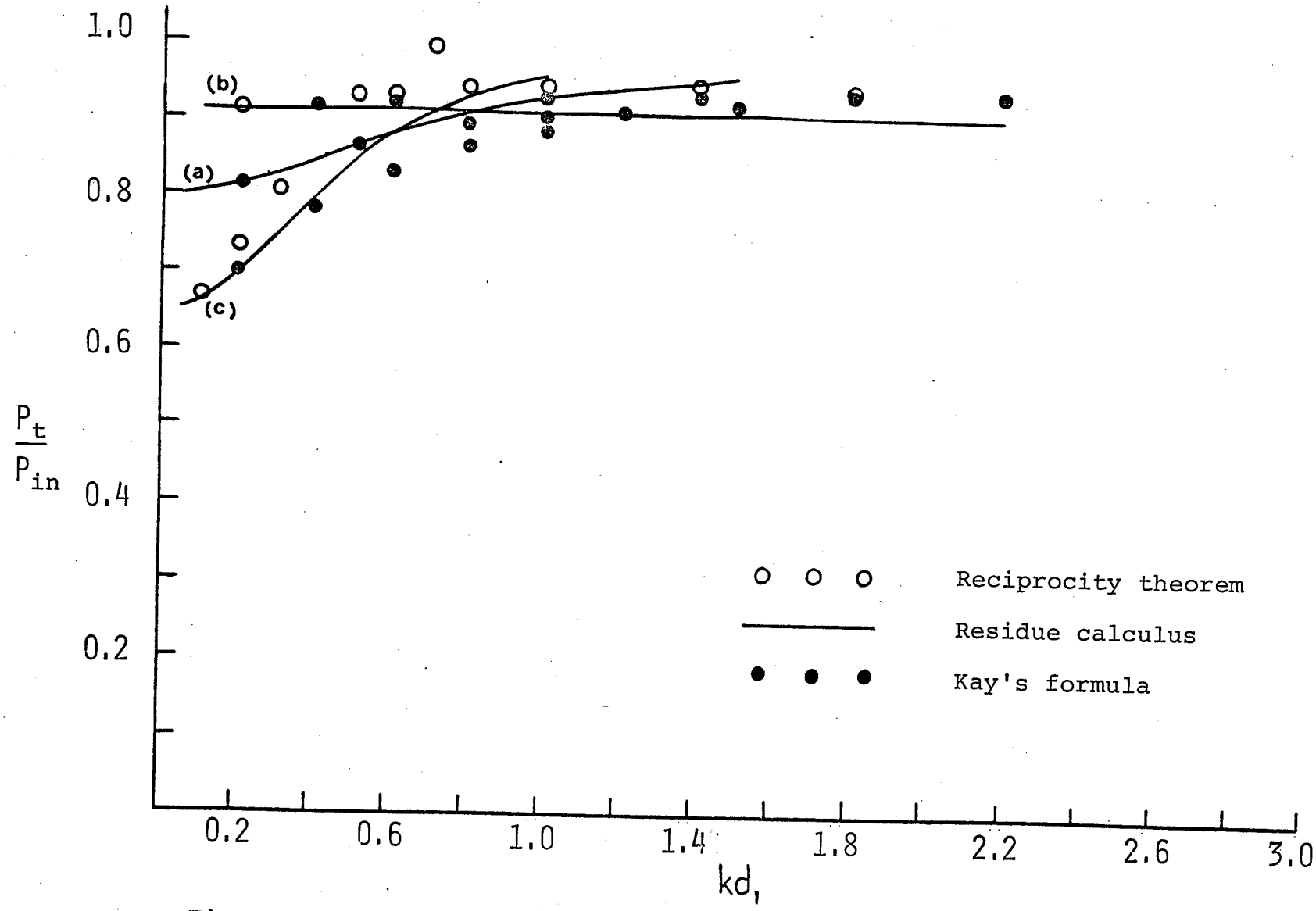

Figure 4.16 Transmitted power for TE incidence with the same parameters as for Fig. 4.14

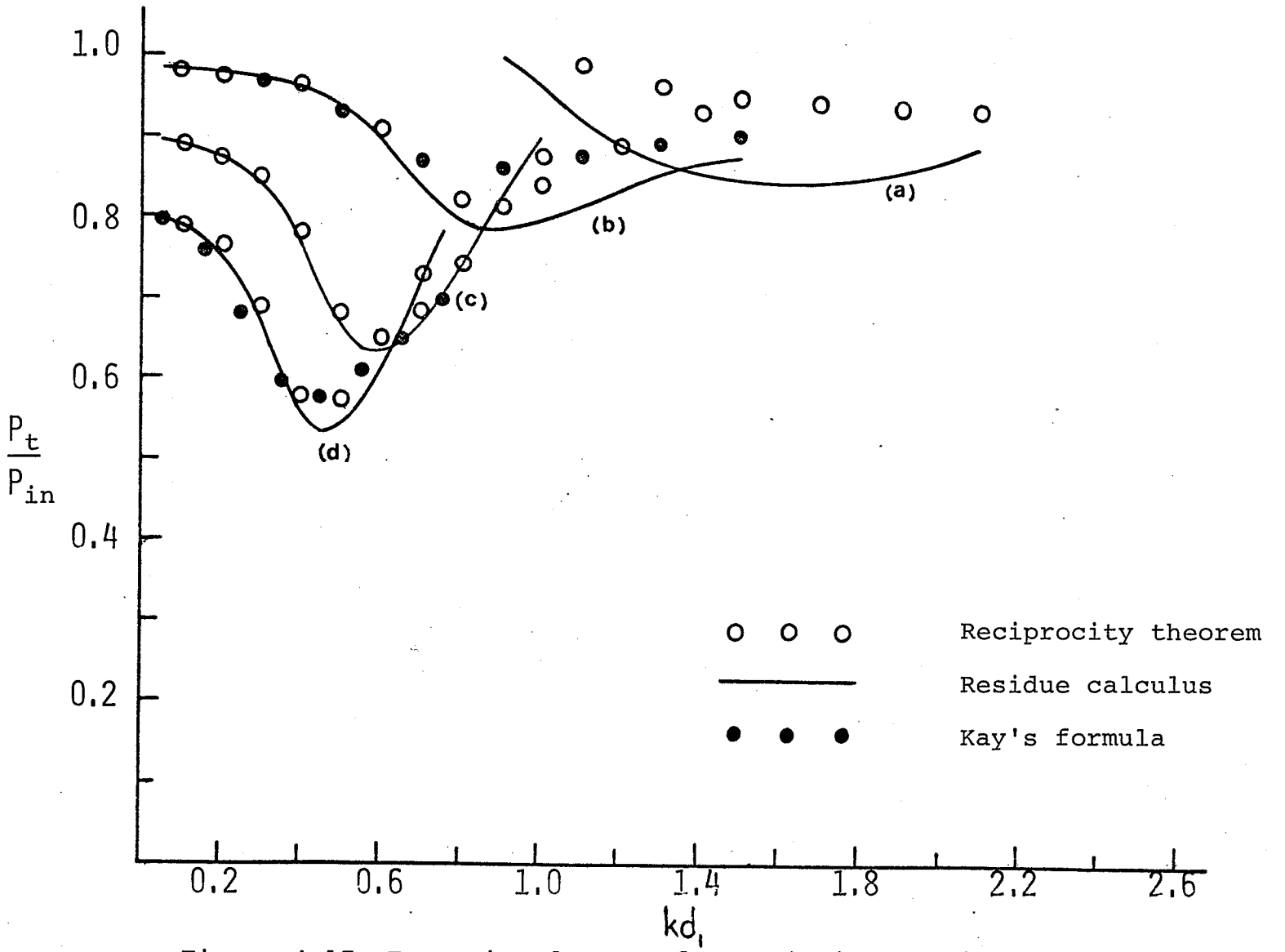

Figure 4.17 Transmitted power for TM incidence with the same parameters as for Fig. 4.13

CHAPTER 5

DISCUSSION AND CONCLUSION

5.1 INTRODUCTION

The problem of discontinuity on a dielectric slab waveguide has been studied for both TE and TM excitations. Because of lack of efficient means to deal with the problem, which generally involves determining the amount of radiation loss, reflected and transmitted powers at the discontinuity, this thesis proposes two new approaches, the Wiener-Hopf and the residue-calculus, to effectively determine these quantities. This study should, therefore, be of interest in designing and evaluating the performance of systems involving dielectric waveguides, such as used in optical communications or surface wave aerial designs. For a better understanding of the proposed techniques, some important features together with the results are discussed in this chapter.

5.2 DISCUSSION

The accuracy of the proposed techniques, the Wiener-Hopf and the residue-calculus are checked by comparing the results obtained with previous results which are available only for simple cases. For more general cases, reliable experimental data over the slab discontinuity is lacking since such experiments are difficult to perform. The results obtained from the proposed techniques are, therefore, compared with those obtained by applications of the reciprocity theorem and Kay's analytical technique. As shown in figures 4.3, 4.4 and 4.5 it is clear that when the residue-calculus method is applied to a step discontinuity involving only a change in slab thickness with the material property remaining the

same on both sides of the junction as considered by Marcuse [23], the results agree very well with his results. As for the general case of step discontinuity, which involves both a change in slab thickness as well as dielectric constant, the results agree with the approximate results obtained by applying the reciprocity theorem and Kay's analytical technique as shown in figures 4.10, 4.11, 4.14, 4.15, 4.16 and 4.17. The agreement of these results are acceptable otherwise deviations can be attributed to the approximations involved in each technique which are discussed later. The good agreement between the Wiener-Hopf and the residue-calculus results is confirmed, as expected, in figures 3.4 and 3.5 from which it appears that the residue-calculus results are more accurate than those obtained by the reciprocity theorem and Kay's analytical technique. It is also found that as the frequency increases, the reflection coefficient is obtained by the residue-calculus and Wiener-Hopf methods converges to the reflection coefficient of the normal plane wave incidence at the junction of two media of infinite dimension, as expected. This is because the dielectric slab will look more like the medium of infinite dimension as frequency increases. However, the results are only presented in the frequency range of single mode operation.

Though the reciprocity theorem and Kay's analytical technique can be applied to approximately solve the general problem of a dielectric slab waveguide discontinuity, they have certain limitations as compared to the Wiener-Hopf and the residue-calculus methods. The limitation of the reciprocity theorem is that it only provides the answer to the amount of transmitted power through the junction. Without a knowledge of the reflected power at the junction, it is impossible to determine the power lost due to radiation. Hence, it is clear that this technique does not

give all the answers to the problem. Moreover, the results obtained are only approximate since the field at the junction is approximated by the incident field. Thus, it is clear from figures 4.10 and 4.16 that the accuracy is lower as either $\varepsilon_{r_2}/\varepsilon_{r_1}$ or d_2/d_1 is increased. On the other hand, Kay's analytical technique can be applied to a dielectric slab discontinuity which can be satisfactorily represented by a discontinuity in surface impedance subject to the condition that $h_2 d \ll 1$ (h_2 is the propagation constant along the x-axis and d is half the slab thickness). When this condition is violated, the representation of a dielectric slab waveguide by surface impedance is not a satisfactory approximation. Thus, the results obtained will be appreciably different from the exact solution. However, it is found from the results presented in Chapter 4 that the application of Kay's analytical technique still gives reasonably good approximate results for the reflected, transmitted and radiated powers for many cases, even though the condition previously mentioned is violated.

The Wiener-Hopf and the residue-calculus techniques, on the contrary, are not subject to those limitations, which restrict the applications of the previous two techniques. Though the Wiener-Hopf technique does not give the exact solution to the problem because the surface wave structures considered always have finite thickness, highly accurate results are still obtained by this technique. It can be seen from the equations (3.2.60), (3.2.61) for TE incidence and (3.2.88), (3.2.89) for TM incidence that the Wiener-Hopf solution contains the unknown constants which are the solution of linear algebraic simultaneous equations of infinite dimension. In order to solve these equations for the unknown constants, they must be first truncated to finite dimension. However, the accuracy of the approximated solutions for the reflected,

transmitted and radiated powers can always be improved by increasing the number of terms "N" in the approximation. From the results shown in Tables (3.1) and (3.2) it is found that in general the nth constant rapidly decreases as n increases. This implies that the convergent solution can be obtained by using only a few terms. The radiation pattern can easily be obtained from equations (3.2.87) and (3.2.94) for TE and TM incidence, respectively. Another advantage of this technique is the possibility of obtaining the diffraction coefficient at the edge of a dielectric slab of finite thickness by following Keller's ray technique [51] and applying equations (3.2.87) and (3.2.94) for TE and TM incidence, respectively.

However, the Wiener-Hopf technique cannot be applied when the thickness on both sides of the junction is not the same. It is found that the formulation for this case by the Wiener-Hopf technique is too complicated. This disadvantage of the Wiener-Hopf technique led to the proposal of the residue-calculus technique which can easily be employed to formulate such problems. This is then the most general technique introduced to solve the problem of a dielectric slab waveguide discontinuity [52]. The technique can for instance be applied to the problem of a step discontinuity which involves both a change in the slab thickness as well as dielectric constant of the guiding structure. Furthermore, the solutions obtained by residue-calculus are in simpler forms than those based on the Wiener-Hopf method, as shown in (4.3.6), (4.3.8), (4.3.9) and (4.3.10) for TE incidence and in (4.3.11), (4.3.12), (4.3.13) and (4.3.14) for TM incidence. This leads to relatively short computer time required by the residue-calculus method as compared to the Wiener-Hopf technique. The major reason for this difference is the step involving factorization and decomposition of the functions, which are quite complicated in the Wiener-Hopf technique. However, this disadvantage

can be improved by further study to somehow perform the factorization and decomposition analytically. The results of the residue-calculus method are highly accurate as already pointed out, even though the asymptotic behaviour (*i.e.*, as $|\rho| \to \infty$) of the constructed function is assumed algebraic of the form ρ^{-2} [40, 41]. When all the requirements as well as the proper boundary conditions are met, as given in Chapter 4, the solution of the residue-calculus method is unique.

Examination of the results for the various numerical examples considered reveals different observations for the TE and TM incidence cases.

For the TE case the numerical results show that the reflection coefficient always increases with frequency up to a certain value beyond which it remains almost constant or decreases slowly. When the thickness on both sides of the junction is the same, the reflection coefficient always increases when ε_{r_2} is increased or decreased with respect to ε_{r_1} (see figure 4.6). However, the rate of increase with frequency is higher for the $\varepsilon_{r_2} > \varepsilon_{r_1}$ case than the $\varepsilon_{r_2} < \varepsilon_{r_1}$ case. The radiated power always increases when ε_{r_2} is increased or decreased with respect to ε_{r_1} and its rate of decrease with frequency is higher for the $\varepsilon_{r_2} < \varepsilon_{r_1}$ case than the $\varepsilon_{r_2} > \varepsilon_{r_1}$ case. (see figure 4.8). This behaviour is opposite to that of the transmitted power (see figure 4.10). When ε_{r_1} and ε_{r_2} are kept constant at 2.56 and 5.12, respectively, and the ratios d_2/d_1 are varied, it is found that the reflection coefficient as well as its rate of increase with frequency is higher for the higher d_2/d_1 ratios as shown in figure 4.12. For the case $d_2/d_1 > 1$, the radiated power at low frequency increases when d_2/d_1 is increased. The rate of decrease of the radiated power with frequency is faster for larger d_2/d_1 ratios as shown in figure 4.14. For the case

$d_2/d_1 < 1$, the radiated power at low frequency increases as d_2/d_1 is decreased. The rate of decrease of radiated power with frequency is higher for small d_2/d_1 ratios. Hence, after a certain frequency, the radiated power becomes smaller for smaller d_2/d_1 ratios as shown in figure 4.14. This behaviour is opposite to that of the transmitted power (figure 4.16).

For TM incidence the numerical examples suggest that the reflection coefficient always increases with frequency. When the thickness on both sides of the junction is the same, the rate of increase of the reflection coefficient with frequency is higher for $\varepsilon_{r_2} > \varepsilon_{r_1}$ case than for $\varepsilon_{r_2} < \varepsilon_{r_1}$ case (see figure 4.7). It is found from the behaviour of the radiated power (figure 4.9), that it increases with frequency when $\varepsilon_{r_2} > \varepsilon_{r_1}$ up to a certain value and then decreases. However, when $\varepsilon_{r_2} < \varepsilon_{r_1}$, the variation of the radiated power with frequency is quite small. This is opposite to the behaviour of the transmitted power when $\varepsilon_{r_2} > \varepsilon_{r_1}$, but the same when $\varepsilon_{r_2} < \varepsilon_{r_1}$ (figure 4.11). By keeping ε_{r_1} and ε_{r_2} constant at 2.56 and 5.12, respectively, while the ratios d_2/d_1 are varied it is found that the rate of increase of the reflection coefficient with frequency is higher for the higher d_2/d_1 ratios (figure 4.13). The radiated power, which increases with frequency up to a certain value then decreases, is greater for the larger d_2/d_1 ratios (figure 4.15). This behaviour is opposite to that of the transmitted power (figure 4.17).

5.3 CONCLUSION

Two new techniques are proposed to solve the problem of discontinuity on the dielectric slab waveguide for single mode operation and for both TE and TM incidence. The Wiener-Hopf method gives a very

accurate result but takes more computer time than the residue-calculus method and can only be applied when the thickness on both sides of the junction are the same. The residue-calculus method, on the other hand, can be applied to a more general class of discontinuities which involves both a change in thickness as well as the dielectric constant of the guide.

Examination of the results reveals that the radiation loss for the TE incidence always decreases with frequency while for the TM case it increases with frequency up to a certain value then decreases. This behaviour is opposite to that of the transmitted power. Thus, for higher transmitted power through the discontinuity junction it is recommended that, for both TE and TM modes, the operating frequency should be close to the value above which the propagation is multimode but the latter can also be operated at the frequency close to its cut-off. The reflected power, on the other hand, is always small compared to the transmitted power for both TE and TM incidence for small step discontinuity.

5.4 SUGGESTIONS FOR FUTURE RESEARCH

As pointed out in the discussion, the factorization and decomposition steps in the Wiener-Hopf technique are performed numerically, which takes rather long computer time. This disadvantage may be removed by further research to obtain these steps analytically. This will also enable the accuracy check, of the technique, based on the conservation of energy at the junction.

In this thesis, the emphasis is on finding new efficient techniques to solve the problem of one dielectric waveguide terminated by another dielectric guide. The techniques can then be applied to generated data in order to find the optimized ratios of $\varepsilon_{r_2}/\varepsilon_{r_1}$ and d_2/d_1

for each type of intended operation (*i.e.*, antenna or surface waveguide). Further research, which can also be done by applying the proposed techniques in this thesis, is necessary to solve the problem of inserting a finite section of one dielectric waveguide into another waveguide. In principle this can be done by expanding the field in each section of a dielectric slab waveguide by surface wave and continuous modes as in Chapter 4. By applying the boundary conditions and orthogonality property at discontinuity junctions, it should be possible to obtain the integral equations for the unknown mode amplitudes which may be solved by the residue-calculus method. The results of this research, if successful, should find applications in surface wave antennas design. It will also help to explain how energy is radiated at a certain designated point of discontinuity along the surface waveguide.

It is generally known that dielectric waveguides are in practice always cylindrical, similar to those applied in fiber optic communications. Further research can, therefore, be done by applying the proposed techniques to the analysis of discontinuities in cylindrical dielectric waveguide.

The diffraction of a plane wave by a thin dielectric half plane was recently reported by Anderson [55], basing his analysis on the impedance boundary condition which requires that the dielectric slab be sufficiently thin. Thus, his results cannot be applied to a thick dielectric half plane. However, it seems possible that the application of the Wiener-Hopf technique to a dielectric slab waveguide discontinuity, Chapter 3, can be modified to solve for the diffraction of a plane wave by a thick dielectric half plane. This research, if successful, will give the more general optical diffraction coefficient at the dielectric edge which will be useful in the study of surface wave antennas.

APPENDIX A

It will be shown in this appendix, that f_n^A and f_n^B for $n = 0, 1, 2, \ldots$ can be obtained from $\Phi_-^{I'}(\alpha,d)$ and $\Phi_+^{III'}(\alpha,d)$ at certain points in the α-plane. For convenience, equations (3.2.28) and (3.2.29) are rewritten

$$\Phi_-^I(\alpha,d) = \frac{\cosh (\alpha^2 - k_1^2)^{\frac{1}{2}} d \; \Phi_-^{I'}(\alpha,d)}{(\alpha^2 - k_1^2)^{\frac{1}{2}} \sinh (\alpha^2 - k_1^2)^{\frac{1}{2}} d} - \frac{2}{d} \sum_{n=0}^{\infty} \frac{\varepsilon_n' (f_n^A + j\alpha f_n^B)}{[\alpha^2 - k_1^2 + (\frac{n\pi}{d})^2]} \cos n\pi \tag{A-1}$$

$$\Phi_+^{III}(\alpha,d) = \left[\Phi_+^{III'}(\alpha,d) + j \frac{A_i (\alpha + \beta_1)(k_1^2 - \beta_1^2)^{\frac{1}{2}} \sin (k_1^2 - \beta_1^2)^{\frac{1}{2}} d}{\sqrt{2\pi}\,(\alpha^2 - k_2^2 + k_1^2 - \beta_1^2)} \right]$$

$$\frac{\cosh (\alpha^2 - k_2^2)^{\frac{1}{2}} d}{(\alpha^2 - k_2^2)^{\frac{1}{2}} \sin (\alpha^2 - k_2^2)^{\frac{1}{2}} d} + \frac{2}{d} \sum_{n=0}^{\infty} \frac{\varepsilon_n' (f_n^A + j\alpha f_n^B)}{[\alpha^2 - k_2^2 + (\frac{n\pi}{d})^2]} \cos n\pi +$$

$$j \frac{A_i (\alpha + \beta_1) \cos (k_1^2 - \beta_1^2)^{\frac{1}{2}} d}{\sqrt{2\pi}\,(\alpha^2 - k_2^2 + k_1^2 - \beta_1^2)} \tag{A-2}$$

where $\varepsilon_n' = 1$ for $n \geq 1$

$= \frac{1}{2}$ for $n = 0$

The two equations above (A-1) and (A-2) are regular in the lower and upper half of α plane satisfying $\mathrm{Im}(\alpha) \leq k_0''$ and $\mathrm{Im}(\alpha) \geq -k_0''$, respectively. Let us first consider (A-2) which is regular in the upper half of the α-plane. It is clear that the left hand side is already regular in the upper half plane but the right hand side has poles at $\alpha = -k_2$, $j\gamma_n'$, $n = 1, 2, 3, \ldots$ where $\gamma_n' = \{(\frac{n\pi}{d})^2 - k_2^2\}^{\frac{1}{2}}$. In order to make the right hand side regular, the residues at these α must vanish, thus we

have

$$\varepsilon_n' \cos n\pi f_n^A - \varepsilon_n' \cos n\pi \gamma_n' f_n^B = j \frac{A_i(\beta_0 + j\gamma_n')(k_1^2 - \beta_1^2)^{\frac{1}{2}} \sin(k_1^2 - \beta_1^2)^{\frac{1}{2}} d}{\sqrt{2\pi}\,(\beta_1^2 + (\frac{n\pi}{d})^2 - k_1^2)} -$$

$$\Phi_+^{III'}(j\gamma_n', d) \quad ; \quad n = 1, 2, 3, \ldots \qquad \text{(A-3)}$$

and for $n = 0$,

$$\varepsilon_0' f_0^A - jk_2\, \varepsilon_0' f_0^B = j \frac{A_i(k_2 - \beta_1) \sin(k_1^2 - \beta_1^2)^{\frac{1}{2}} d}{2\sqrt{2\pi}\,(k_1^2 - \beta_1^2)^{\frac{1}{2}}} - \frac{\Phi_+^{III'}(-k_2, d)}{2} \qquad \text{(A-4)}$$

Following similar arguments applying to (A-1) in the lower half plane, we have for $n \geq 1$

$$\varepsilon_n' \cos n\pi f_n^A + \varepsilon_n' \cos n\pi \gamma_n f_n^B = \Phi_-^{I'}(-j\gamma_n, d) \qquad \text{(A-5)}$$

and for $n = 0$,

$$\varepsilon_0' f_0^A + jk_1 \varepsilon_0' f_0^B = \frac{\Phi_-^{I'}(k_1, d)}{2} \qquad \text{(A-6)}$$

where $\gamma_n = \{(\frac{n\pi}{d})^2 - k_1^2\}^{\frac{1}{2}}$

Solving equations (A-3) and (A-5) gives,

$$\varepsilon_n' \cos n\pi f_n^A = \frac{\gamma_n' \Phi_-^{I'}(-j\gamma_n, d) - \gamma_n \Phi_+^{III'}(j\gamma_n', d)}{(\gamma_n + \gamma_n')} +$$

$$j \frac{A_i \gamma_n (\beta_1 + j\gamma_n')(k_1^2 - \beta_1^2)^{\frac{1}{2}} \sin(k_1^2 - \beta_1^2)^{\frac{1}{2}} d}{\sqrt{2\pi}\,(\beta_1^2 + (\frac{n\pi}{d})^2 - k_1^2)(\gamma_n + \gamma_n')} \qquad \text{(A-7)}$$

$$\varepsilon_n' \cos n\pi f_n^B = \frac{\Phi_-^{I'}(-j\gamma_n, d) + \Phi_+^{III'}(j\gamma_n', d)}{(\gamma_n + \gamma_n')} -$$

$$j \frac{A_i(\beta_1 + j\gamma_n')(k_1^2 - \beta_1^2)^{\frac{1}{2}} \sin(k_1^2 - \beta_1^2)^{\frac{1}{2}} d}{\sqrt{2\pi}\,(\gamma_n + \gamma_n')(\beta_1^2 + (\frac{n\pi}{d})^2 - k_1^2)} \qquad \text{(A-8)}$$

Similarly solving equations (A-4) and (A-6) gives,

$$\varepsilon_0' f_0^A = \frac{k_2 \Phi_-^{I'}(k_1,d) - k_1 \Phi_+^{III'}(-k_2,d)}{2(k_1 + k_2)} + j \frac{A_i k_1 (k_2 - \beta_1) \sin(k_1^2 - \beta_1^2)^{\frac{1}{2}} d}{2\sqrt{2\pi}\,(k_1 + k_2)(k_1^2 - \beta_1^2)^{\frac{1}{2}}} \tag{A-9}$$

and

$$\varepsilon_0' f_0^B = \frac{\Phi_-^{I'}(k_1,d) + \Phi_+^{III'}(-k_2,d)}{2j(k_1 + k_2)} - \frac{A_i (k_2 - \beta_1) \sin(k_1^2 - \beta_1^2)^{\frac{1}{2}} d}{2\sqrt{2\pi}\,(k_1 + k_2)(k_1^2 - \beta_1^2)^{\frac{1}{2}}} \tag{A-10}$$

APPENDIX B

The modified Lee and Mittra factorization formulas [39] are given in this appendix for k_0 with the negative imaginary part defined by

$$k_0 = k_0' - jk_0'' \quad ; \quad k_0' \text{ and } k_0'' > 0$$

Theorem: Let $G(\alpha)$ be an analytic function of α, $(\alpha = \sigma + j\tau)$ and let it satisfy the following conditions in the strip $|\tau| < \tau_+$:

(a) $G(\alpha)$ is regular in the strip.

(b) $G(\alpha)$ is non-zero and even, that is $G(-\alpha) = G(+\alpha) \neq 0$.

(c) $G(\alpha) \sim B\alpha^{\nu} e^{-h|\alpha|}$ as $|\sigma| \to \infty$, where ν and h are real constants.

Furthermore, let $G(\alpha)$ have the following properties in the upper half plane $\tau > -\tau_+$.

(a) a finite number of simple zeros at $\alpha = -\xi_m$, where $\text{Im}(\xi_m) < -\tau_+$, $m = 1, 2, 3, \ldots, M$.

(b) a finite number of simple poles at $\alpha = -\eta_n$, where $\text{Im}(\eta_n) < -\tau_+$, $n = 1, 2, 3, \ldots, N$.

(c) at most one branch singularity at $\alpha = -k_0$ in the form $\gamma = (\alpha^2 - k_0^2)^{\frac{1}{2}}$.

Then for α within the strip, we have

$$G(\alpha) = G_+(\alpha)\, G_-(\alpha) \tag{B-1}$$

where $G_+(\alpha)$ and $G_-(\alpha)$ are non-zero in the upper $(\tau > -\tau_+)$ and lower $(\tau < \tau_+)$ α-plane, respectively. The expressions for $G_+(\alpha)$ and $G_-(\alpha)$ are

$$G_+(\alpha) = G_-(-\alpha) = \sqrt{G(0)}\,\left(1 - \frac{\alpha}{k_0}\right)^{\nu_0/2} \prod_{m=1}^{M}\left(1 - \frac{\alpha}{\xi_m}\right) \prod_{n=1}^{N}\left(1 - \frac{\alpha}{\eta_n}\right)^{-1}$$

$$\exp\left[j\,\frac{k_0 h}{2} + j\,\frac{h\gamma}{\pi}\,\ell n\,\left(\frac{\alpha - \gamma}{k_0}\right) + q(\alpha) + \sum_n R_n(\alpha)\right] \tag{B-2}$$

where

$$\gamma = (\alpha^2 - k_0^2)^{\frac{1}{2}} \quad \text{with the branch} \quad \mathrm{Re}(\gamma) > 0 \quad \text{is chosen} \tag{B-3}$$

$$q(\alpha) = -\fint_0^\infty K(w)\, \ell n \left[1 - \frac{\alpha}{(k_0^2 - w^2)^{\frac{1}{2}}} \right] dw \tag{B-4}$$

and $\fint$ implies that the integral is a principal value.

$$K(w) = -\frac{h}{\pi} - \frac{1}{2\pi j} [B(w) + B(w\, e^{j\pi})] \tag{B-5}$$

$$B(w) = \frac{d}{dw}\, \ell n\, [G(\beta)] = \frac{G_w'(\beta)}{G(\beta)} \tag{B-6}$$

$$\beta = -(k_0^2 - w^2)^{\frac{1}{2}} = j(w^2 - k_0^2)^{\frac{1}{2}} \tag{B-7}$$

$$\nu_0 = \lim_{w \to 0} w\, B(w) \tag{B-8}$$

$\sum_n R_n$ = the residue contributions from the poles of $B(w)$ on the positive real axis.

APPENDIX C

The factorizations of $M(\alpha)$ and $N(\alpha)$ are obtained by applying the theorem given in the Appendix B.

$$M(\alpha) = M_-(\alpha)\, M_+(\alpha) \quad ; \quad |\tau| < k_0'' \tag{C-1}$$

$$M_+(\alpha) = M_-(-\alpha) = \left[j\sqrt{\frac{\sin k_2 d}{k_2}}\,(k_2 - \alpha) \prod_{n=1}^{\infty} (1 + \frac{\alpha}{j\gamma_n'}) e^{j\,\alpha d/n\pi} \right]^{-1} \cdot$$

$$\left[\sqrt{H(0)}\,(1 - \frac{\alpha}{k_0})^{\frac{1}{2}} (1 - \frac{\alpha}{\beta_2})^{-1} \exp(j\,\frac{k_0 d}{2} + j\,\frac{d\gamma}{\pi}\,\ell n(\frac{\alpha - \gamma}{k_0}) \right.$$

$$\left. + q_0(\alpha) \right]^{-1} \tag{C-2}$$

where

$$H(0) = \frac{jk_0}{-k_2 \sin k_2 d + jk_0 \cos k_2 d} \tag{C-3}$$

$$q_0(\alpha) = -\int_0^{\infty} \dot{K}_0(w)\, \ell n \left[1 - \frac{\alpha}{(k_0^2 - w^2)^{\frac{1}{2}}} \right] dw \tag{C-4}$$

$$K_0(w) = -\frac{d}{\pi} + \frac{(w^2 d + (w^2/w' - w') \sin w'd \cos w'd)}{\pi(w'^2 \sin^2 w'd + w^2 \cos^2 w'd)} \tag{C-5}$$

$$w' = (w^2 + k_2^2 - k_0^2)^{\frac{1}{2}} \tag{C-6}$$

$$N(\alpha) = N_-(\alpha)\, N_+(\alpha) \quad ; \quad |\tau| < k_0'' \tag{C-7}$$

$$N_+(\alpha) = N_-(-\alpha) = \left[j\sqrt{\frac{\sin k_1 d}{k_1}}\,(k_1 - \alpha) \prod_{n=1}^{\infty} (1 + \frac{\alpha}{j\gamma_n})\, e^{j\alpha d/n\pi} \right]^{-1} \cdot$$

$$\left[\sqrt{H_1(0)}\,(1 - \frac{\alpha}{k_0})^{\frac{1}{2}}\,(1 - \frac{\alpha}{\beta_1})^{-1} \exp(j\,\frac{k_0 d}{2} + j\,\frac{\gamma d}{\pi}\,\ell n(\frac{d - \gamma}{k_0}) \right.$$

$$\left. + q_1(\alpha) \right]^{-1} \tag{C-8}$$

where $$H_1(0) = \frac{j\, k_0}{-k_1 \sin k_1 d + j\, k_0 \cos k_1 d} \qquad \text{(C-9)}$$

$$q_1(\alpha) = -\int_0^{\infty} K_1(w)\, \ell n \left[1 - \frac{\alpha}{(k_0^2 - w^2)^{\frac{1}{2}}} \right] dw \qquad \text{(C-10)}$$

$$K_1(w) = -\frac{d}{\pi} + \frac{(w^2 d + (w^2/w'' - w'') \sin w'' d \cos w'' d)}{\pi(w''^2 \sin^2 w'' d + w^2 \cos^2 w'' d)} \qquad \text{(C-11)}$$

$$w'' = (w^2 + k_1^2 - k_0^2)^{\frac{1}{2}} \qquad \text{(C-12)}$$

In general, for electromagnetic field problems the asymptotic behaviour of factorized functions is algebraic. This implies that $M_+(\alpha)$, $M_-(\alpha)$, $N_+(\alpha)$, $N_-(\alpha)$ should be multiplied by $e^{x(\alpha)}$ where $x(\alpha)$ is an entire function which has to be determined for each case. But for the problems considered in this thesis, the functions $M(\alpha)$ and $N(\alpha)$ are very similar and have the same asymptotic behaviour and moreover, they can always be encountered in the forms $M_+(\alpha)/N_+(\alpha)$, $M_-(\alpha)/N_-(\alpha)$ and $M_-(\alpha)\, N_+(\alpha)$, hence, we need not concern ourselves about these entire functions since they will finally cancel each other.

$$K(\alpha) = \frac{\varepsilon_{r_2}(\alpha^2 - k_0^2)^{\frac{1}{2}} \cosh (\alpha^2 - k_2^2)^{\frac{1}{2}} d + (\alpha^2 - k_2^2)^{\frac{1}{2}} \sinh (\alpha^2 - k_2^2)^{\frac{1}{2}} d}{\varepsilon_{r_2}(\alpha^2 - k_0^2)^{\frac{1}{2}} (\alpha^2 - k_2^2)^{\frac{1}{2}} \sinh (\alpha^2 - k_2^2)^{\frac{1}{2}} d} \qquad \text{(C-13)}$$

$$K_+(\alpha) = K_-(-\alpha) = \left[j \sqrt{\frac{\varepsilon_{r_2} \sin k_2 d}{k_2}} (k_2 - \alpha) \prod_{n=1}^{\infty} (1 + \frac{\alpha}{j\gamma_n'}) e^{j\, \alpha d/n\pi} \right]^{-1} \cdot$$

$$\left[\sqrt{H_2(0)} (1 - \frac{\alpha}{k_0})^{\frac{1}{2}} (1 - \frac{\alpha}{\beta_2})^{-1} \exp(j \frac{k_0 d}{2} + j \frac{d\gamma}{\pi} \ell n(\frac{\alpha - \gamma}{k_0}) \right.$$

$$\left. + q_2(\alpha) \right]^{-1} \qquad \text{(C-14)}$$

where

$$H_2(0) = \frac{j\, k_0}{-k_2 \sin k_2 d + j\, \varepsilon_{r_2} k_0 \cos k_2 d} \tag{C-15}$$

$$q_2(\alpha) = -\int_0^{\infty} K_2(w)\, \ell n \left[1 - \frac{\alpha}{(k_0^2 - w^2)^{\frac{1}{2}}}\right] dw \tag{C-16}$$

$$K_2(w) = -\frac{d}{\pi} + \frac{\varepsilon_{r_2} (w^2 d + (w^2/w_2 - w_2) \cos w_2 d \sin w_2 d)}{\pi[w_2^2 \sin^2 w_2 d + (w\varepsilon_{r_2})^2 \cos^2 w_2 d]} \tag{C-17}$$

$$w_2 = (w^2 + k_2^2 - k_0^2)^{\frac{1}{2}} \tag{C-18}$$

$$L(\alpha) = \frac{\varepsilon_{r_1} (\alpha^2 - k_0^2)^{\frac{1}{2}} \cosh (\alpha^2 - k_1^2)^{\frac{1}{2}} d + (\alpha^2 - k_1^2)^{\frac{1}{2}} \sinh (\alpha^2 - k_1^2)^{\frac{1}{2}} d}{\varepsilon_{r_1} (\alpha^2 - k_0^2)^{\frac{1}{2}} (\alpha^2 - k_1^2)^{\frac{1}{2}} \sin (\alpha^2 - k_1^2)^{\frac{1}{2}} d} \tag{C-19}$$

$$L_+(\alpha) = L_-(-\alpha) = \left[j \sqrt{\frac{\varepsilon_{r_1} \sin k_1 d}{k_1}} (k_1 - \alpha) \prod_{n=1}^{\infty} (1 + \frac{\alpha}{j\gamma_n}) e^{j\, \alpha d/n\pi}\right]^{-1} \cdot$$

$$\left[\sqrt{H_3(0)} (1 - \frac{\alpha}{k_0})^{\frac{1}{2}} (1 - \frac{\alpha}{\beta_1})^{-1} \exp[j \frac{k_0 d}{2} + j \frac{d\gamma}{\pi} \ell n (\frac{\alpha - \gamma}{k_0}) + q_3(\alpha)\right]^{-1} \tag{C-20}$$

where $$H_3(0) = \frac{j\, k_0}{-k_1 \sin k_1 d + j\, \varepsilon_{r_1} k_0 \cos k_1 d} \tag{C-21}$$

$$q_3(\alpha) = -\int_0^{\infty} K_3(w)\, \ell n \left[1 - \frac{\alpha}{(k_0^2 - w^2)^{\frac{1}{2}}}\right] dw \tag{C-22}$$

$$K_3(w) = -\frac{d}{\pi} + \frac{\varepsilon_{r_1} (w^2 d + (w^2/w_3 - w_3) \cos w_3 d \sin w_3 d)}{[w_3^2 \sin^2 w_3 d + (w\varepsilon_{r_1})^2 \cos^2 w_3 d]} \tag{C-23}$$

$$w_3 = (w^2 + k_1^2 - k_0^2)^{\frac{1}{2}} \tag{C-24}$$

The following decompositions can be done by applying the theorem 1.3B of Noble [38].

$$U(\alpha) = U_+(\alpha) + U_-(\alpha) = \frac{1}{L_+(\alpha)\ K_-(\alpha)} \left[\frac{1}{(\alpha - \beta_1)} - \frac{(\beta_1^2 - k_0^2)^{\frac{1}{2}}}{(\alpha^2 - k_0^2)^{\frac{1}{2}}\ (\alpha - \beta_1)} \right] \tag{C-25}$$

$$V(\alpha) = V_+(\alpha) + V_-(\alpha) = \frac{1}{L_+(\alpha)\ K_-(\alpha)} \left(\frac{\varepsilon_{r_2}\beta_1}{\varepsilon_{r_1}} + \alpha\right) \left[\frac{1}{(\alpha^2 - k_2^2 + k_1^2 - \beta_1^2)} + \right.$$

$$\left. \frac{\varepsilon_{r_1}\ (\beta_1^2 - k_0^2)^{\frac{1}{2}} \cosh\ (\alpha^2 - k_2^2)^{\frac{1}{2}}\, d}{(\alpha^2 - k_2^2 + k_1^2 - \beta_1^2)(\alpha^2 - k_2^2)^{\frac{1}{2}} \sin(\alpha^2 - k_2^2)^{\frac{1}{2}}\, d} \right] \tag{C-26}$$

$$W_1^n(\alpha) = W_{1+}^n(\alpha) + W_{1-}^n(\alpha) = \frac{1}{L_+(\alpha)\ K_-(\alpha)} \left(\frac{1}{\alpha^2 - k_1^2 + \left(\frac{n\pi}{d}\right)^2}\right) \tag{C-27}$$

$$\bar{W}_1^n(\alpha) = \bar{W}_{1+}^n(\alpha) + \bar{W}_{1-}^n(\alpha) = \frac{j\alpha}{L_+(\alpha)\ K_-(\alpha)} \left(\frac{1}{\alpha^2 - k_1^2 + \left(\frac{n\pi}{d}\right)^2}\right) \tag{C-28}$$

$$W_2^n(\alpha) = W_{2+}^n(\alpha) + W_{2-}^n(\alpha) = \frac{1}{L_+(\alpha)\ K_-(\alpha)} \left(\frac{1}{\alpha^2 - k_2^2 + \left(\frac{n\pi}{d}\right)^2}\right) \tag{C-29}$$

$$\bar{W}_2^n(\alpha) = \bar{W}_{2+}^n(\alpha) + \bar{W}_{2-}^n(\alpha) = \frac{j\alpha}{L_+(\alpha)\ K_-(\alpha)} \left(\frac{1}{\alpha^2 - k_2^2 + \left(\frac{n\pi}{d}\right)^2}\right) \tag{C-30}$$

APPENDIX D

Expressions for C_0, C_1, F_0, F_1, M_0, M_1, N_0, N_1, R_0, R_1, S_0, S_1, T_0, T_1, S_0', S_1', T_0', T_1'

The expressions for C_0, C_1, F_0, F_1, M_0, M_1, R_0, R_1, S_0, S_1, T_0, T_1, S_0', N_0, N_1, S_1', T_0', T_1' are given by

$$C_0 = \frac{\{(\varepsilon_{r_2} - \varepsilon_{r_1})\, k_0^2 - \beta_2^2 + \beta_1^2\}\{(\varepsilon_{r_1} - 1)k_0^2 + \beta_2^2 - \beta_1^2\}}{F_0 N_0} \tag{D-1}$$

$$C_1 = \frac{\{(\varepsilon_{r_2} - \varepsilon_{r_1})\, k_0^2 - \beta_2^2 + \beta_1^2\}\{(\varepsilon_{r_2} - 1)k_0^2 - \beta_2^2 + \beta_1^2\}}{F_0 M_0} \tag{D-2}$$

$$F_0 = \frac{2}{\{(d_1 + \frac{1}{\gamma_1})(d_2 + \frac{1}{\gamma_2})\}^{\frac{1}{2}}} \tag{D-3}$$

$$F_1 = \frac{2}{\pi^{\frac{1}{2}}\{(d_2 + \frac{1}{\gamma_2})(\cos^2 \sigma d_1 + \frac{\sigma^2}{\rho^2} \sin^2 \sigma d_1)\}^{\frac{1}{2}}} \tag{D-4}$$

$$\begin{aligned} M_0 = {} & (\gamma_2^2 - \gamma_1^2)(\gamma_1^2 + k_2^2)\{k_2 \sin k_2 d_1 \cos k_1 d_1 - k_1 \sin k_1 d_1 \cos k_2 d_1\} + \\ & (\gamma_2^2 - \gamma_1^2)(k_2^2 - k_1^2) \cos k_1 d_1 \{(k_2 \sin k_2 d_2 - \gamma_1 \cos k_2 d_2) e^{-\gamma_1 (d_2 - d_1)} - \\ & (k_2 \sin k_2 d_1 - \gamma_1 \cos k_2 d_1)\} + (k_2^2 - k_1^2)(\gamma_1^2 + k_2^2)(\gamma_2 - \gamma_1) \cos k_1 d_1 \\ & \cos k_2 d_2\, e^{-\gamma_1 (d_2 - d_1)} \end{aligned} \tag{D-5}$$

$$\begin{aligned} M_1 = {} & (k_2^2 - \rho^2)(\gamma_2^2 + \rho^2)\{k_2 \sin k_2 d_1 \cos \sigma d_1 - \sigma \cos k_2 d_1 \sin \sigma d_1\} + \\ & (k_2^2 - \sigma^2)(\gamma_2^2 + \rho^2)\{D_0 \cos \rho (d_2 - d_1) - D_1 \sin \rho (d_2 - d_1) - \\ & (k_2 \sin k_2 d_1 \cos \sigma d_1 - \sigma \cos k_2 d_1 \sin \sigma d_1)\} + (k_2^2 - \sigma^2)(k_2^2 - \end{aligned}$$

$$\rho^2) \cos k_2 d_2 \{D_2 \cos\rho(d_2 - d_1) - D_3 \sin\rho(d_2 - d_1)\} \quad \text{(D-6)}$$

$$D_0 = k_2 \sin k_2 d_2 \cos \sigma d_1 - \sigma \cos k_2 d_2 \sin \sigma d_1 \quad \text{(D-7)}$$

$$D_1 = \rho \cos k_2 d_2 \cos \sigma d_1 + \frac{k_2 \sigma}{\rho} \sin k_2 d_2 \sin \sigma d_1 \quad \text{(D-8)}$$

$$D_2 = \gamma_2 \cos \sigma d_1 - \sigma \sin \sigma d_1 \quad \text{(D-9)}$$

$$D_3 = \rho \cos \sigma d_1 + \frac{\gamma_2 \sigma}{\rho} \sin \sigma d_1 \quad \text{(D-10)}$$

$$N_0 = (\gamma_2^2 - \gamma_1^2)(\gamma_2^2 + k_1^2) \{k_2 \sin k_2 d_2 \cos k_1 d_2 - k_1 \cos k_2 d_2 \sin k_1 d_2\} +$$

$$(\gamma_2^2 - \gamma_1^2)(k_2^2 - k_1^2) \cos k_2 d_2 \{(k_1 \sin k_1 d_1 - \gamma_2 \cos k_1 d_1) e^{-\gamma_2 (d_1 - d_2)} +$$

$$(\gamma_2 \cos k_1 d_2 - k_1 \sin k_1 d_2)\} + (k_2^2 - k_1^2)(\gamma_2^2 + k_1^2)(\gamma_2 - \gamma_1) \cos k_1 d_1$$

$$\cos k_2 d_2 \, e^{-\gamma_2 (d_1 - d_2)} \quad \text{(D-11)}$$

$$N_1 = (\gamma_2^2 + \rho^2)(\gamma_2^2 + \sigma^2) \{k_2 \sin k_2 d_2 \cos \sigma d_2 - \sigma \cos k_2 d_2 \sin \sigma d_2\} +$$

$$(\gamma_2^2 + \rho^2)(k_2^2 - \sigma^2) \cos k_2 d_2 \{(\sigma \sin \sigma d_1 - \gamma_2 \cos \sigma d_1) e^{-\gamma_2 (d_1 - d_2)}$$

$$+ (\gamma_2 \cos \sigma d_2 - \sigma \sin \sigma d_2)\} + (k_2^2 - \sigma^2)(\gamma_2^2 + \sigma^2) \cos k_2 d_2 \, e^{-\gamma_2 (d_1 - d_2)}$$

$$(\gamma_2 \cos \sigma d_1 - \sigma \sin \sigma d_1) \quad \text{(D-12)}$$

$$R_0 = \frac{2(\varepsilon_{r_1} \varepsilon_{r_2})^{\frac{1}{2}}}{\left[d_2 + \frac{\varepsilon_{r_2}}{\gamma_2} \left(\frac{\gamma_2^2 + k_2^2}{k_2^2 + \varepsilon_{r_2}^2 \gamma_2^2} \right) \right]^{\frac{1}{2}} \left[d_1 + \frac{\varepsilon_{r_1}}{\gamma_1} \left(\frac{\gamma_1^2 + k_1^2}{k_1^2 + \varepsilon_{r_1}^2 \gamma_1^2} \right) \right]^{\frac{1}{2}}} \quad \text{(D-13)}$$

$$R_1 = \frac{2(\varepsilon_{r_1} \varepsilon_{r_2})^{\frac{1}{2}}}{\left[\pi(\varepsilon_{r_1} \cos^2 \sigma d_1 + \frac{\sigma^2}{\varepsilon_{r_1} \rho^2} \sin^2 \sigma d_1) \right]^{\frac{1}{2}} \left[d_2 + \frac{\varepsilon_{r_2}}{\gamma_2} \left(\frac{\gamma_2^2 + k_2^2}{k_2^2 + \varepsilon_{r_2}^2 \gamma_2^2} \right) \right]^{\frac{1}{2}}}$$

$$\text{(D-14)}$$

$$S_0 = \left[\frac{1}{\varepsilon_{r_2}} \{k_2 \sin k_2 d_2 \cos k_1 d_2 - k_1 \cos k_2 d_2 \sin k_1 d_2\} (\gamma_2^2 - \gamma_1^2)(\gamma_2^2 + k_1^2)\right.$$

$$+ (\gamma_2^2 - \gamma_1^2)(k_2^2 - k_1^2) \cos k_2 d_2 \{(k_1 \sin k_1 d_1 - \gamma_2 \cos k_1 d_1) e^{-\gamma_2 (d_1 - d_2)}$$

$$+ (\gamma_2 \cos k_1 d_2 - k_1 \sin k_1 d_2)\} + (k_2^2 - k_1^2)(\gamma_2^2 + k_1^2)(\gamma_2 - \gamma_1)$$

$$\left.\cos k_1 d_1 \cos k_2 d_2 \, e^{-\gamma_2 (d_1 - d_2)}\right] \qquad \text{(D-15)}$$

$$S_1 = \left[\frac{1}{\varepsilon_{r_1}} \{k_2 \sin k_2 d_2 \cos k_1 d_2 - k_1 \cos k_2 d_2 \sin k_1 d_2\} (\gamma_2^2 - \gamma_1^2)(\gamma_2^2 + k_1^2)\right.$$

$$+ \frac{1}{\varepsilon_{r_1}} (\gamma_2^2 - \gamma_1^2)(k_2^2 - k_1^2) \cos k_2 d_2 \{(k_1 \sin k_1 d_1 - \gamma_2 \cos k_1 d_1) e^{-\gamma_2 (d_1 - d_2)}$$

$$+ (\gamma_2 \cos k_1 d_2 - k_1 \sin k_1 d_2)\} + (k_2^2 - k_1^2)(\gamma_2^2 + k_1^2)(\gamma_2 - \gamma_1)$$

$$\left.\cos k_1 d_1 \cos k_2 d_2 \, e^{-\gamma_2 (d_1 - d_2)}\right] \qquad \text{(D-16)}$$

$$T_0 = \left[\frac{1}{\varepsilon_{r_2}} \{k_2 \sin k_2 d_2 \cos \sigma d_2 - \sigma \cos k_2 d_2 \sin \sigma d_2\} (\gamma_2^2 + \rho^2)(\gamma_2^2 + \sigma^2)\right.$$

$$+ (\gamma_2^2 + \rho^2)(k_2^2 - \sigma^2) \cos k_2 d_2 \{(\sigma \sin \sigma d_1 - \gamma_2 \cos \sigma d_1) e^{-\gamma_2 (d_1 - d_2)}$$

$$+ (\gamma_2 \cos \sigma d_2 - \sigma \sin \sigma d_2)\} + (k_2^2 - \sigma^2)(\gamma_2^2 + \sigma^2) \cos k_2 d_2 \, e^{-\gamma_2 (d_1 - d_2)}$$

$$\left.\{\gamma_2 \cos \sigma d_1 - \frac{\sigma}{\varepsilon_{r_1}} \sin \sigma d_1\}\right] \qquad \text{(D-17)}$$

$$T_1 = \left[\frac{1}{\varepsilon_{r_1}} \{k_2 \sin k_2 d_2 \cos \sigma d_2 - \sigma \cos k_2 d_2 \sin \sigma d_2\} (\gamma_2^2 + \rho^2)(\gamma_2^2 + \sigma^2)\right.$$

$$+ \frac{1}{\varepsilon_{r_1}} (\gamma_2^2 + \rho^2)(k_2^2 - \sigma^2) \cos k_2 d_2 \{(\sigma \sin \sigma d_1 - \gamma_2 \cos \sigma d_1) e^{-\gamma_2 (d_1 - d_2)}$$

$$+ (\gamma_2 \cos \sigma d_2 - \sigma \sin \sigma d_2)\} + (k_2^2 - \sigma^2)(\gamma_2^2 + \sigma^2) \cos k_2 d_2 \, e^{-\gamma_2 (d_1 - d_2)}$$

$$\left.\{\gamma_2 \cos \sigma d_1 - \frac{1}{\varepsilon_{r_1}} \sin \sigma d_1\}\right] \qquad \text{(D-18)}$$

$$S_0' = [\frac{1}{\varepsilon_{r_2}} \{k_2 \sin k_2 d_1 \cos k_1 d_1 - k_1 \cos k_2 d_1 \sin k_1 d_1\} (\gamma_2^2 - \gamma_1^2)(\gamma_1^2 + k_2^2)$$
$$+ \frac{1}{\varepsilon_{r_2}} (\gamma_2^2 - \gamma_1^2)(k_2^2 - k_1^2) \cos k_1 d_1 \{(k_2 \sin k_2 d_2 - \gamma_1 \cos k_2 d_2)$$
$$e^{-\gamma_1 (d_2 - d_1)} - (k_2 \sin k_2 d_1 - \gamma_1 \cos k_2 d_1)\} + (k_2^2 - k_1^2)(\gamma_1^2 + k_2^2)$$
$$(\gamma_2 - \gamma_1) \cos k_1 d_1 \cos k_2 d_2 \, e^{-\gamma_1 (d_2 - d_1)}] \qquad \text{(D-19)}$$

$$S_1' = [\frac{1}{\varepsilon_{r_1}} \{k_2 \sin k_2 d_1 \cos k_1 d_1 - k_1 \cos k_2 d_1 \sin k_1 d_1\}(\gamma_2^2 - \gamma_1^2)(\gamma_1^2 + k_2^2)$$
$$+ (\gamma_2^2 - \gamma_1^2)(k_2^2 - k_1^2) \cos k_1 d_1 \{(k_2 \sin k_2 d_2 - \gamma_i \cos k_2 d_2) e^{-\gamma_1 (d_2 - d_1)}$$
$$- (k_2 \sin k_2 d_1 - \gamma_1 \cos k_2 d_1)\} + (k_2^2 - k_1^2)(\gamma_1^2 + k_2^2)(\gamma_2 - \gamma_1)$$
$$\cos k_1 d_1 \cos k_2 d_2 \, e^{-\gamma_1 (d_2 - d_1)}] \qquad \text{(D-20)}$$

$$T_0' = [\frac{1}{\varepsilon_{r_2}} \{k_2 \sin k_2 d_1 \cos \sigma d_1 - \sigma \cos k_2 d_1 \sin \sigma d_1\} (k_2^2 - \rho^2)(\gamma_2^2 + \rho^2)$$
$$+ \frac{1}{\varepsilon_{r_2}} (k_2^2 - \sigma^2)(\gamma_2^2 + \rho^2) \{D_0' \cos\rho(d_2 - d_1) - D_1' \sin\rho(d_2 - d_1)$$
$$- (k_2 \sin k_2 d_1 \cos \sigma d_1 - \frac{\sigma}{\varepsilon_{r_1}} \cos k_2 d_1 \sin \sigma d_1)\} + (k_2^2 - \sigma^2)(k_2^2 - \rho^2)$$
$$\cos k_2 d_2 \{D_2' \cos\rho(d_2 - d_1) - D_3' \sin\rho(d_2 - d_1)\}] \qquad \text{(D-21)}$$

$$T_1' = [\frac{1}{\varepsilon_{r_1}} \{k_2 \sin k_2 d_1 \cos \sigma d_1 - \sigma \cos k_2 d_1 \sin \sigma d_1\} (k_2^2 - \rho^2)(\gamma_2^2 + \rho^2)$$
$$+ (k_2^2 - \sigma^2)(\gamma_2^2 + \rho^2) \{D_0' \cos\rho(d_2 - d_1) - D_1' \sin\rho(d_2 - d_1)$$
$$- (k_2 \sin k_2 d_1 \cos \sigma d_1 - \frac{\sigma}{\varepsilon_{r_1}} \cos k_2 d_1 \sin \sigma d_1)\} + (k_2^2 - \sigma^2)(k_2^2 - \rho^2)$$
$$\cos k_2 d_2 \{D_2' \cos\rho(d_2 - d_1) - D_3' \sin\rho(d_2 - d_1)\}] \qquad \text{(D-22)}$$

$$D_0' = k_2 \sin k_2 d_2 \cos \sigma d_1 - \frac{\sigma}{\varepsilon_{r_1}} \cos k_2 d_2 \sin \sigma d_1 \qquad \text{(D-23)}$$

$$D_1' = \rho \cos k_2 d_2 \cos \sigma d_1 + \frac{k_2 \rho}{\varepsilon_{r_1} \rho} \sin k_2 d_2 \sin \sigma d_1 \qquad \text{(D-24)}$$

$$D_2' = \gamma_2 \cos \sigma d_1 - \frac{\sigma}{\varepsilon_{r_1}} \sin \sigma d_1 \qquad \text{(D-25)}$$

$$D_3' = \rho \cos \sigma d_1 + \frac{\gamma_2 \sigma}{\varepsilon_{r_1} \rho} \sin \sigma d_1 \qquad \text{(D-26)}$$

BIBLIOGRAPHY

[1] H.M. Barlow and J. Brown, *Radio Surface Waves*, Oxford: The Clarendon Press, 1962, Ch. 1.

[2] L. Lewin, "Radiation from curved dielectric slabs and fibers", IEEE Trans. Microwave Theory and Techniques, Vol. MTT-22, pp. 718-727, July 1974.

[3] E.A.J. Marcatili, "Bends in optical dielectric guides", Bell System Technical Journal, Vol. 48, pp. 2103-2132, September 1969.

[4] D. Marcuse, *Light Transmission Optics*, New York: Van Nostrand Reinhold Company, 1972, Ch. 9.

[5] D. Marcuse, *Theory of Dielectric Optical Waveguides*, New York: Academic Press, 1974, Ch. 4.

[6] G. Goubau, "Surface waves and their application to transmission lines", J. of Applied Phys., Vol. 21, pp. 1119-1128, November 1950.

[7] L. Young, *Advances in Microwaves*, New York: Academic Press, Vol. 4, 1969, pp. 191-300.

[8] J.A. Arnaud, *Beam and Fiber Optics*, New York: Academic Press, 1976, Ch. 5.

[9] J. Jordan, "Fiber-optic links for data communications", Telecommunications, Vol. 13, No. 9, pp. 107-108, September 1979.

[10] L. Campbell, "Fiber optics for telecommunications", Microwave J., Vol. 22, No. 7, p. 24, July 1979.

[11] A.E. Karbowiak, *Advances in Microwaves*, New York: Academic Press, Vol. 1, 1966, pp. 75-113.

[12] R.M. Gagliardi and S. Karp, *Optical Communications*, New York: John Wiley & Sons, 1976, Ch. 1.

[13] H.M. Barlow and J. Brown, *Radio Surface Waves*, Oxford: The Clarendon Press, 1962, Ch. 13.

[14] C.H. Walter, *Traveling Wave Antennas*, New York: Dover Publications, Inc., 1965. Ch. 8.

[15] N. Marcuvitz, "On field representations in terms of leaky modes or eigenmodes", IEEE Trans. on Antennas and Propagation, Vol. AP-5, p. 100, January 1956.

[16] H.M. Barlow and J. Brown, *Radio Surface Waves*, Oxford: The Clarendon Press, 1962, Ch. 12.

[17] C.M. Angulo, "Diffraction of surface wave by a semi-infinite dielectric slab", IEEE Trans. on Antennas and Propagation, Vol. AP-5, pp. 100-108, January 1957.

[18] V.V. Shevchenko, *Continuous Transitions in Open Waveguides*, Boulder, Colorado: The Golem Press, 1971, pp. 9-21.

[19] W.R. Jones, "A new approach to the diffraction of a surface wave by a semi-infinite grounded dielectric slab", IEEE Trans. on Antennas and Propagation, Vol. AP-12, pp. 767-777, November 1964.

[20] A.F. Kay, "Scattering of a surface wave by a discontinuity in reactance", IEEE Trans. on Antennas and Propagation, Vol. AP-7, pp. 22-31, January 1959.

[21] E.L. Johansen, "Surface wave scattering by step", IEEE Trans. on Antennas and Propagation, Vol. AP-15, pp. 442-448, May 1967.

[22] R.A. Waldron, *The Theory of Waveguide and Cavity*, London: Maclaren and Sons, Ltd., 1967, Ch. 5.

[23] D. Marcuse, "Radiation losses of tapered dielectric slab waveguides", Bell System Technical Journal, Vol. 49, pp. 273-290, February 1970.

[24] F.J. Zucker, *Antenna Theory, Part 2*, New York: McGraw-Hill, 1969, Ch. 21.

[25] P.J.B. Clarricoats and A.B. Sharpe, "Modal matching applied to a discontinuity in a planar surface waveguide", Electronics Letters, Vol. 8, pp. 28-29, January 1972.

[26] E.W. Hu and L. Bergstein, "Analysis of surface waveguide discontinuities", Annual Summary of Res. in Elect., Microwave Research Ins., pp. 22-26, September 1976.

[27] S.F. Mahmoud and J.C. Beal, "Scattering of surface waves at a dielectric discontinuity on a planar waveguide", IEEE Trans. on Microwave Theory and Techniques, Vol. MTT-23, pp. 193-198, February 1975.

[28] B. Rulf, "Discontinuity radiation in surface waveguides", J. Opt. Soc. Am., Vol. 65, pp. 1248-1252, November 1975.

[29] G.A. Hockham and A.B. Sharpe, "Dielectric-waveguide discontinuities", Electronics Letters, Vol. 8, pp. 230-231, May 1972.

[30] T.E. Rozzi, "Rigorous analysis of the step discontinuity in a planar dielectric waveguide", IEEE Trans. on Microwave Theory and Techniques, Vol. MTT-26, pp. 738-746, October 1978.

[31] R.E. Collin, *Field Theory of Guided Waves*, New York: McGraw-Hill, 1960, Ch. 11.

[32] H.M. Barlow and J. Brown, *Radio Surface Waves*, Oxford: The Clarendon Press, 1962, Chs. 2 & 8.

[33] R.F. Harrington, *Time-Harmonic Electromagnetic Fields*, New York: McGraw-Hill, 1961, Ch. 4.

[34] D. Marcuse, *Light Transmission Optics*, New York: Van Nostrand Reinhold Company, 1972, Ch. 8.

[35] D. Marcuse, *Theory of Dielectric Optical Waveguides*, New York: Academic Press, 1974, Chs. 1 & 2.

[36] N.S. Kapany and J.J. Burke, *Optical Waveguides*, New York: Academic Press, 1972, Chs. 2 & 4.

[37] C.H. Walter, *Traveling Wave Antennas*, New York: Dover Publications, Inc., 1965, Ch. 6.

[38] B. Noble, *Methods Based on the Wiener-Hopf Technique*, London: Pergamon Press, 1958, Chs. 1 & 5.

[39] R. Mittra and S.W. Lee, *Analytical Techniques in the Theory of Guided Waves*, New York: The Macmillan Company, 1971, Ch. 3.

[40] R.E. Collin, "Scattering by an infinite array of thin dielectric sheets", IEEE Trans. on Antennas and Propagation, Vol. AP-8, pp. 62-67, January 1960.

[41] J.B. Andersen and V.V. Solodukhov, "Field behaviour near a dielectric wedge", IEEE Trans. on Antennas and Propagation, Vol. AP-26, pp. 598-602, July 1978.

[42] H.F. Weinberger, *A First Course in Partial Differential Equations*, New York: Blaisdell Publishing Company, 1965, Ch. 4.

[43] L.B. Felsen and N. Marcuvitz, *Radiation and Scattering of Waves*, Englewood Cliffs, New Jersey: Prentice-Hall, Inc., 1973, Ch. 4.

[44] B.W. Roos, *Analytic Functions and Distributions in Physics and Engineering*, New York: John Wiley & Sons, Inc., 1969, Ch. 3.

[45] P.M. Morse and H. Feshbach, *Methods of Theoretical Physics*, New York: McGraw-Hill, 1953, Ch. 8.

[46] R. Mittra and S.W. Lee, *Analytical Techniques in the Theory of Guided Waves*, New York: The Macmillan Company, 1971, Ch. 2.

[47] A.I. Markushevich, *Theory of Functions of a Complex Variable, Vol. II*, Englewood Cliffs, New Jersey: Prentice-Hall, Inc., 1965, Ch. 2.

[48] L.L. Pennisi, *Elements of Complex Variables*, New York: Holt Reinhart and Winston, 1963, Ch. 7.

[49] E.T. Copson, *Theory of Functions of a Complex Variable*, Oxford University Press, 1935, Ch. 6.

[50] V.V. Shevchenko, *Continuous Transitions in Open Waveguides*, Boulder, Colorado: The Golem Press, 1971, Ch. 2.

[51] J.B. Keller, "Geometrical theory of diffraction", J. Opt. Soc. Am., Vol. 52, pp. 116-130, February 1962.

[52] A. Ittipiboon and M.A.K. Hamid, "Scattering of surface waves at a slab waveguide discontinuity", Proc. IEE., Vol. 126, pp. 798-804, September 1979.

[53] D.T. Paris and F.K. Hurd, *Basic Electromagnetic Theory*, New York: McGraw-Hill, 1969, Ch. 8.

[54] J.A. Stratton, *Electromagnetic Theory*, New York: McGraw-Hill, 1941, Ch. 9.

[55] J. Anderson, "Plane wave diffraction by a thin dielectric half plane", IEEE Trans. on Antennas and Propagation, Vol. AP-27, pp. 584-589, September 1979.

[56] A. Hessel, *Antenna Theory, Part 2*, New York: McGraw-Hill, 1969, Ch. 19.

[57] T. Tamir, *Antenna Theory, Part 2*, New York: McGraw-Hill, 1969, Ch. 20.